SYNTHESIS AND EVALUATION OF THE ANTIBACTERIAL AND ANTIOXIDANT ACTIVITIES AND *IN SILICO* MOLECULAR DOCKING ANALYSIS OF QUINOLINE DERIVATIVES

Bayan Abdi Ahmed

A Thesis Submitted to Department of Applied Chemistry

School of Applied Natural Science

Presented in partial Fulfillment of the Requirements for Master of Science Degree in Applied Chemistry (Synthetic Organic Chemistry)

Office of Graduate Studies

Adama Science and Technology University

June, 2021
Adama, Ethiopia

SYNTHESIS AND EVALUATION OF THE ANTIBACTERIAL AND ANTIOXIDANT ACTIVITIES AND *IN SILICO* MOLECULAR DOCKING ANALYSIS OF QUINOLINE DERIVATIVES

Bayan Abdi Ahmed

Advisor : Yadessa Melaku (PhD)

Co-Advisor : Rajalakshmanan Eswaramoorthy (PhD)

A Thesis Submitted to Department of Applied Chemistry

School of Applied Natural Science

Presented in partial Fulfillment of the Requirements for Master of Science Degree in Applied Chemistry (Synthetic Organic Chemistry)

Office of Graduate Studies

Adama Science and Technology University

June, 2021
Adama, Ethiopia

DECLARATION

I hereby declare that this MSc Thesis entitled "**Synthesis and Evaluation of the Antibacterial and Antioxidant Activities and *In silico* Molecular Docking Analysis of Quinoline Derivatives"** is my original work. That is, it has not been presented for any degree or diploma in this or in any other university. All sources of materials used for this thesis have been duly acknowledged.

_____	_____	_____
Name of the student	Signature	Date

RECOMMENDATION

We, the advisors of this thesis, hereby certify that we have read the revised version of the thesis entitled "**Synthesis and Evaluation of the Antibacterial and Antioxidant Activities and *In silico* Molecular Docking Analysis of Quinoline Derivatives**" prepared under our guidance by Bayan Abdi submitted in partial fulfillment of the requirements for the degree of Master of Science in Applied Chemistry (Synthetic Organic Chemistry). Therefore, we recommend the submission of revised version of the thesis to the department following the applicable procedures.

_____	_____	_____
Name of major advisor	Signature	Date
_____	_____	_____
Name of co-advisor	Signature	Date

APPROVAL OF BOARD OF EXAMINERS

We, the advisors of the thesis entitled "**Synthesis and Evaluation of the Antibacterial and Antioxidant Activities and *In silico* Molecular Docking Analysis of Quinoline Derivatives**" and developed by Bayan Abdi, hereby certify that the recommendation and suggestions made by the board of examiners are appropriately incorporated into the final version of the thesis.

Name of major advisor	Signature	Date
Name of co-advisor	Signature	Date

We, the undersigned, members of the Board of Examiners of the final open defense by Bayan Abdi have read and evaluated his thesis entitled "**Synthesis and Evaluation of the Antibacterial and Antioxidant Activities and *In silico* Molecular Docking Analysis of Quinoline Derivatives**" and examined the candidate during open defense. This is, therefore, to certify that the thesis has been accepted in partial fulfillment of the requirement of the Degree of Master's in Applied Chemistry (Synthetic Organic Chemistry).

Advisor	Signature	Date
Chairperson	Signature	Date
Internal Examiner	Signature	Date
External Examiner	Signature	Date

Finally approval and acceptance of the thesis is contingent upon submission of its final copy to the Office of Postgraduate Studies (OPGS) through the Department Graduate committee (DGC) and School Graduate Committee (SGC).

Department Head	Signature	Date
School Dean	Signature	Date
Office of Postgraduate Studies, Dean	Signature	Date

TABLE OF CONTENT

ACKNOWLEDGEMENTS

First and foremost, I would like to thanks the Almighty God for giving me the strength, knowledge, ability, and opportunity to undertake this research study and to persevere and complete it successfully. Without his supports and blessings, this achievement would not have been possible.

I would like to express my deepest thanks to my advisor Yadessa Melaku (PhD), for his constructive advice, useful discussion, continuous guidance, friendly treatment, frequently visits during laboratory work and careful supervision of the research project at all time. His unwavering enthusiasm, optimism, and kindness have been invaluable sources of encouragement, and the knowledge he has passed on to me is essential. For these reasons and more, I am ceaselessly grateful. He also my teachers of patience and behavioral changes.

I would like to thank my co-advisor Rajalakshmanan Eswaramoorthy (PhD) for his very good support on *in silico* molecular docking analysis.

My special thanks to Digafie Zeleke (PhD) for his continuous support throughout the practical or lab research by preparing all materials needed and giving advice on how to use the materials. He shares endless solid knowledge and shows to me, the short pathway how to achieve the research in short time.

I would also like to thank all my coworkers for their encouragement and supports in chemistry laboratory. These include Mr. Mona Fikadu, Mr. Fitsum Lemilemu, Mr. Tadewos Damena, Mr. Mamaru Bitew and Mr. Damis Zelelew.

I would like to acknowledge Adama Science and Technology University Department of Applied Chemistry for supporting materials, some chemicals required for this research and opportunity to pursue MSc study.

I am thankful to the Department of Chemistry, Addis Ababa University, for their cooperation in running of NMR spectroscopy sample analysis.

Finally, this work would not have been possible without the support and encouragement of my family. So that, I want to thank my family for their continuous support that helped me to pursue every academic endeavor to the fullest. They have always been the driving force behind every success I have achieved so far. I would not be where I am today without their love, patience and continued faith in me.

LIST OF ABBREVIATIONS

ADT	AutoDock tool
DMF	Dimethylformamide
DMSO	Dimethyl sulfoxide
DNA	Deoxyribonucleic acid
DPPH	1,1-diphenyl-2-picryl hydrazyl
EC	Effective concentration
EDC	1-Ethyl-3-(3-dimethylaminopropyl) carbodiimide
LD	Lethal dose
LRP	Luciferase reporter phage
MHA	Mueller-Hinton agar
MIC	Minimum inhibition concentration
NHA	Number of hydrogen acceptor
NHD	Number of hydrogen donor
NMR	Nuclear magnetic resonance
NRB	Number of rotatable bonds
PPA	Polyphosphoric acid
R_f	Retention factor
RMSD	Root mean square deviation
THF	Tetrahydrofuran
TLC	Thin layer chromatography
TPSA	Total polar surface area
UV-Vis	Ultra violate-visible
WHO	World health organization

LIST OF FIGURES

LIST OF SCHEMES

LIST OF TABLES

LIST OF APPENDIXS

ABSTRACT

*The quinoline heterocycle is a useful scaffold to develop bioactive molecules. In the present work, a series of novel quinoline derivatives were synthesized by Vilsmeier–Haack reaction. Methoxy and Ethoxyl (nucleophiles) were introduced into 2,7-dichloroquinoline-3-carbaldehyde by substitution of chlorine at 2-position using potassium carbonate in DMF. The carbaldehyde functional group of 2,7-dichloroquinoline-3-carbaldehyde and 2-chloroquinoline-3-carbaldehyde was further manipulated to nitriles using phosphorous oxychloride and sodium azide. The nitrile functional group of 2,7-dichloroquinoline-3-carbonitrile was converted to amide using acetic acid and sulfuric acid. All synthesized compounds were characterized by ^{1}H NMR, ^{13}C NMR, and UV-Vis spectroscopy. The antibacterial activity of the synthesized compounds (**129-133**) were screened against two Gram negative (E. coli and P. aeruginosa) and two Gram positive (S. aureus and S. pyogenes) pathogenic bacteria. Most of the compounds displayed good activity against two or more bacterial strains. Among them, compounds **132** and **130** showed good activities against E. coli with mean inhibition zones of 12.00 ± 0.00 and 11.00 ± 0.04 mm respectively. The compound **129** also had good activity against S. aureus and P. aeruginosa with mean inhibition of 11.00 ± 0.03 mm at 200 µg/mL relative to standard amoxicillin. Compound **131** at 200 µg/mL concentration showed good activity against S. pyrogenes with mean inhibition of 11.00 ± 0.02 mm. The radical scavenging activity of these compounds was evaluated using 1,1-diphenyl-2-picryl hydrazyl (DPPH), and compounds **130** and **129** displayed strongest antioxidant activity with IC_{50} of 0.31 and 2.17 µg/mL relative to ascorbic acid (2.41 µg/mL) respectively. The molecular docking study of the synthesized compounds was conducted to investigate their binding pattern with topoisomerase IIα or anticancer potency and E. coli gyraseB. The in silico interaction results match with the in vitro analysis of the synthesized compounds showed good activities against E. coli, among synthesized compounds **130** (-6.4 kcal/mol) and **132** (-6.6 kcal/mol) exhibited better activity. The synthesized compounds (**129-133**) were found to have minimum binding energy ranging from -6.9 to -7.3 kcal/mol against topoisomerase IIα, with best results achieved with compound **132** (-7.3 kcal/mol), **129** (-7.1 kcal/mol) and **130** (-7.1 kcal/mol) of these, compound **132** displayed binding affinity of -7.3 Kcal/mol compared to vosaroxin (-7.2 Kcal/mol).*

Key words: Antibacterial, Antioxidant, Quinoline, Disk diffusion

1. INTRODUCTION

Nowadays, heterocyclic compounds play an important role towards the development of organic synthesis and have got wide applications in the field of medicinal chemistry. The ring system containing nitrogen, oxygen and sulfur as heteroatom has important role in many biological processes and as therapeutic agents.

1.1 Background

Heterocyclic compounds play an important role in designing new classes of structural entities of medicinal importance with potentially new mechanisms of action. These heterocyclic compounds are well known to possess diverse pharmacological properties, namely, antimicrobial, anticancer, anticonvulsant, antimalarial activities etc. [1]. Quinoline was first extracted from coal tar in 1834 by German chemist Friedlieb Ferdinand Runge; he called quinoline *leukol* ("white oil" in Greek). Coal tar remains the principal source of commercial quinoline. In 1842, the French chemist Charles Gerhardt obtained a compound by dry distilling quinine, strychnine, or cinchonine with potassium hydroxide; he called the compound *Chinoilin* or *Chinolein*. Runge's and Gephardt's compounds seemed to be distinct isomers because they reacted differently. However, the German chemist August Hoffmann eventually recognized that the differences in behaviors were due to the presence of contaminants and that the two compounds were actually identical. The report of quinoline as a natural product is from the Peruvian stick insect *Oreophoetes peruana*. They have a pair of thoracic glands from which they discharge a malodorous fluid containing quinoline when disturbed [2]. Chemical names of quinoline (**1**) are benzo-pyridine or 1-aza-napthalene. These are weak tertiary base with alkaloidal nature and contain nitrogenous heterocyclic aromatic ring [3]. Quinoline nucleus occurs in several natural compounds and pharmacologically active substances displaying a broad range of biological activity. Quinoline nucleus shows the same reactions as in pyridine and benzene. The main chemical reactions are nucleophilic and electrophilic substitution in nature [3]. Quinolines exhibits wide range of activity such as antiprion, antimicrobial, antibacterial, antitubercular and anticancer activities [1]. Quinoline ring plays an important role in new anti-cancer agents development as its derivatives have shown excellent results through different mechanism of action such as growth inhibitors by cell cycle arrest, apoptosis, inhibition of

angiogenesis, disruption of cell migration, and modulation of nuclear receptor responsiveness [1].

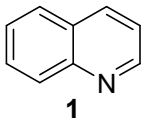

1

Figure 1: Quinoline (1-Aza Naphthalene) structure.

Quinoline derivatives are great importance to chemists and biologists as it is found in a large variety of naturally occurring compounds and also chemically useful molecules having diverse biological activities. A large variety of quinoline derivatives have been used as antimalarial (**2-5**) [4], anti-inflammatory (**6**) [5, 6], anticancer (**7-9**) [7], antibacterial (**10, 11**) [8], and antihypertensive (**12, 13**) [9]. In addition to the medicinal importance, multi-substituted quinolines are valuable synthons used for the preparation of nano- and mesostructures with enhanced electronic and photonic properties [10].

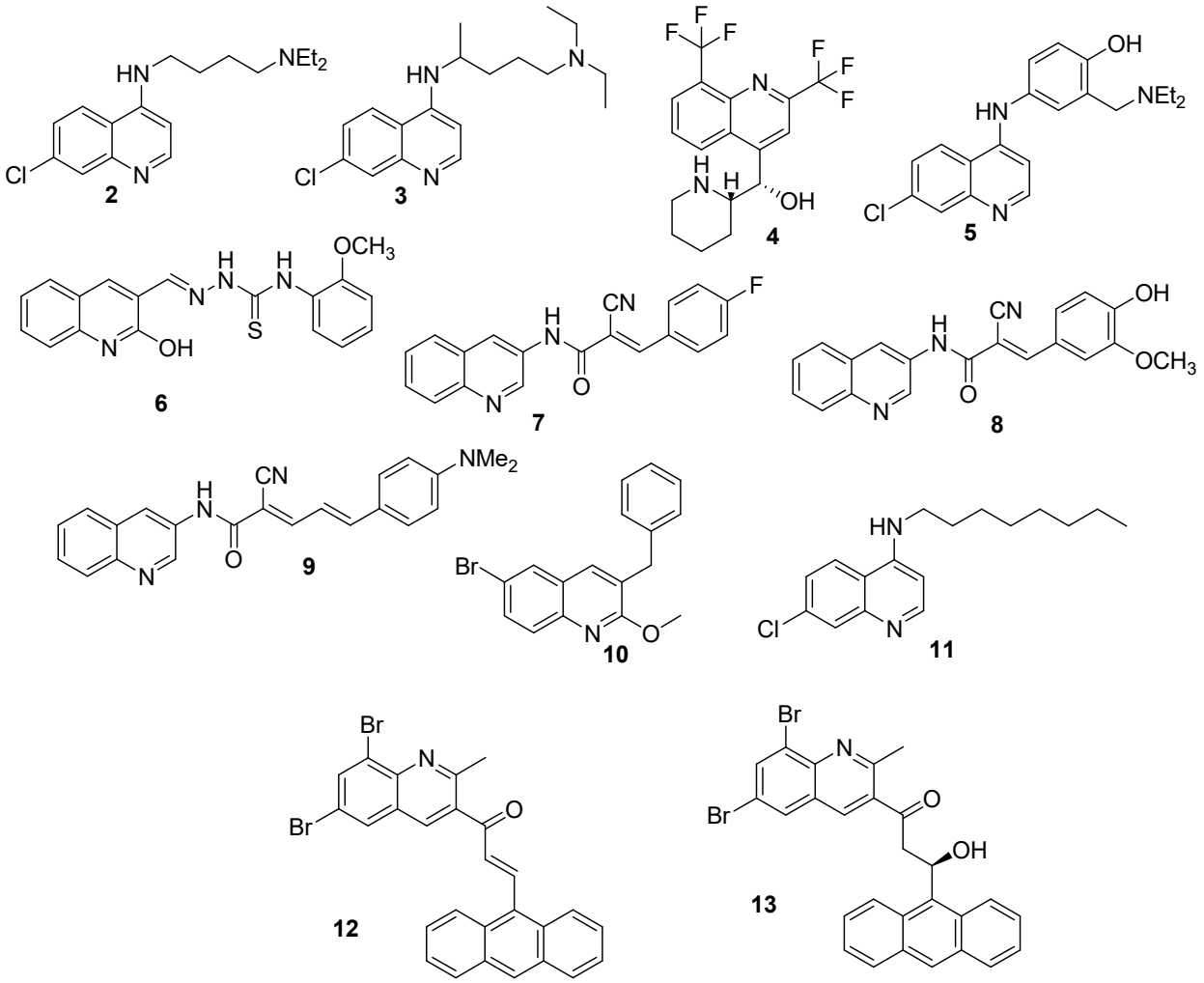

Figure 2: Some structures of bioactive quinoline derivatives.

1.2 Statement of the problem

Recent reports from the World Health Organization (WHO) state that public health has become a major concern due to the population explosion and an increase in endemic and epidemic diseases. Treatment of microbial infection is a major emerging health issue. In spite of the existence of a number of drugs that are used for the treatment of antimicrobial infections, the mortality and morbidity caused by microbes have an alarming worldwide impact on the human population due to the increasing number of multidrug-resistant and the rise of multidrug resistant had made the treatment of microbial infections complicated. Genomic studies on various microorganisms indicate that the prolonged use of antimicrobials and antibiotics makes these

microorganisms more resistant to them. New infectious diseases are discovered every year, including an increase in the numbers of antibiotic-resistant pathogens.

To address this dilemma, it is crucial to develop new compounds with more effective antimicrobial agent with less side effects. The quinoline derivatives have also attracted much attention due to their considerable biological and pharmacological activities. Inspired by these reports, this study was designed to synthesize antibacterial and antioxidant compounds using disk diffusion and DPPH scavenging free radical methods.

1.3 Objectives

1.3.1 General objective

The overall objective of this study is synthesis and evaluation of the antibacterial and antioxidant activities and *in silico* molecular docking analysis of quinoline derivatives.

1.3.2 Specific objectives

- ✓ To synthesize quinoline derivatives through Vilsmeier–Haack reaction.
- ✓ To characterize the synthesized compounds with spectroscopic techniques including UV-Vis and NMR.
- ✓ To evaluate antibacterial activity of the synthesized compound using disk diffusion method against some selected Gram-negative (*E. coli* and *Pseudomonas aeruginosa*) and Gram-positive (*Staphylococcus aureus* and *Streptococcus pyogenes*) pathogenic bacteria.
- ✓ To evaluate antioxidant activity of synthesized compounds using DPPH (1,1-Diphenyl-2-2-picrylhydrazyl) radical scavenging method.
- ✓ To evaluate *in silico* molecular docking analysis of synthesized compounds using the ADT (AutoDock Tools) against *E. coli* DNA gyrase and *topoisomerase IIα.*

1.4 Significance of the study

- ✓ The synthetic methodologies and biological evaluation methods utilized in this project may provide information to conduct further research in the area.
- ✓ This research might bring new drug candidates, which are used to treat various diseases effectively.
- ✓ Attraction of many researchers toward the synthesis of quinoline derivatives.

- ✓ The research may enhance knowledge, confidence, interest and development toward synthesis.

2. **LITERATURE REVIEW**

2.1 Synthesis of quinoline derivatives

The structural core of quinoline has been generally synthesized by various conventional named reactions such as Skraup, Doebner-Von Miller, Friedlander, Pfitzinger, Conrad-Limpach, Combes, Vilsmeier–Haack synthesis and others.

The synthesis of quinolines has been practiced since Koenigs published the first in 1879, in which he passed allylaniline over heated lead (II) oxide [11]. Soon afterwards, in 1880, Czech chemist Zdenko Hans Skraup developed one of the most well-known syntheses of quinolines (**16**): heating anilines (**14**) and glycerol (**15**) with an oxidant in concentrated sulfuric acid (Scheme 1) [12].

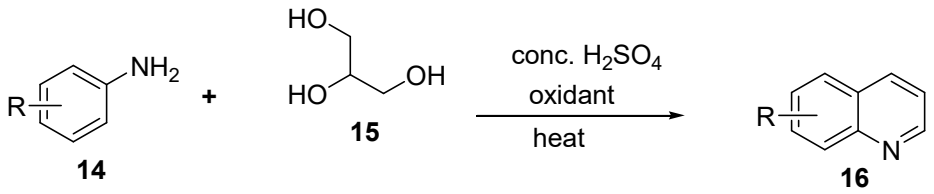

Scheme 1: Classical Skraup quinoline synthesis.

For nearly a century and a half, numerous modifications of the Skraup quinoline synthesis have been developed in an attempt to improve product yield, introduce various functional groups, and minimize harsh reaction conditions. The beginning of the last century saw various attempts at improving the efficiency of this method. In the late 1920s and early 1930s, Essie White Cohn of the University of Denver introduced acetic and boric acid modifications in order to reduce the violence of the reaction [13]. Around the same time, Clarke and Davis introduced the addition of ferrous sulfate; and Darzens, Delaby, and Hiron implemented a thorium-vanadium oxide modification. Employing the generally held belief that acrolein is the active intermediate in the cyclization mechanism, in 1947 Yale reacted this component with 3-nitro-4-aminoanisole in a mixture of concentrated sulfuric acid and arsenic pentoxide [14]. This group also found success with 85% phosphoric acid and arsenic acid in place of the previously used acid catalyst and oxidant [15]. However, none of these modifications completely addressed or alleviated the problems inherent in the method, namely low yield, violent reactions, toxic reagents, and

inconvenient isolation processes [13]. More recently, microwave-assisted Skraup reactions have provided a means of decreasing reaction time and slightly increasing yield, but these methods still required large amounts of sulfuric acid [16] or toxic arsenic oxide as an oxidant [17].

In 1881, Doebner and Von Miller conducted similar quinoline synthesis experiments; they replaced the glycerol component of the reaction with ethylene glycol and produced 2-methylquinoline. They also heated aniline (**14**) with paraldehyde (the cyclic trimer of acetaldehyde) in sulfuric acid and again obtained 2-methylquinoline. Through these experiments they determined that crotonaldehyde was the key reactive intermediate, signifying that the use of any α, β-unsaturated aldehyde or ketone (**17**) as the annulation partner to aniline would similarly result in quinoline (**18**) (Scheme 2) [18].

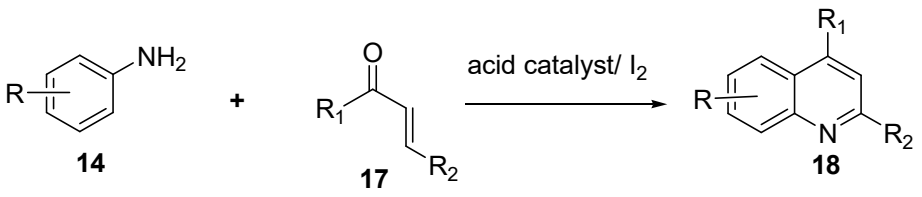

Scheme 2: Doebner-Von Miller quinoline synthesis.

Of the other quinoline (**21**) syntheses regularly performed, the Friedländer reaction is one of the simplest and most well-established [19]. Traditionally, a Friedländer annulation combines a 2-amino aryl carbonyl (**19**) with another carbonyl compound (**20**) containing an active α-carbon; these two components are either refluxed in acid or base or subjected to microwave heating to perform the cyclization (Scheme 3) [19].

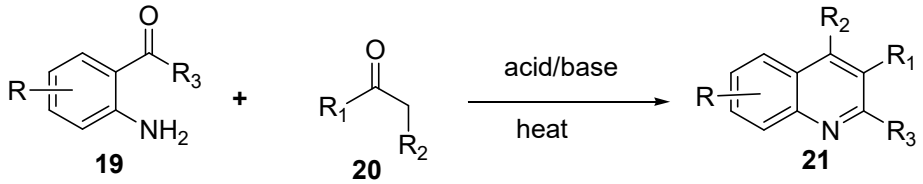

Scheme 3: Friedlander quinoline synthesis.

The synthetic utility of this reaction lies in its remarkable compatibility with a wide variety of functional groups, as long as those groups are stable to the acidic or basic reaction conditions or intense heating. However, this method is not without its limitations. Unsymmetrical ketone

annulation partners exhibit poor regioselectivity, thereby significantly reducing yield of the desired product.

Pfitzinger reaction represents a powerful method in the construction of quinoline-4-carboxylic acids (**24**) by the condensation of isatin (**22**) with carbonyl compound (**23**) (Scheme 4a) [7]. However, its procedure is generally based on strong base and acid in a two-step process, and is unable to form quinoline-4-carboxylic esters. Enaminones, available and versatile synthons in organic synthesis [8], have been extensively used in various transformations for the concise construction of diverse heterocyclic compounds [9]. Recently, Elghamry and coworkers (2016) reported a novel Pfitzinger reaction of *N,N*-dimethylenaminones (**25**) and isatins (**22**) to synthesize quinoline-4-carboxylic acids (**26**) (Scheme 4b) [10]. Interestingly, Pan Zhou *et al.,* (2018) reported a novel synthesis of pyrroloquinolines (**27**) through cascade cyclization of isatins and *N,N*-dimethylenaminones in the presence of amines under different catalytic system, respectively (Scheme 4c) [20]. Inspired by the above-mentioned synthesis of quinoline derivatives based on isatins and *N,N*-dimethylenaminones, and our ongoing interest in improved Pfitzinger reaction [21] and enaminone chemistry [22], Pan Zhou *et al.,* pursued a one-step protocol Pfitzinger reaction that could be used to construct quinoline-4-carboxylic esters/acids (**28**) from isatins and *N,N*-dimethylenaminones in alcohols/water promoted by TMSCl (Scheme 4d) the 61-82% yields were produced [20].

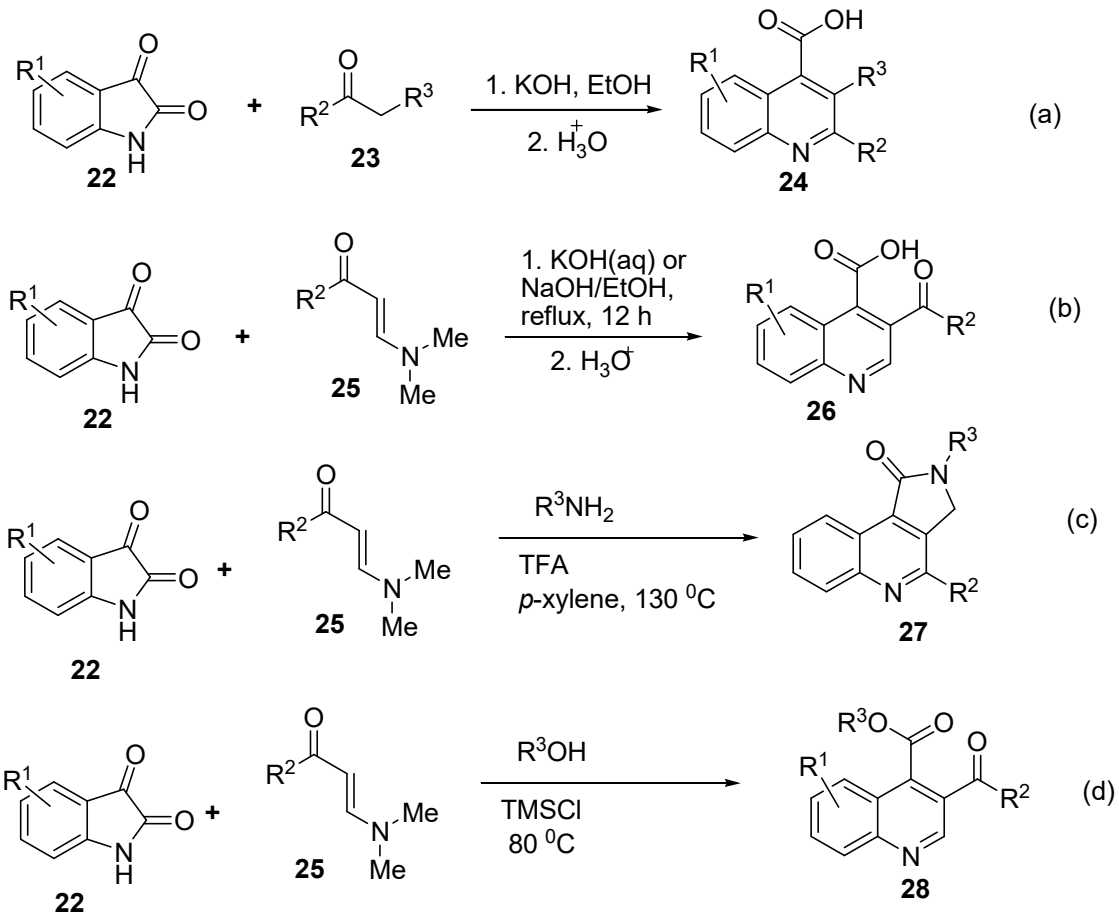

Scheme 4: The classic Pfitzinger reaction and synthesis of quinolines based on isatins and *N,N*-dimethylenaminones.

One the other quinoline syntheses regularly performed is Conrad–Limpach synthesis from aryl amines (**14**) and *β*-ketoesters (**29**) are combined under thermal conditions to form quinoline-4-ols (**30**) (Scheme 5). Although this is considered a universal process [23], it presents several challenges

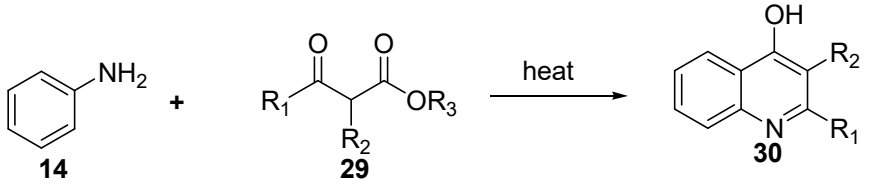

Scheme 5: Conrad–Limpach quinoline syntheses.

The original solvent-free method was relatively inefficient, however the high-energy imine-enol intermediate compulsory for cyclization necessitated any solvent added to the mixture to be

high-boiling. The mineral oil, diphenyl ether, and Dowtherm (mixture of diphenyl with diphenyl oxide). A commonly used as solvents are either prohibitively expensive or difficult to remove from the product [23, 24].

The Combes quinoline synthesis is a chemical reaction, which was first reported by Combes in 1888. It involves the condensation of unsubstituted anilines (**14**) with β-diketones (**31**) to form substituted quinolines (**18**) (Scheme 6) after an acid-catalyzed ring closure of an intermediate Schiff base [25].

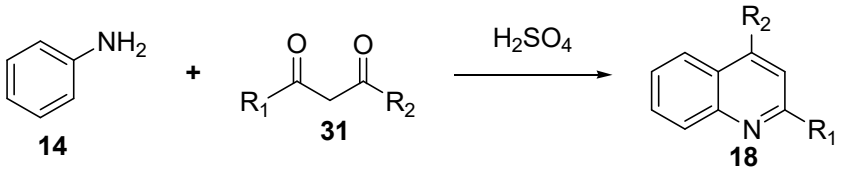

Scheme 6: Combes quinoline syntheses.

The Combes quinoline synthesis is often used to prepare the 2,4-substituted quinoline (**18**) backbone and is unique in that it uses a β-diketone substrate (**31**), which is different from other quinoline preparations, such as the Conrad-Limpach synthesis and the Doebner reaction.

Kubba *et al*., (2016) showed a synthesis of novel series of quinoline derivative compounds, which have been synthesized by cyclization of ethyl *p*-aminobenzoate (**32**), formaldehyde (**33**), and pyruvic acid (**34**) which affords, 6-(ethoxycarbonyl) quinoline-4-carboxylic acid (**35**) with 71% yield (Scheme 7) [21].

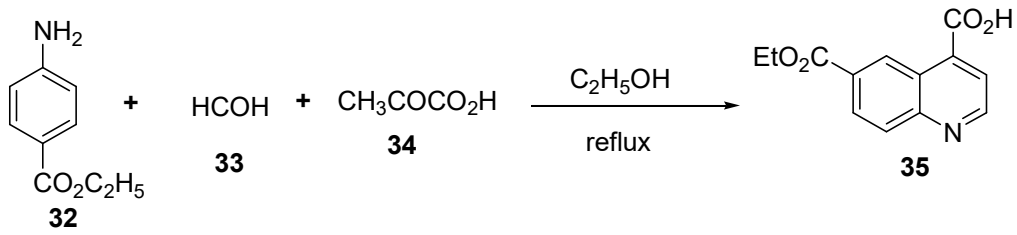

Scheme 7: Synthesis of 6-(ethoxycarbonyl) quinolone-4-carboxylic acid.

Thomas *et al*., (2010) reported the title derivative compounds were synthesized by a series of reactions as shown in Scheme 10. The intermediate, 3-(4-methoxy-phenyl-amino)-but-2-enoic acid ethyl ester (**37**) was synthesized from corresponding 4-methoxyaniline (**36**) by treating it with ethylacetoacetate in presence of magnesium sulfate in ethanol at 90 ^{0}C. The intermediate **37**

was then converted to 6-methoxy-2-methylquinolin-4-ol (**38**) by heating it at 270 ^{0}C using Dowtherm for 20 min. The required key intermediate 4-azido-6-methoxy-2-methylquinoline (**40**) was obtained by heating the compound **38** with phosphorous oxychloride, followed by treating the chloro derivative **39** with sodium azide in presence of 1:1 aqueous ethanol as solvent. The conversion of chloro intermediate **39** to an azide compound **40** was carried out in an autoclave by heating to 100 ^{0}C and maintaining the reaction for 12 h. The title derivatives of compound **41** in (Scheme 8) were then synthesized by sequential one pot reaction of intermediate **40** with propargyl bromide and different primary and secondary amines in presence of triethylamine and copper iodide [26].

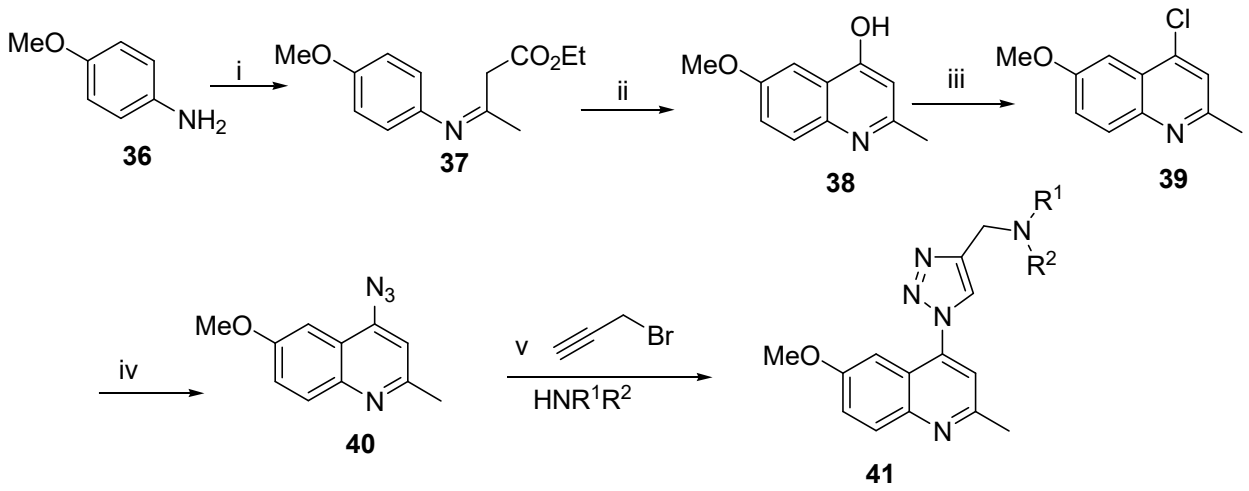

Scheme 8: 1-[1-(6-methoxy-2-methylquinolin-4-yl)-1H-1,2,3-triazol-4-yl] methanamine derivatives. Reagents and conditions: (i) Ethylacetoacetate, EtOH, $MnSO_4$, 90 ^{0}C, 5 h (ii) Dowtherm, 270 ^{0}C, 20 min (iii) $POCl_3$, 105 ^{0}C, 2 h (iv) sodium azide, EtOH/H_2O, 100 ^{0}C, 12 h. (v) Propargyl bromide, CuI, substituted amines, THF/H_2O (1:1), reflux, 2h.

Aghera *et al*., (2008) used Vilsmeier–Haack reagent to produce quinoline derivatives at moderate reaction conditions. The synthesized *p*-substituted acetaniline compounds (**43**) starting from *p*-substituted aniline (4**2**) and acetic anhydride in ethanol. A *p*-substituted acetaniline compounds treated with Vilsmeier–Haack reagent to produce quinoline derivatives (**44**) in scheme 9 [22].

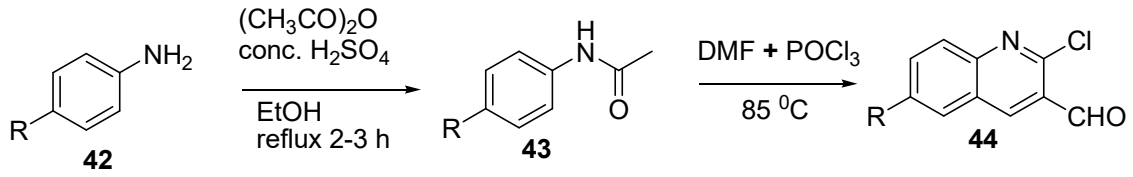

Scheme 9: Synthesis of 6-substituted 2-chloroquinoline-3-caraldehydes.

Pankaj B. A. *et al.,* (2013) have been reported the novel series synthesize of 2-Chloroquinoline nucleus clubbed with the pyrazole ring [27]. The synthesis of 2-chloroquinoline-3-carbaldehyde derivatives (**44a-c**) [28] from acetanilide derivatives, **43a–c** was dissolved in dimethylformamide and to this solution phosphorus oxychloride was added gradually at 0°C. The reaction mixture was taken in a round bottom flask equipped with reflux condenser and refluxed for 5–6 h on oil bath at 80–90°C. The solution was cooled to room temperature and then poured on ice water the products in scheme 10 [29]. The synthesis of 2-chloroquinoline chalcones (**46a-f**) [30] from 2-chloroquinoline-3-carbaldehyde derivatives, 40% sodium hydroxide solution and methanol in an ice-bath and substituted acetophenone (**45**) for 24 h at room temperature. At the end of the period, the reaction mixture was poured in ice cold water, neutralized with dilute hydrochloric acid and the resultant solid was filtered, dried to give titled compounds **46a–f**. Scheme of synthesis of 2-chloroquinoline chalcones is described in scheme 11 [29]. The synthesis of 2-chloroquinoline pyrazole derivatives [31] from a mixture of compounds **46a–f**, hydrazine hydrate and AcOH was placed into an open Pyrex-glass vessel. The above mixtures were subjected to microwave irradiation with magnetic stirring for 5–7 min and with a maximum power of 300 W. The reaction mixture was poured in ice cold water and yield compounds (**47**). Scheme of synthesis of 2-chloroquinoline pyrazole derivatives is described in scheme 12 [29].

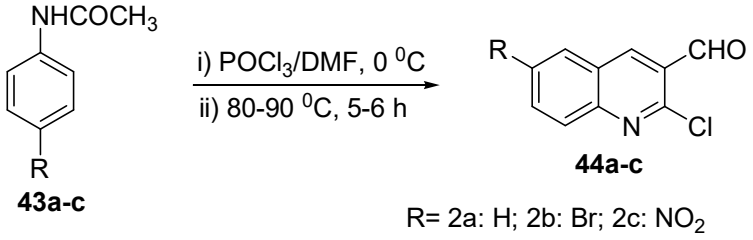

Scheme 10: Synthesis of compounds **44a-c**.

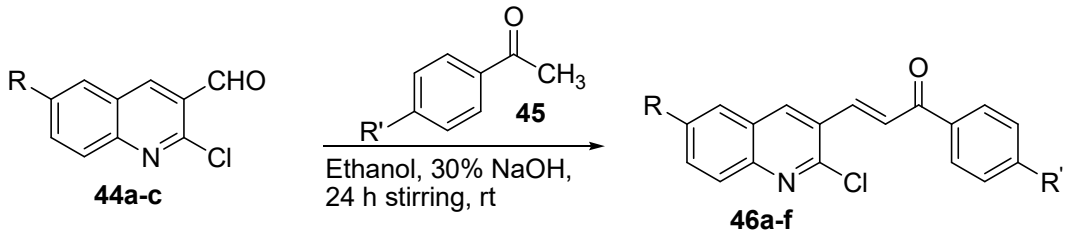

Compound code	R	R'
46a	H	H
46b	H	Br
46c	H	F
46d	H	NH_2
46e	NO_2	Br
46f	Br	Br

Scheme 11: Synthesis of compounds **46a-f**.

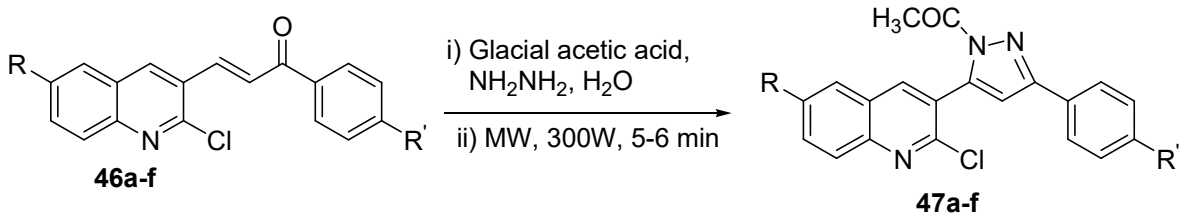

Scheme 12: Synthesis of compounds **47a-f**.

Bakr F *et al.,* (2013) reported the synthesis of quinoline derivatives (**49)** from acetanilide and acetoacetanilide (**48**) *via* Vilsmeier–Haack reaction (Scheme 13a). It was reported that one-pot synthesis of pyrido[2,3-*b*]quinolin-2-ones (**50**) in moderate yields (22–59%) was archived by treatment of substituted acetanilide with DMF and $POCl_3$, to produce compound **49**; to this reaction mixture a secondary amide was added in $POC1_3$ solution containing one drop of DMF, and the mixture was heated for a further 2-3 h at 75 ^{0}C (Scheme 13b) [32]. 3-Formylquinoline-2(1*H*)-thione (X = S) and -seleno I (X = Se) **51** have been prepared from reaction of **49** with NaXH (X = S, Se). Compounds **51** reacted with primary amine to produce Schiff's bases **52** (Scheme 13c) [32, 33].

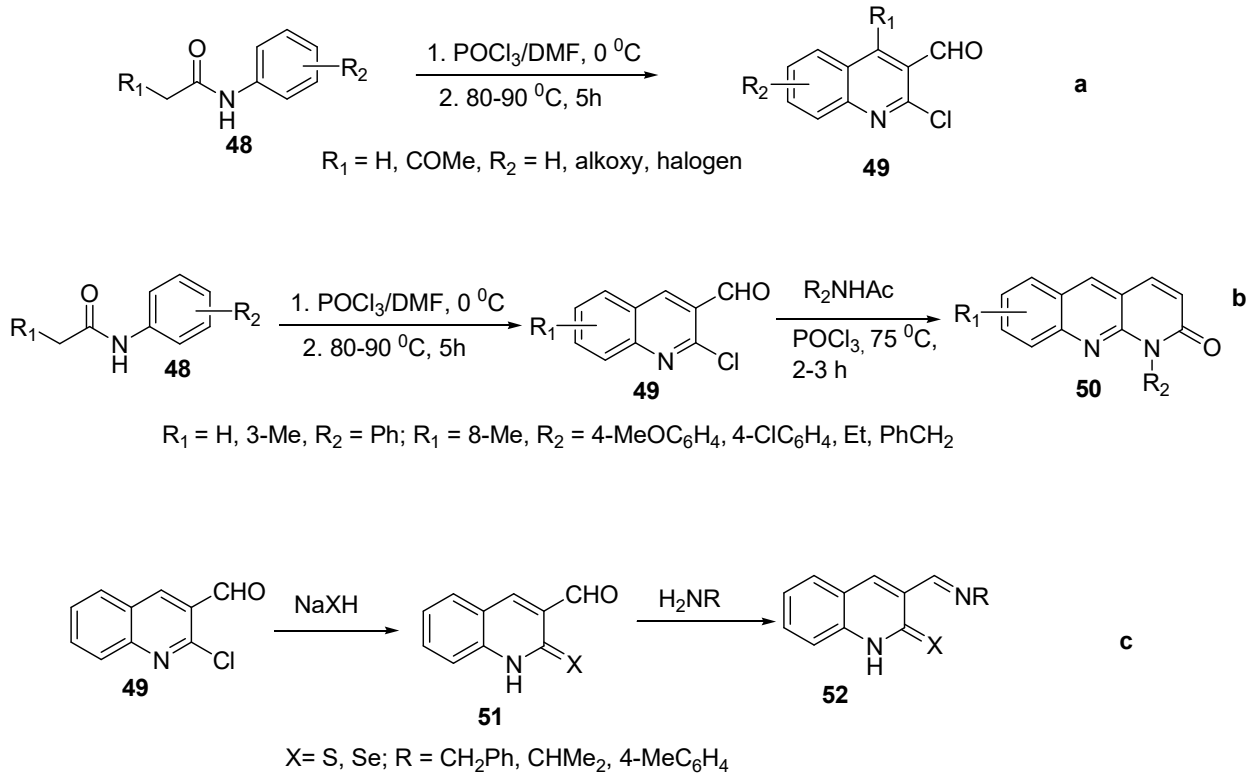

Scheme 13: Synthesis of quinoline derivatives from acetanilide and acetoacetanilide.

Reaction of compound **53** with acetic acid at reflux temperature leads to formation of quinoline **54** which was condensed with ethyl bromoacetate (**55**) to give ethyl 6-methylfuro [2,3-**b**] quinoline-2-carboxylate **56** (Scheme 14a) [32]. 2*H*-Pyrano[2,3-**b**] quinolin-2-ones **59** were prepared in 46–95% by treating compound **53** with HCl to give quinolines **57***,* which reacted with malonic acid in ethanol in the presence of pyridine and piperidine followed by cyclization in polyphosphoric acid [32, 34]. In a similar manner the related cyanoacrylic acid (**60**) and its ethyl ester (**60**) with compound **61** both gave pyranoquinoline-3-carboxylic acid **62** in 90% yield on treatment with PPA (Scheme 14b) [32].

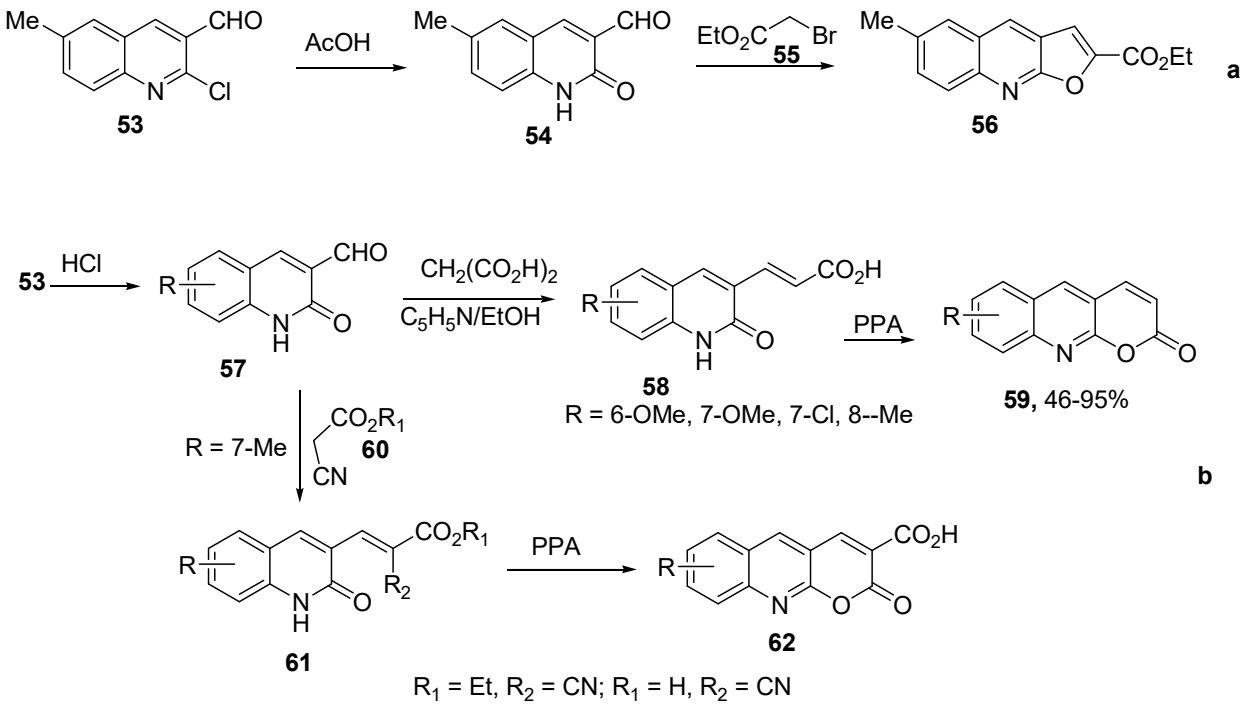

Scheme 14: Synthesis of quinoline derivatives from 2-chloro-6-methylquinoline-3-carbaldehydes.

Preparation of pyrazolo[3,4-*b*]quinolines **66** as antiviral agents was reported by treatment of compound **63** with hydroxylamine in EtOH to give oxime **64**. Stirring a solution of **64** and $SOCl_2$ in DMF at 0∘C yielded nitrile **65** which was refluxed with hydrazine in EtOH to give target compounds, which showed MIC of 1.5 μg/mL against herpes simplex virus type 2 and vasodilator activity with an EC_{50} of 31 Mm (Scheme 15) [32].

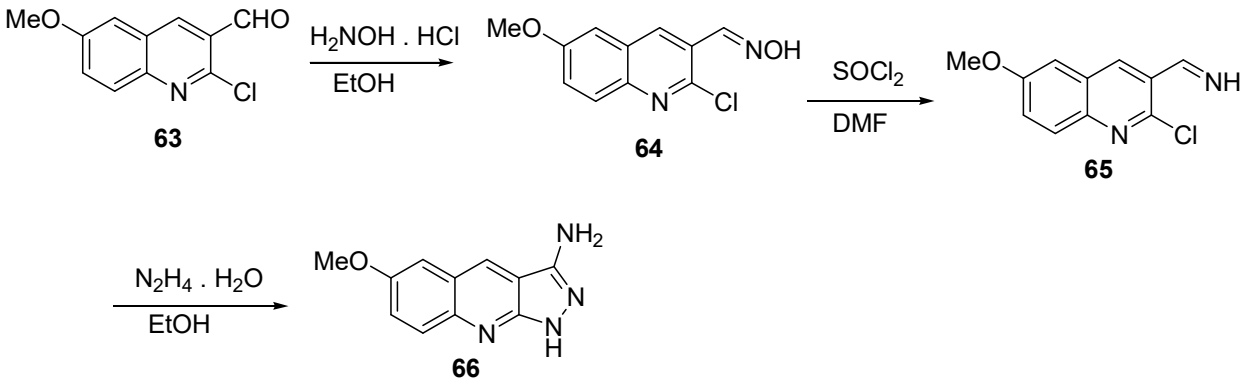

Scheme 15: Synthesis of 6-methoxy-1H-pyrazolo[3,4-b] quinolin-3-amine.

Sujeet K. G. and Ashutosh M. (2016) reported the synthesis of 3-chloro-1-(substituted)-4-(tetrazolo [1,5-a] quinolin-4-yl) azetidin-2-one derivatives (**70a-l**) in scheme 16 starting with acetanilide (**43**). Initially, acetanilide (**43**) was allowed to react with Vilsmeier-Haack reagent (DMF + $POCl_3$) to form 2-chloro-3-formyl quinoline (**49**). The 2-chloro-3-formyl quinoline (**49**) was further treated with *p*-toluenesulphonic acid and sodium azide which yielded Tetrazolo [1,5-1]quinoline-4-carbaldehyde (**67**). The reaction of formyl group with various substituted amines (**68a-l**) formed corresponding Schiff base intermediates (**69a-l**), which were further allowed to react with chloroacetyl chloride to produce 3-chloro-1-(substituted)-4-(tetrazolo [1,5-a]quinolin-4-yl) azetidin-2-one derivatives (**70a-l**) [5].

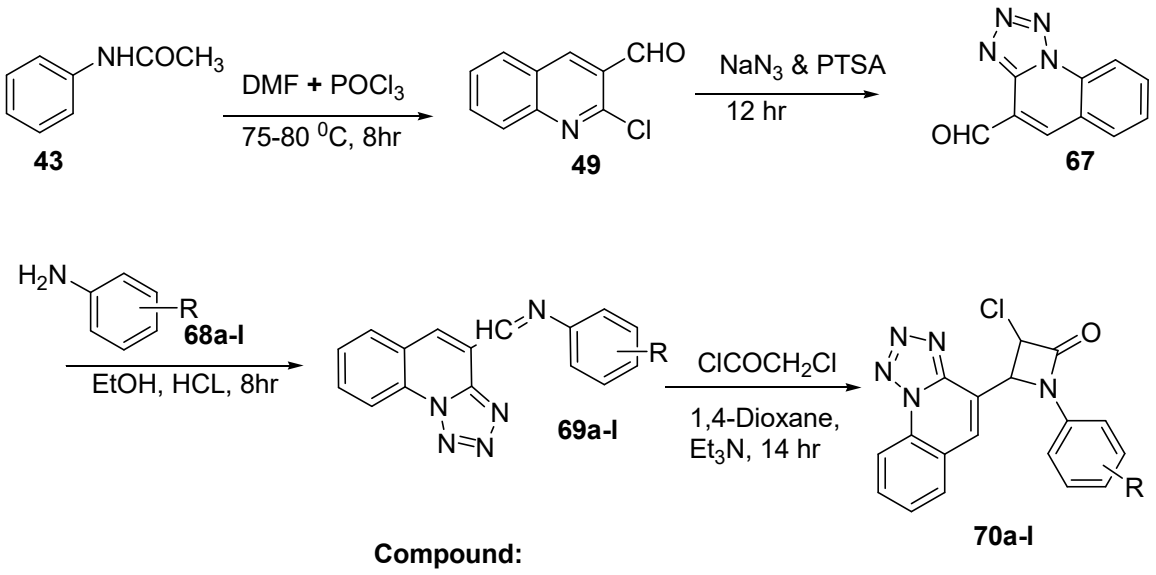

Scheme 16: Synthetic protocol of compounds (**70a-l**).

Digafie Z. *et al.,* (2020) reported synthesis of 2-Chloroquinoline-3-carbaldehyde derivatives (**72, 73, 74, 75, and 78**) (Scheme 17) and 2-chloro-8-methylquinoline-3-carbaldehyde (**82, 83 and 84**) (Scheme 18) derivatives were synthesized through Vilsmeier formulation of acetanilide (**43**) and N-(o-tolyl)acetamide (**80**). In the process, N-(o-tolyl)acetamide (**80)** and acetanilide (**43**) were prepared by refluxing the corresponding aniline (**14**) in acetic acid and acetic anhydride (**71**) mixtures. Then 2-chloroquinoline-3-carbaldehyde (**49**) and 2-chloro-8-methylquinoline-3-carbaldehyde (**81**) were prepared from the acetanilide (**43**) by the Vilsmeier approach. The chlorine in position 2 of quinolines was substituted by various nucleophiles by refluxing 2-

chloroquinoline-3-carbaldehyde (**49**) and 2-chloro-8-methylquinoline-3-carbaldehyde (**81**) in *N,N*-dimethylformamide with various nucleophilic reagents in basic medium. Potassium carbonate was used to induce the basic medium. Refluxing 2-chloro-8-methylquinoline-3-carbaldehyde (**81**) in 6M HCl and acetic acid (1:1) mixture afforded 8-methyl-2-oxoquinoline-3-carbaldehyde (**82**). The carbaldehyde functional group of quinoline was oxidized to carboxylic acid by permanganate method and was subsequently reduced to alcohol using metallic sodium. The overall sequence of reactions used in the synthesis of various targeted quinoline derivatives are illustrated in Schemes 17 and 18 [35, 36].

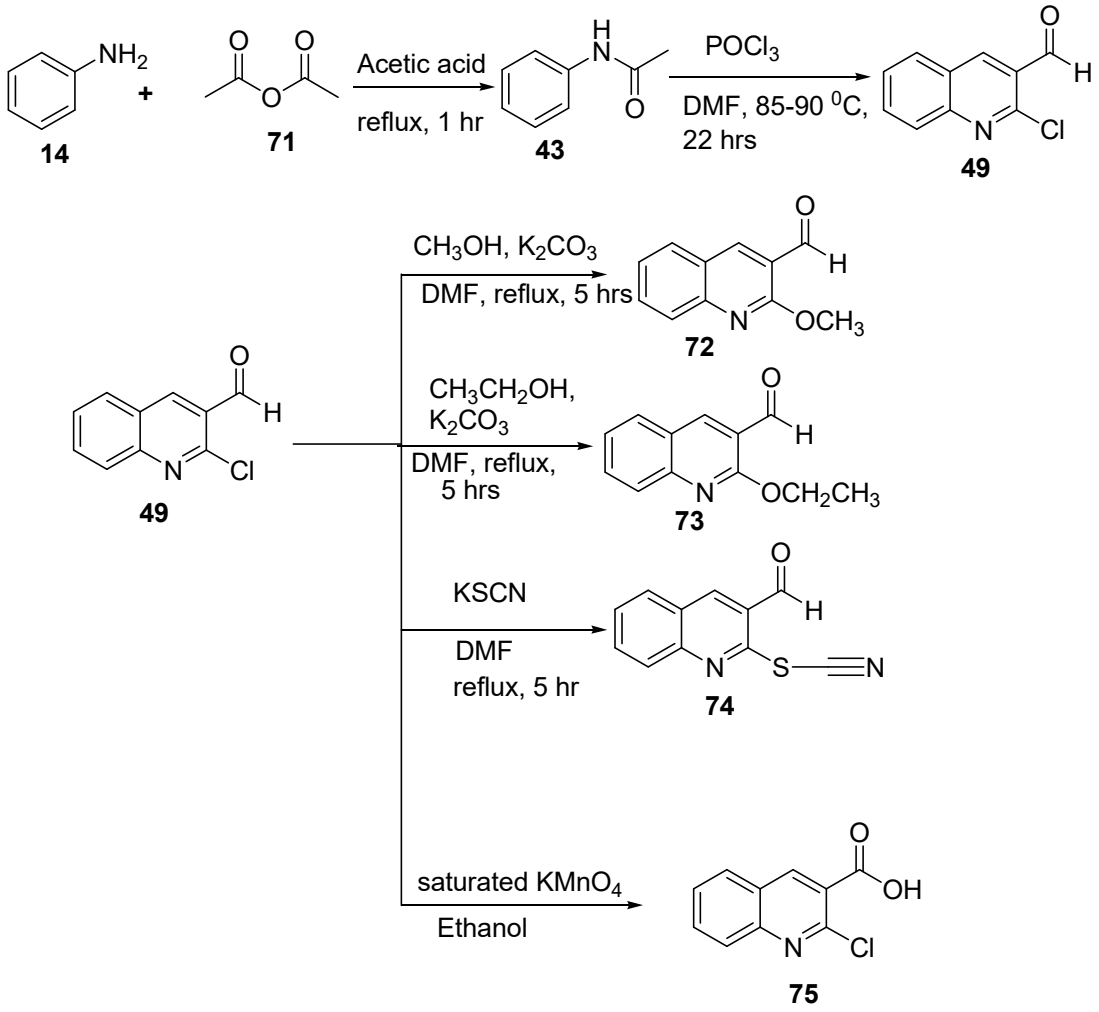

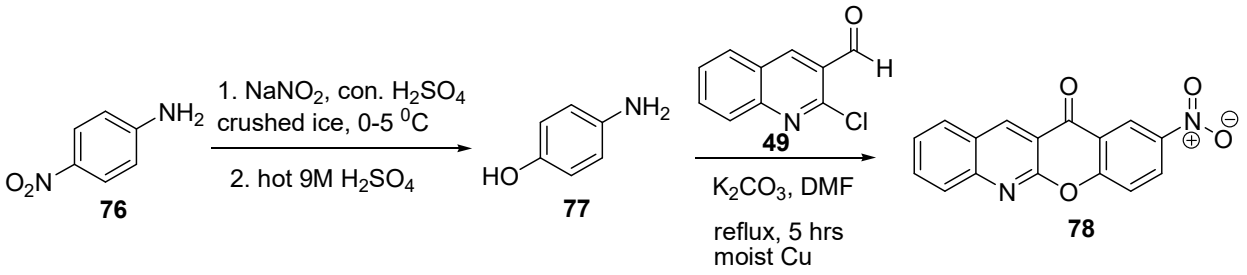

Scheme 17: Synthesis of 2-chloroquinoline-3-carbaldehyde and its derivatives.

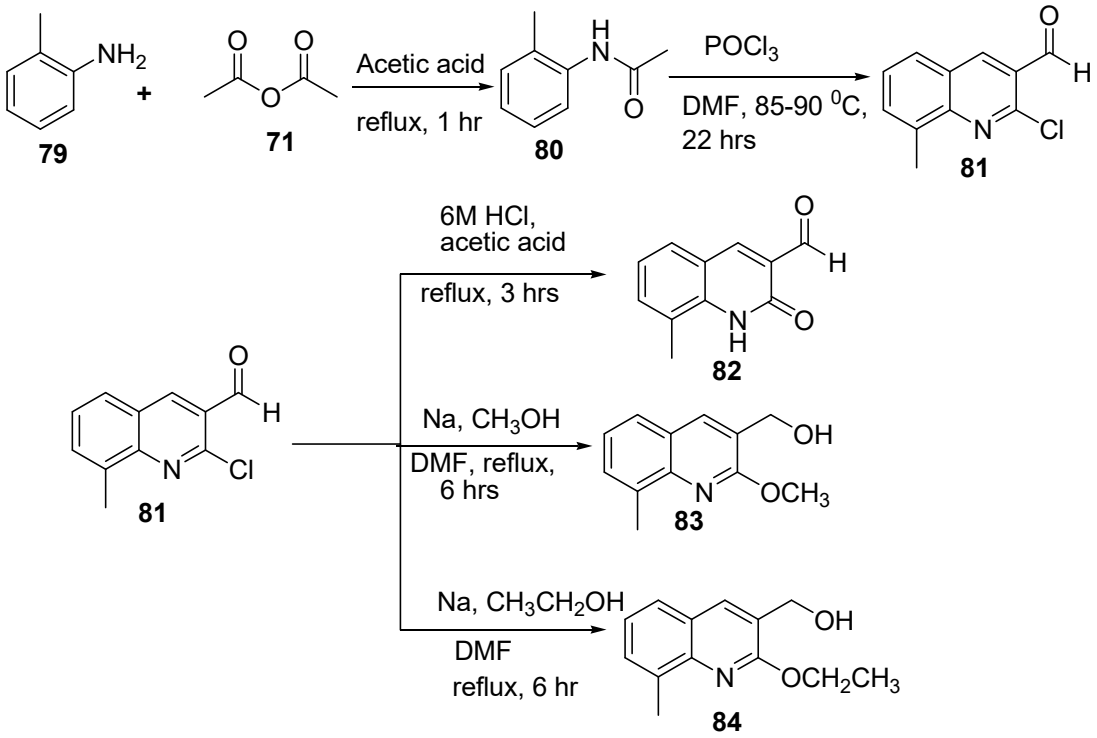

Scheme 18: Synthesis of 2-chloro-8-methylquinoline-3-caraldehyde and its derivatives.

Jayakumar Swamy B.H. *et al.,* (2012) reported the synthesis of 3-formyl 2-hydroxy quinoline thiosemicarbazides (**87**) (Scheme 19) from DMF, phosphorus oxychloride and acetanilide (**43**) through Vilsmeier reaction the 2-chloro-3-formyl quinoline (**49**) was formed. The 2-chloro-3-formyl-quinoline (**49**) and aqueous hydrochloric acid was heated under reflux for 1 hr and then allowed to cool to room temperature then the reaction mixture was poured on to crushed ice when 3-formyl 2-hydroxy quinoline (**85**) separated as yellow solid. The 3-formyl-2-hydroxy quinoline compound was heated with a solution of the 4-aryl substituted thiosemicarbazide (**86**) in ethanol or methanol containing a few drops of glacial acetic acid the mixture was refluxed for

2-3 hours and then concentrated. The crude product was purified by recrystallization from aqueous DMF to get a pure crystalline compound [6, 37].

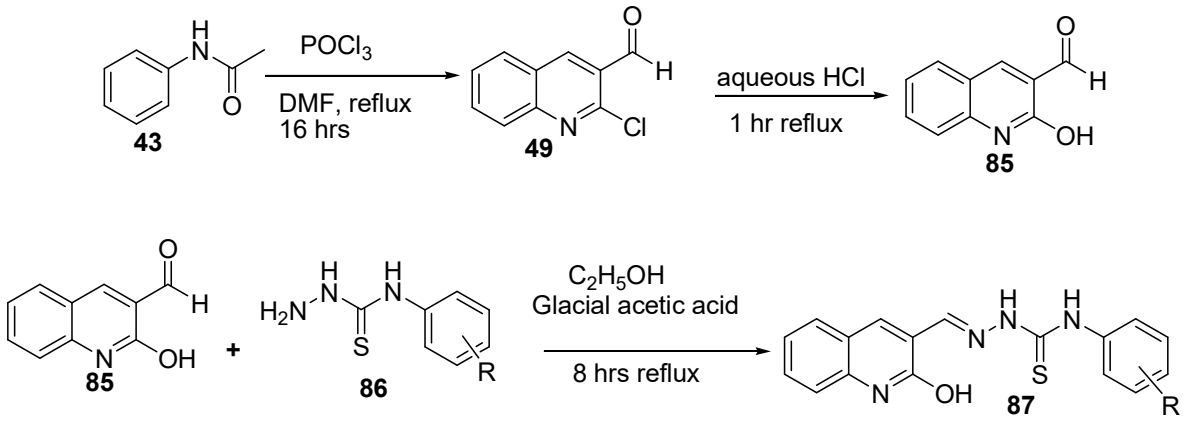

Scheme 19: Synthesis of 3-formyl 2-hydroxy quinoline thiosemicarbazides.

In order to generate a diverse array of analogues, a convergent synthesis was visualized, whereby the targeted hydrazide-hydrazone structure could be formed by an amide-coupling reaction between an alkyl carboxylic acid and aryl hydrazone (Scheme 20). The alkyl acids **88–91** were prepared following literature methods [38]. Similarly, the substituted 2-chloroquinoline-3-carbaldehydes **92–94** were isolated in yields of 47%–60% following Vilsmeier cyclisation of the corresponding acetanilides **95–97** with Vilsmeier reagents (Scheme 20). Following aqueous work-up, carbaldehydes **92–94** were then treated with neat hydrazine hydrate at room temperature in ethanol to generate the quinoline hydrazones **98–100** in 74%–87% yields (Scheme 20). Finally, the desired hydrazide-hydrazones **101–106** were obtained by EDC coupling of the hydrazones (**98-100**) to the appropriate carboxylic acids **88-91** using 1-ethyl-3-(3-dimethylaminopropyl)-carbodiimide hydrochloride (EDC), which gave hydrazide-hydrazones **101**–**106** in yields of 62%–68% (Scheme 20) [39].

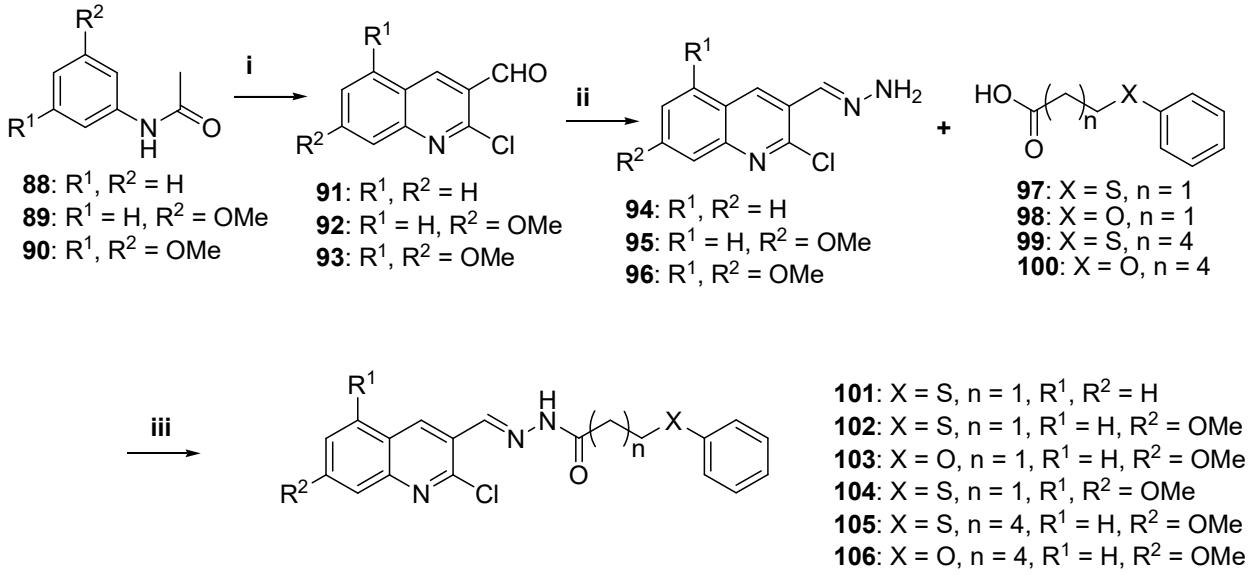

Scheme 20: Synthesis of quinoline-based hydrazide-hydrazones. Reagents and conditions: (i) DMF, $POCl_3$, 90 ^{0}C, 12 h; (ii) NH_2NH_2. H_2O, EtOH, rt, 18 h; (iii) EDC, DMF, Et_3N, rt, 18 h.

2-Chloroquinoline-3-carboxylic acid was prepared by oxidation of **49** using silver nitrate in the presence of sodium hydroxide [40]. Esterification of the carboxylic acid derivative **75** using absolute ethanol and sulfuric acid afforded the ester derivative **107**, in a good yield, followed by subsequent hydrazinolysis in boiling ethanol to afford 2-chloroquinoline-3-carbohydrazide **108.** The later compound **108** was subjected to react with carbon disulfide in ethanol in the presence of KOH under reflux followed by acidification by using diluted hydrochloric acid to give 5-(2-chloro-quinolin-3-yl)-1,3,4-oxadiazole-2-thiol (**109**) (Scheme 21) [41].

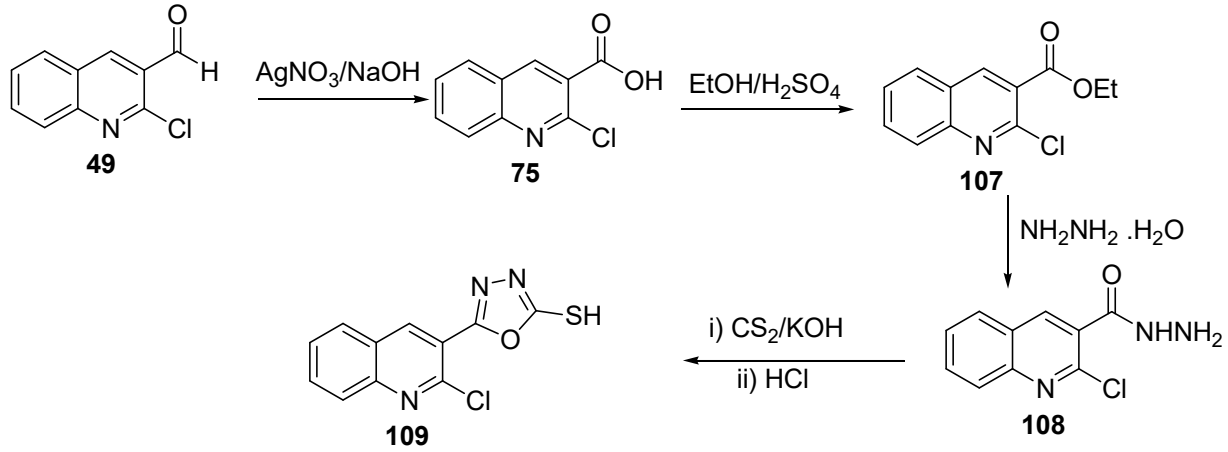

Scheme 21: Synthesis of quinoliny 1,3,4-oxadiazole (**109**).

2.2 Biological activities

2.2.1 Antimalarial activity

Antimalarials are classified based on their activities against the malaria life stages within the human host. This classification includes [42] (Figure 3): The tissue schizontocidal drugs which can be classified as causal drugs and they hinder erythrocytic stages are primaquine **110**, which also prevent a relapse caused by hypnozoites of Plasmodium vivax and Plasmodium ovale in the liver; hypnozoitocidal drugs act against exo-erythrocytic hypnozoites of Plasmodium vivax and Plasmodium ovale such as primaquine; blood schizontocidal drugs act on the blood forms of the parasite thereby eliminating clinical attacks of malaria. These include quinine (**111**), chloroquine (**112**), mefloquine (**113**). Gametocytocides such as primaquine, chloroquine and quinine prevent gametocyte forms in the blood, thereby hindering mosquito infection and sporontocides such as primaquine hinder the development of oocyst and multiplication of the parasites in the mosquito gut when it takes a blood meal from the human host [43].

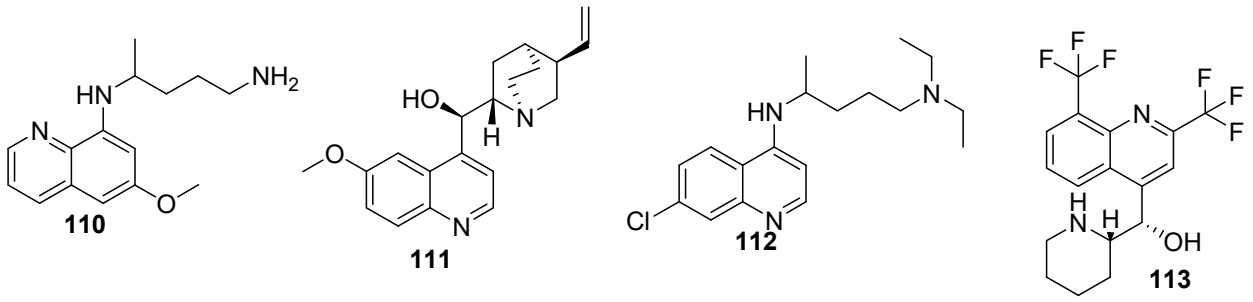

Figure 3: Examples of antimalarials classified based on their activity against malaria life stage.

Antimalarial drugs are also classified based on their structures into groups such as 4-aminoquinolines, like chloroquine and amodiaquine (**114**)*;* 8-aminoquinolines such as primaquine; 4-quinolinemethanols, e.g., mefloquine; quinoline-containing cinchona alkaloids, e.g., quinine and quinidine (**115**). [42, 43] (Figure 4). Each of these classes has its own unique mode of action and mechanism of resistance against the malaria parasite.

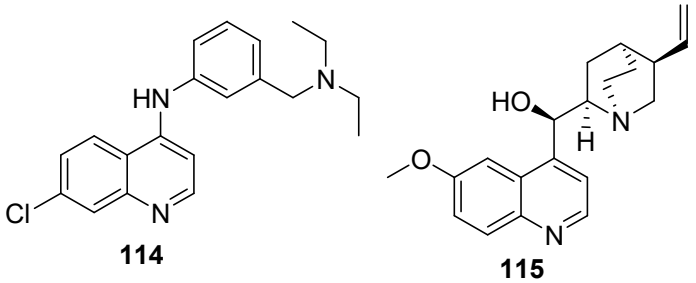

Figure 4: Examples of antimalarials classified based on their structure.

2.2.2 Antiinflammatory activity

The quinoline ring system is ubiquitous in the areas of medicinal chemistry [12]. Several promising anti-inflammatory [44] agents that have been recently developed contain the quinoline scaffold. Some example of quinoline scaffold including compound **116** [44] and compound **117 [**45] (Figure 5) were used as anti-inflammatory agents.

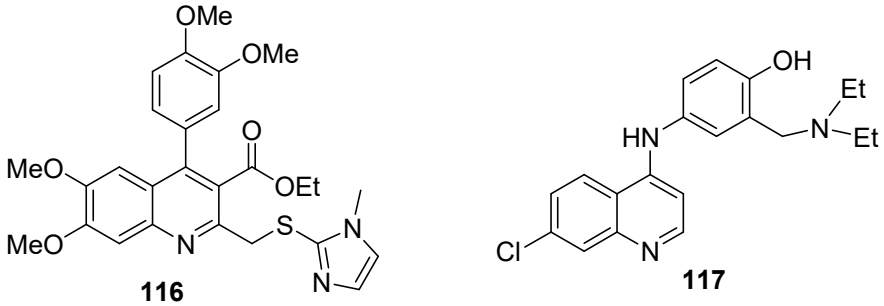

Figure 5: Structure of compounds used for anti-inflammatory activity.

2.2.3 Anticancer activity

Quinoline is a pharmacologically valuable scaffold that is prevalent in a variety of biologically active synthetic and natural compounds. Throughout the 20th century, the chemistry of quinolines has been the subject of intense study and different interesting bioactivity [39, 46]. This anticancer activity is quite broad, with quinoline derivatives having been used against many cancers, such as those of the breast, prostate, gastrointestinal tract, colon and liver [39,47,48,]. Importantly, a number of quinoline-based anticancer drugs have also been used clinically, including camptothecin (**118**) and its analogues (irinotecan (**119**) and topotecan (**120**)) [39] and bosutinib (**121**) (Figure 6) [39, 49, 50].

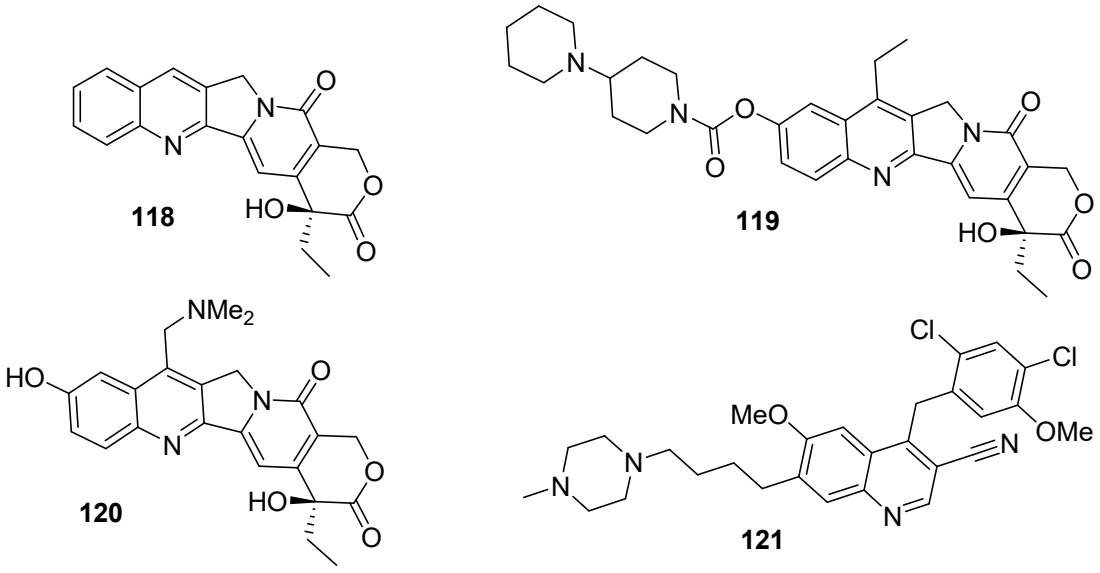

Figure 6: Structure of quinolone-containing anticancer drugs.

2.2.4 Antibacterial activity

Fluoroquinolones are classified in four generations basis of their spectrum of activity and their pharmacokinetic profile. First generation including; Naldixic acid, Oxolinic acid and Pipemidic acid which were active against some Gram negative bacteria, highly protein bound drugs and short half-life. Second generation including; Norfloxacin, Enoxacin, Ciprofloxacin, Ofloxacin and Lomefloxacin were protein binding (50%), longer half-life than previous agents and improved activity against Gram negative bacteria. Third generation including; Temafloxacin, Sparafloxacin, and Grepafloxacin were active against Gram negative bacteria and Gram positive bacteria. Fourth generation including; Gatifloxacin (**122**), Moxifloxacin (**123**), Trovafloxacin (**124**), and Clinafloxacin (**125**) (Figure 7) were Show extended activity against both strains of bacteria [51].

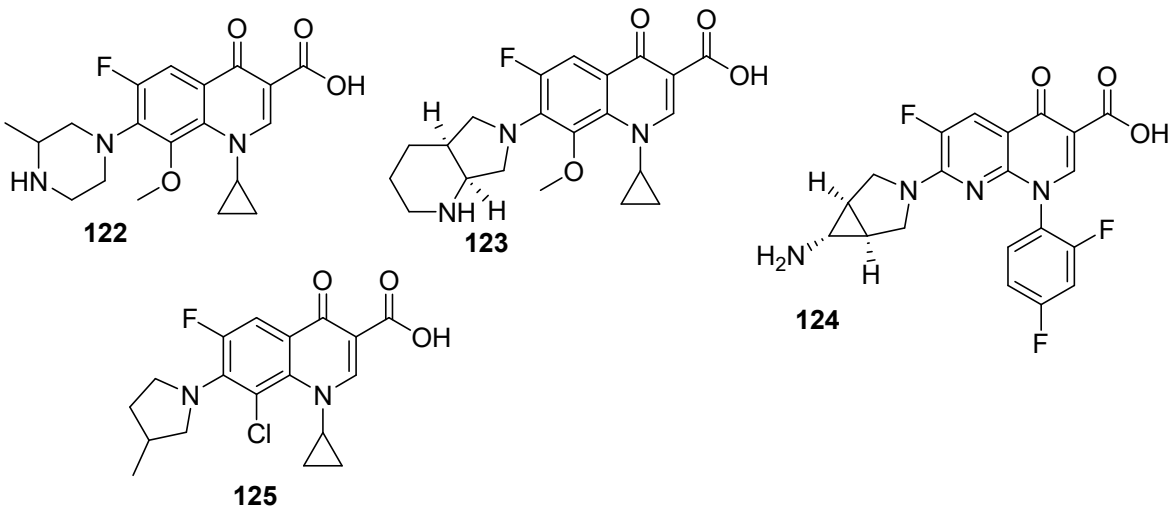

Figure 7: Some structure of quinolone derivatives containing antibacterial activity.

3. MATERIAL AND METHODS

3.1 General

Thiele tube was used to check melting points. Column chromatography was performed on normal silica gel. Thin Layer Chromatography (TLC) was done using silica gel 60 F254 (Merck) precoated plates. NMR analyses were carried out on Bruker avance 400 MHz spectrometer using $CDCl_3$, MeOD-*d4* and DMSO-*d6* as a solvent at the Chemistry Department of Addis Ababa University. All chemicals were purchased from Loba Chemie PVT, Ltd.

3.2 Chemicals, Reagents and Equipment

The chemicals and reagents used in this study are aniline, *m*-chloroaniline, acetic anhydride, glacial acetic acid, *N, N*-dimethylformamide, potassium carbonate, sodium azide, phosphorus oxychloride, zinc powder, calcium chloride, dichloromethane, magnesium sulfate anhydrous, sulfuric acid, n-hexane, ethyl acetate, ethanol and methanol. All these necessary analytical chemicals and reagents were purchased from Fine chemicals PLC, Ranchem industry and trading and scientific chemical supplier, Addis Ababa, Ethiopia. Some of the apparatus used are funnels, round bottom flasks, vials, glass wares, refrigerator, Whatmann No.1 filter papers, drying oven, measuring cylinders, TLC Chamber, condenser, electronic balance, dropper, shaker, beakers, capillary tubes, hot plate, Thiele tube etc.

3.3 Methods

3.3.1. Synthesis of acetanilide. In 250 mL round flask, aniline (25 mL), acetic anhydride (25 mL), zinc powder (0.2 g), and acetic acid (25 mL) were added. The mixture was boiled under reflux using water condenser for 2 hours. Then, it was cooled to room temperature and poured into 300 mL of crushed ice water. The solid product was collected by suction filtration. White crystal; yield 89%, mp 112–113 ^{o}C (Lit. mp 114.3 ^{o}C) [37].

3.3.2. Synthesis of 3-chloroacetanilide. In 250 mL round flask, 3-chloroaniline (25 mL), acetic anhydride (25 mL), zinc powder (0.2 g), and acetic acid (25 mL) were added. The mixture was boiled under reflux using water condenser for 2 hours. Then, it was cooled to room temperature

and poured into 300 mL of crushed ice water. The solid product was collected by suction filtration. White crystal; yield 91%, mp 72–74 ^{o}C (Lit. mp 76 ^{o}C) [29].

3.3.3. Synthesis analytical data of 2-chloroquinoline-3-carbaldehyde

N,N-dimethylformamide (21.1 mL, 0.27 mol) was added to a 250 mL round-bottom flask guarded with drying tube; it was cooled to 0 ^{o}C using ice bath. Then, phosphorus oxychloride (60 mL, 0.64 mol) was added dropwise to it from separatory funnel guarded by drying tube while being stirred by magnetic stirrer. This addition was done for 30 minutes. Then 3-chloroacetamide (12.34 g, 0.09 mol) was added to it. After 5 minutes, the dropper funnel was replaced by air condenser with guarding tube at its end, and the mixture was heated for 22 hours on oil bath at 94–98 ^{o}C. Then it was cooled to room temperature, poured into a beaker containing 400 mL crushed ice water, and stirred for 20 minutes. The yellow solid product was collected by suction filtration and washed with cold water. The crude yield was 14.6 g (83%) and was recrystallized from ethyl acetate. yellow crystal; m.p 146–148 ^{o}C; yield 5.2 g (30%).

3.3.4. Synthesis of 2,7-dichloroquinoline-3-carbaldehyde (128)

N,N-dimethylformamide (16.5 mL, 0.21 mol) was added to a 250 mL round-bottom flask guarded with drying tube; it was cooled to 0 °C using ice bath. Then, phosphorus oxychloride (46.5 mL, 0.50 mol) was added dropwise to it from separatory funnel guarded by drying tube while being stirred by magnetic stirrer. This addition was done for 30 minutes. Then 3-chloroacetamide (12 g, 0.05 mol) was added to it. After 5 minutes, the dropper funnel was replaced by air condenser with guarding tube at its end, and the mixture was heated for 22 hours on oil bath at 100–105°C. Then it was cooled to room temperature, poured into a beaker containing 300 mL crushed ice water, and stirred for 20 minutes. The yellow solid product was collected by suction filtration and washed with cold water.

3.3.5. Synthesis of 2,7-dichloroquinoline-3-carbonitrile (129)

The 2,7-dichloroquinoline-3-carbaldehyde (0.3 g, 1.3 mmol), sodium azide (0.13 g, 2 mmol) and phosphorus oxychloride (2 mL) were added to test tube in 1:1:5 ratios. The mixture was stirred for 20 minutes and heated for 6 hrs in water bath by checking progress of reaction using TLC profile. The mixture was cooled and poured to the beaker containing 20 mL of crushed ice water

with stirring. The product was filtered by suction filtration and washed with cold water. The Rf = 0.71 (Hexane: EtOAc = 2:1). The product was purified over silica gel column chromatography *n*-hexane: EtOAc (2:1) as eluent.

3.3.6. Synthesis of 2,7-dichloroquinoline-3-carboxamide (130)

A100 mL round-bottom flask was charged with 2,7-dichloroquinoline-3-carbonitrile (0.19 g, 0.85 mmol), acetic acid (2 mL) and sulfuric acid (1 mL); the mixture was refluxed using water condenser with stirring for 3 hrs and the progress of reaction was monitored with TLC. After completion of the reaction, the mixture was cooled and poured to beaker containing 100 mL of ice water. The dark crystal was collected by suction filtration with Rf = 0.77 (Dichloromethane: Methanol = 9:1).

3.3.7. Synthesis of 7-chloro-2-methoxyquinoline-3-carbaldehyde (131)

A 100 mL round-bottom flask was charged with 2,7-dichloroquinoline-3-caraldehyde (0.99 g, 4.4 mmol), methanol (10 mL), *N,N*-dimethylformamide (13 mL) and potassium carbonate (0.57 g, 8.8 mmol); the mixture was refluxed using water condenser with stirring for 4 hrs and the progress of reaction was monitored by TLC. After completion of reaction the mixture was cooled and poured to 60 ml crushed ice water. The yellow crystal was collected by using suction filtration with Rf = 0.71 (*n*-hexane: EtOAc = 5:1).

3.3.8. Synthesis of 7-chloro-2-ethoxyquinoline-3-carbaldehyde (132)

A 100 mL round bottom flask was charged with 2,7-dichloroquinoline-3-carbaldehyde (0.5 g, 2.2 mmol), potassium carbonate (0.6 g, 4.3 mmol), ethanol (10 mL), and *N,N*-dimethylformamide (10 mL); the mixture was refluxed with water condenser for 4 hrs and the progress of reaction was monitored with TLC. At the end ethanol was removed by distillation, and the remaining cooled mixture was poured into 80 mL crushed ice water. The solid product was collected by suction filtration with Rf = 0.75 (*n*-hexane: EtOAc = 4:1).

3.3.9. Synthesis of 2-chloroquinoline-3-carbonitrile (133)

In the test tube 2-chloroquinoline-3-carbaldehyde (1 g, 5.2 mmol), sodium azide (0.68 g, 10.5 mmol) and phosphorus oxychloride (4 mL) in 1:1:5 ratios were added and stirring for 30 minutes

in the hood. The mixture was heated in water bath for 6 hrs and the progress of reaction was monitored by TLC. Then, the mixture was cooled to room temperature and poured into beaker containing 60 mL of crushed ice water. The yellow crystal was collected by suction filtration with Rf = 0.66 (*n*-hexane: EtOAc = 5:1). The product was purified over silica gel column chromatography *n*-hexane: EtOAc (3:1) as eluent. Add spectral data

3.4 Work-up and purification

Column chromatography on silica gel was conducted for separation of the mixture of the synthesized compounds using various eluent selected depending on the TLC profile. In some cases, purification of compounds was achieved using recrystallization.

3.5 Characterization of synthesized compounds

The synthesized compounds were characterized by spectroscopic techniques including UV-Vis and NMR (^{1}H, ^{13}C-NMR and DEPT-135). Some of the intermediate compounds were characterized by comparing their melting point with literature reported for the same compounds.

3.6 Preparation of discs containing synthesized compounds

Each synthetic compound (5 mg) was dissolved in DMSO (5 mL) to give 1 mg/mL. This was used as standard solution. The standard solution was serially diluted in DMSO to furnish 100 and 200 µg/mL. The concentrations were incorporated into sterile blank paper discs and were dried at 37 ^{o}C. The paper discs were weighed carefully for confirming exact amount of the synthesized compounds being incorporated.

3.7 Bacterial culture

Four strains of bacterial species, two Gram-positive bacteria (*S. aureus* (ATCC25923), *S. pyogenes* (ATCC19615)) and two Gram-negative bacteria (*E. coli* (ATCC, 25922), *P. aeruginosa* (ATCC27853)) which were provided by Adama Public Health Research & Referral Laboratory Center were used to evaluate antibacterial activity of the synthetic compounds.

3.8 Antibacterial activity

In vitro antibacterial susceptibility test was determined by disc diffusion method. The medium was prepared by dissolving 38 g of Mueller Hinton agar (MHA) medium in 1000 mL of distilled water and the autoclaved at 121 °C for 15 min. The autoclaved medium was poured into sterile plates (20-25 mL/plate) and the plates were allowed to solidify under sterile condition at room temperature. After solidification, the plates were seeded with overnight grown culture approximately 1.5 X 10^8 CFU/mL by swabbing evenly on to the surface of the medium with a sterile cotton swab.

The synthesized compound at the concentrations of (100 and 200 µg/mL) was prepared by dissolving in DMSO. Whatman filter paper no. 1 was used to prepare discs approximately 6 mm in diameter. The sterile discs were infused with the synthesized compounds and position on the surface of the medium with sterile forceps and gently pressed down to ensured contact with the MHA. Amoxicillin was used as standard antibiotic and then plates were inverted and then incubated at 37 ℃ for 24 hrs. After incubation the inhibition zone produced by the synthesized compounds were evaluated by measuring the diameter (mm) of the clear zone around the disc against the test organisms using a ruler.

3.9 Antioxidant activity

Antioxidant activity of the synthesized compounds was assessed according reported procedure [52] by the DPPH radical scavenging method. The nitrogen centered stable free radical DPPH has often been used to characterize antioxidants. It is reversibly reduced and therefore the odd electron within the DPPH radical gives a robust absorption maximum at 517 nm using spectrophotometer, which was purple in color. The radical scavenging activity of the synthesized target compounds was evaluated with 1,1-diphenyl-2-picryl hydrazyl (DPPH). In the process, 0.04 mg/mL (0.004% (w/v)) solution of DPPH in methanol was prepared and used as standard solution. The synthesized compounds were serially diluted in methanol to furnish four different concentrations (1.25, 2.50, 5.00, 10.00 µg/mL). Likewise the control was made by adding 1 mL of the DPPH solution to 4 mL of methanol, while 4 mL methanol was used as a blank.

After a 30 min incubation period at room temperature, the absorbance was measured against blank at λ 517 nm [53]. Ascorbic acid was used as the standard. The activity was expressed as IC_{50}, which is the concentration of the test compound required to give a 50% decrease of the absorbance from that of the control solution. The inhibition curves were prepared and to obtain IC_{50} values were obtained. The percent of inhibition (I %) of free radical production from DPPH was calculated by the following equation:

$$\%\ \text{of I} = \frac{(\text{A control} - \text{A sample})}{\text{A control}} \times 100$$

Where A control is the absorbance of the control reaction, A sample is the absorbance of the test compound.

3.10 *In silico* molecular docking of the synthesized compounds

Synthesized compounds were subjected to molecular docking studies using the Auto Dock Tool (ADT) version 1.5.2 and Auto Dock version 4.2 docking program to investigate the potential binding mode. The crystal structure of the enzyme (PDB ID: 3S7S) with resolution 2.3 Å were chosen as the protein model. The structures of ligands were optimized using the Chem Office software. Auto Dock version 4.2 was used to prepare the molecules and parameters before submitting it for docking analysis with Auto Dock. Polar hydrogen atoms were added while non-polar hydrogen atoms were merged and then, Gasteiger partial atomic charges were assigned to the ligands. All rotatable bonds of ligands, defined by default of the program, were allowed to rotate during the automated docking process and then prepared protein and ligand structures were saved in the PDBQT format suitable for calculating energy grid maps. A grid box size of 46×46×46 Å points with a grid spacing of 0.375 Å was considered. Lamarckian genetic algorithm (LGA) program with an adaptive whole method search in the Auto Dock was chosen to calculate the different ligand conformers. After 200 independent docking runs for each ligand, a cluster analysis was done. In according to the root mean square deviation (RMSD) tolerance of 2.0 Å conformations were clustered and ranked by energy of which the conformation with the best scored pose with the lowest binding energy was selected for these ligands [54].

4. RESULTS AND DISCUSSION

4.1 Synthesis of compounds 128-133

In attempt to generate novel quinoline derivatives which have antimicrobial properties, various quinoline derivatives were prepared using different reaction conditions. In the process, 3-chloroacetanilide was prepared by refluxing the 3-chloroaniline and acetic anhydride in acetic acid (Scheme 22). Then 2,7-dichloroquinoline-3-carbaldehyde (**128**) was prepared from 3-chloroacetanilide by Vilsmeier reaction method. The chlorine in position 2 of quinoline was substituted using methoxy and ethoxy by refluxing 2,7-dichloroquinoline-3-carbaldehyde (**128**) in *N,N*-dimethylformamide with methanol and ethanol as nucleophile in potassium carbonate (Scheme 22). In other process, 2-chloroquinoline-3-carbaldehyde (**39**) was synthesized from acetanilide, DMF and phosphorous oxychloride through Vilsmeier reaction and 2-chloroquinoline-3-carbonitrile (**133**) from 2-chloroquinoline-3-carbaldehyde (**39**) in the presence of sodium azide and phosphorous oxychloride (Scheme 23). DMF was chosen as appropriate solvent, because of its attractive features such as high dielectric constant, its aprotic nature, wide liquid range, low volatility, dissolve all polar reactants and able to supply sufficient activation energy for the reactions because of its high boiling point (153 ^{o}C). Additionally, it is also miscible in water which eases to isolation of the desired product by adding the reaction mixture into cold ice-water which causes water insoluble product to precipitate out. Potassium carbonate was used to induce the basic medium since it weak base and poor nucleophile, it doesn't interfere in most nucleophilic substitution reaction. Refluxing 2,7-dichloroquinoline-3-carbaldehyde (**128**) with methanol and ethanol in the presence of potassium carbonate in DMF to afford 7-chloro-2-methoxyquinoline-3-carbaldehyde (**131**) and 7-chloro-2-ethoxyquinoline-3-carbaldehyde (**132**), respectively. Treating 2,7-dichloroquinoline-3-carbaldehyde (**128**) with sodium azide in phosphorus oxychloride to afford 2,7-dichloroquinoline-3-carbonitrile (**129**) and this product was refluxed with acetic acid and sulfuric acid to furnish 2,7-dichloroquinoline-3-carboxamide (**130**). The overall sequence of reactions used in the synthesis of various targeted quinoline derivatives are illustrated in Scheme 22 and 23. The structure elucidation of the synthesized compounds was accomplished using UV-Vis and NMR spectroscopic methods.

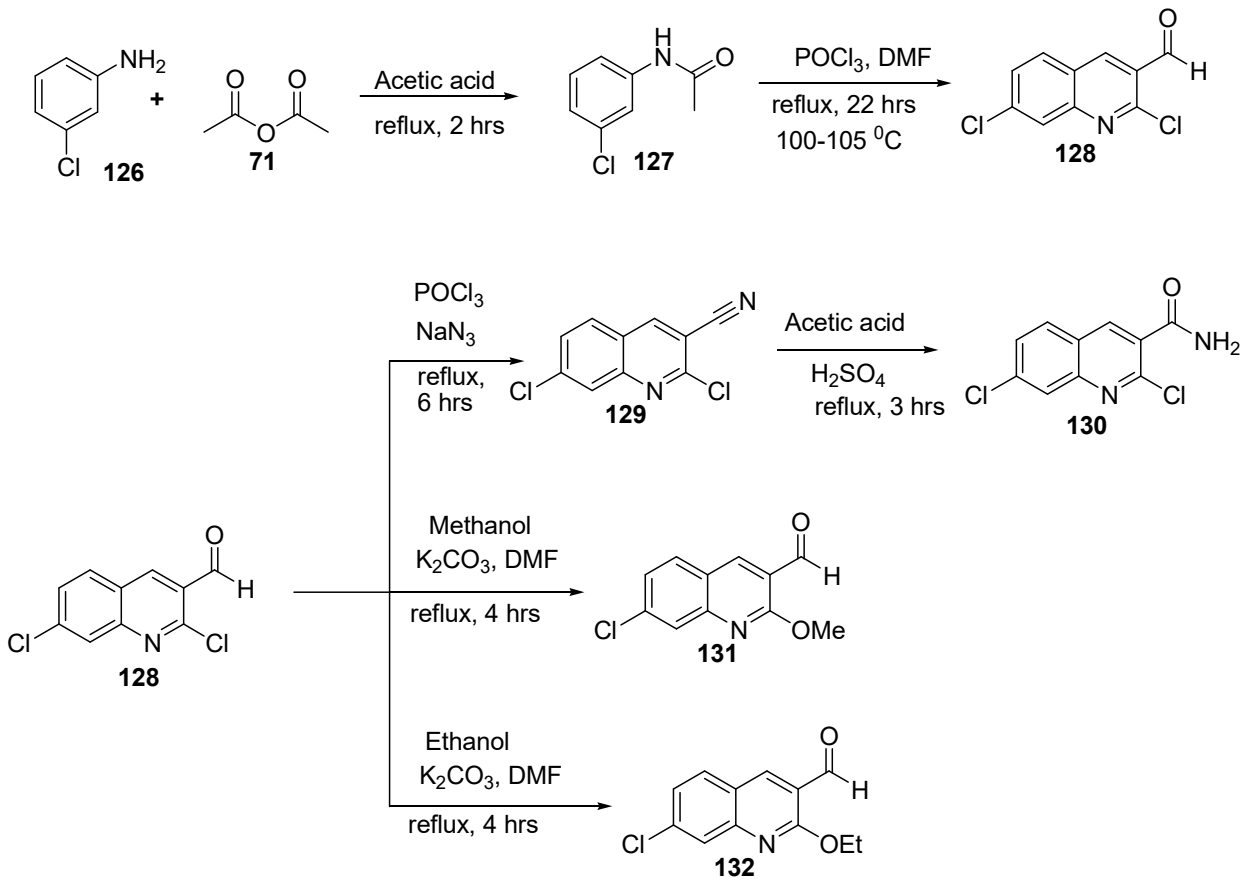

Scheme 22: Synthesis of 7-chloroquinoline-3-carbaldehyde and its derivatives

.

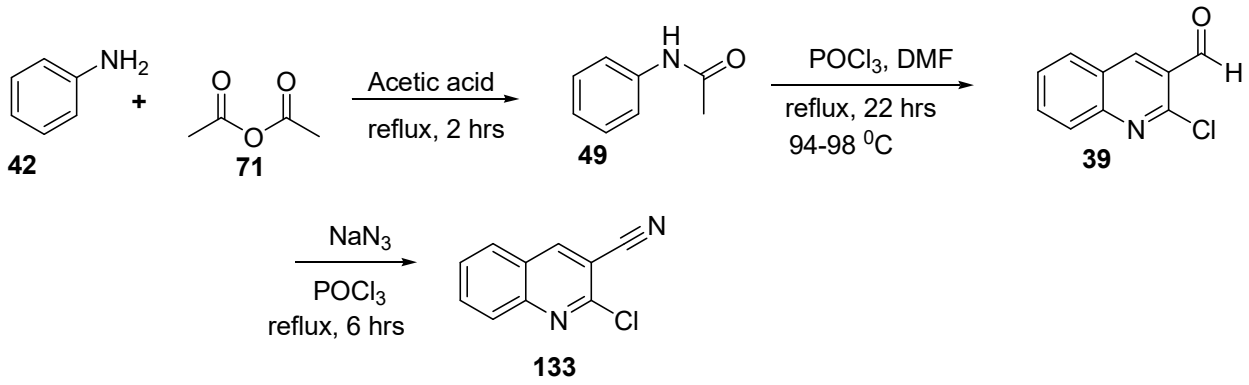

Scheme 23: Synthesis of 2-chloroquinoline-3-carbonitrile (**133**).

4.2 Characterization of synthesized compounds

4.2.1 Characterization of 2,7-dichloroquinoline-3-carbaldehyde (128)

Compound **128** was obtained as yellow crystal melting point 170–174 °C with yield 28%. TLC (*n*-hexane: EtOAc, 4:1) gave rise to a spot at Rf = 0.55, visualized under UV lamp at long-wave (365 nm). The UV-Vis spectrum (MeOH) of this compound displayed absorption band at λmax 324 nm presumably due to π→π* transition of bonding electron to empty ant-bonding orbital caused by energy.

The ^{1}H NMR spectrum (400 MHz, MeOD-d_4 and $CDCl_3$) of compound **128** (Table 1, Appendix 1) showed peaks due to the presence of benzene ring (ring B) fused to pyridine having the ABX spin pattern at δ_H 7.40 (1H, m, H-6), 7.75 (1H, m, H-5) and 8.33 (1H, s, H-8). The two singlet signals at 8.58 (1H, s, H-4) and 10.33 (1H, s) were accounted to proton on the pyridine ring (ring A) fused to benzene ring and aldehyde proton, respectively.

The proton decoupled ^{13}C NMR spectrum (100 MHz, MeOD-d_4 and $CDCl_3$) of compound **128** (Table 1 and Appendix 2) revealed the presence of ten carbon resonances at δ_C 125.3 (C-3), 126.3 (C-10), 129.2 (C-8), 130.8 (C-6), 136.0 (C-5), 140.2 (C-7), 141.7 (C-4), 147.0 (C-9), 151.4 (C-2) and 188.7. The latter is accounted to the presence of carbonyl functional group in the structure of compound **128**. Analysis of the DEPT-135 NMR spectrum of compound **128** revealed the presence of five peaks at δ_C 141.7 (C-4), 136.1 (C-5), 130.8 (C-6), 129.2 (C-8) and 188.7 (carbonyl carbon).

Table 1: The ^{1}H, ^{13}C NMR and DEPT-135 spectral data of compound **128** in MeOD-*d4* and $CDCl_3$ mixture.

Position	^{1}H	^{13}C	DEPT-135
2	-	151.4	-
3	-	125.3	-
4	8.58 (1H, s)	141.7	141.7
5	7.75 (1H, m)	136.0	136.1
6	7.40 (1H, m)	130.8	130.8
7	-	140.2	-
8	8.33 (1H, s)	129.2	129.2
9	-	147.0	-
10	-	126.3	-
-CHO	10.33 (1H, s)		188.7

Based on the above analysis, the structure **128** has been assigned to this compound (Figure 8).

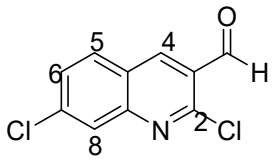

128

Figure 8: Structure of 2,7-dichloroquinoline-3-carbaldehyde (**128**)

4.2.2 Characterization of 2,7-dichloroquinoline-3-carbonitrile (129)

Compound **129** was obtained as yellow crystal melting point 150-156 °C with yield 64%. TLC (*n*-hexane: EtOAc, 2:1) gave rise to a spot at Rf = 0.71, visualized under UV lamp at long-wave (365 nm). The UV-Vis spectrum (MeOH) of this compound displayed absorption band at λmax 359 nm presumably due to π→π* transition of bonding electron to empty ant-bonding orbital caused by energy.

The ^{1}H NMR spectrum (400 MHz, MeOD-*d*$_4$ and $CDCl_3$) of compound **129** (Table 2, Appendix 3) showed peaks due to the presence of benzene ring (ring B) fused to pyridine having the ABX spin pattern was the evidenced from peaks at δ_H 7.64 (1H, d, *J* = 8.00 Hz, H-6), 7.86 (1H, d, *J* = 8.00 Hz, H-5) and 8.02 (1H, s, H-8). The singlet signals at 8.57 (1H, s, H-4) was accounted to proton on the pyridine ring (ring A) fused to benzene ring.

The proton decoupled ^{13}C NMR spectrum (100 MHz, MeOD-*d*$_4$ and $CDCl_3$) of compound **129** (Table 2, Appendix 4) revealed the total of ten peaks at δ_C 108.0 (C-3), 123.6 (C-10), 127.9 (C-8), 129.3 (C-5), 130.0 (C-6), 140.4 (C-7), 144.7 (C-4), 148.4 (C -9), 149.6 (C-2) and 114.8. The latter is accounted to the presence of nitrile functional group in the structure of compound **129**. Analysis of the DEPT-135 NMR spectrum of compound **129** revealed the presence of four peaks at δ_C 144.7 (C-4), 129.3 (C-5), 130.0 (C-6) and 127.9 (C-8).

Table 2: The ^{1}H, ^{13}C NMR and DEPT-135 spectral data of compound **129** in MeOD-*d4* and $CDCl_3$ mixture.

Position	^{1}H	^{13}C	DEPT-135
2	-	149.6	-
3	-	108.0	-
4	8.57 (1H, s)	144.7	144.7
5	7.86 (1H, d, *J* = 8.00 Hz)	129.3	129.3
6	7.64 (1H, d, *J* = 8.00 Hz)	130.0	130.0
7	-	140.4	-
8	8.02 (1H, s)	127.9	127.9
9	-	148.4	-
10	-	123.6	-
-C≡N	-	114.8	-

Based on the above analysis, the structure **129** has been assigned to this compound (Figure 9).

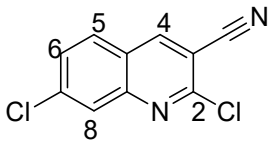

129

Figure 9: Structure of 2,7-dichloroquinoline-3-carbonitrile (**129**)

4.2.3 Characterization of 2,7-dichloroquinoline-3-carboxamide (130)

Compound **130** was obtained as dark crystal melting point 206-208 °C with yield 73%. TLC (Dichloromethane: Methanol, 9:1) gave rise to a spot at Rf = 0.77, visualized under UV lamp at long-wave (365 nm). The UV-Vis spectrum (MeOH) of this compound displayed absorption band at λmax 261 nm presumably due to n→π* transition of non-bonding electron to empty ant-bonding orbital caused by energy.

The ^{1}H NMR spectrum (400 MHz, DMSO-d_6) of compound **130** (Table 3, Appendix 5) showed peaks due to the presence of benzene ring (ring B) fused to pyridine having the ABX spin pattern was the evidenced from peaks at δ_H 7.30 (1H, J = 12.00 Hz, d, H-6), 7.94 (1H, J = 8.00 Hz, d, H-5) and 8.82 (1H, s, H-8). The singlet signals at 8.98 (1H, s, H-4) was accounted to proton on the pyridine ring (ring A) fused to benzene ring. The broad peak at 12.42 was evidenced for the presence of two amine proton (-NH_2).

The proton decoupled ^{13}C NMR spectrum (100 MHz, DMSO-d_6) of compound **130** (Table 3, Appendix 6) revealed the total of ten peaks at δ_C 115.0 (C-8), 117.8 (C-10), 122.9 (C-3), 123.4 (C-6), 132.0 (C-5), 137.5 (C-7), 140.8 (C-9), 144.1 (C-4), 162.3 (C-2), and 164.3. The latter is accounted to the presence of amide functional group in the structure of compound **130**. Analysis of the DEPT-135 NMR spectrum of compound **130** revealed the presence of four peaks at δ_C 144.1 (C-4), 132.0 (C-5), 123.4 (C-6) and 115.0 (C-8).

Table 3: The ^{1}H, ^{13}C NMR and DEPT-135 spectral data of compound **130** in DMSO-*d6*.

Position	^{1}H	^{13}C	DEPT-135
2	-	162.3	-
3	-	122.9	-
4	8.98 (1H, s)	144.1	144.1
5	7.94 (1H, d, *J* = 8.00 Hz)	132.0	132.0
6	7.30 (1H, d, *J* = 12.00 Hz)	123.4	123.4
7	-	137.5	-
8	8.82 (1H, s)	115.0	115.0
9	-	140.8	-
10	-	117.6	-
$CONH_2$	12.4 (broad)	164.3	-

Based on the above analysis, the structure **130** has been assigned to this compound (Figure 10).

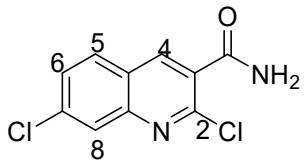

130

Figure 10: Structure of 2,7-dichloroquinoline-3-carboxamide (**130**)

4.2.4 Characterization of 7-chloro-2-methoxyquinoline-3-carbaldehyde (131)

Compound **131** was obtained as dark crystal melting point 102-104 °C with yield 74%. TLC (*n*-hexane: EtOAc, 5:1) gave rise to a spot at Rf = 0.71, visualized under UV lamp at long-wave (365 nm). The UV-Vis spectrum (MeOH) of this compound displayed absorption band at λmax 368 nm presumably due to π→π* transition of bonding electron to empty ant-bonding orbital caused by energy.

The ^{1}H NMR spectrum (400 MHz, MeOD-*d*$_4$ and $CDCl_3$) of compound **131** (Table 4, Appendix 7) showed peak due to the presence of methoxy proton was evidenced from peak at 4.09 (3H, s). The presence of benzene ring (ring B) fused to pyridine having the ABX spin pattern was the evidenced from peaks at δ_H 7.30 (1H, s, H-6), 7.65 (1H, s, H-5) and 7.72 (1H, s, H-8). The two singlet signals at 8.44 (1H, s, H-4) and 10.32 (1H, s) were accounted to proton on the pyridine ring (ring A) fused to benzene ring and aldehyde proton, respectively.

The proton decoupled ^{13}C NMR spectrum (100 MHz, MeOD-*d*$_4$ and $CDCl_3$, Appendix 8) of compound **131** (Table 4, Appendix 8) at δ_C 53.6 was accounted to proton of methoxy carbon on 2-position. Also the ^{13}C NMR spectrum revealed another ten peaks at 119.6 (C-3), 122.4 (C-10), 124.7 (C-6), 125.8 (C-8), 130.5 (C-5), 137.7 (C-7), 139.5 (C-4), 149.0 (C-9), 161.5 (C-2) and 188.9. The latter is accounted to the presence of carbonyl functional group in the structure of compound **131**. Analysis of the DEPT-135 NMR spectrum of compound **131** revealed the presence of six peaks at δ_C 53.6 (methoxy), 139.5 (C-4), 130.5 (C-5), 124.7 (C-6), 125.8 (C-8) and 188.9 (carbonyl carbon).

Table 4: The ^{1}H, ^{13}C NMR and DEPT-135 spectral data of compound **131** in MeOD-*d4* and $CDCl_3$ mixture.

Position	^{1}H	^{13}C	DEPT-135
2	-	161.5	-
3	-	119.6	-
4	8.98 (1H, s)	139.5	139.5
5	7.65 (1H, s)	130.5	130.5
6	7.30 (1H, s)	124.7	124.7
7	-	137.7	-
8	8.72 (1H, s)	125.8	125.8
9	-	149.0	-
10	-	122.4	-
-CHO	10.32 (1H, s)	188.9	188.9
$-OCH_3$	4.09 (3H, s)	53.6	53.6

Based on the above analysis, the structure **131** has been assigned to this compound (Figure 11).

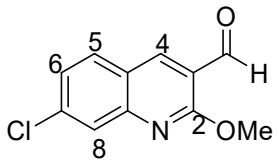

131

Figure 11: Structure of 7-chloro-2-methoxyquinoline-3-carbaldehyde (**131**)

4.2.5 Characterization of 7-chloro-2-ethoxyquinoline-3-carbaldehyde (132)

Compound **132** was obtained as yellow crystal melting point 94-96 °C with yield 67%. TLC (*n*-hexane: EtOAc, 4:1) gave rise to a spot at Rf = 0.75, visualized under UV lamp at long-wave (365 nm). The UV-Vis spectrum (MeOH) of this compound displayed absorption band at λmax

379 nm presumably due to π→π* transition of bonding electron to empty ant-bonding orbital caused by energy.

The ^{1}H NMR spectrum (400 MHz, $CDCl_3$) of compound **132** (Table 5, Appendix 9) showed the presence of methylene attached to oxygen and methyl proton were evidenced from peaks at δ_H 4.61 (2H, q, J = 8.00 Hz) and 1.50 (3H, t, J = 6.00 Hz), respectively. The presence of benzene ring (ring B) fused to pyridine having the ABX spin pattern was the evidenced from peaks at δ_H 7.33 (1H, d, J = 12 Hz, H-6), 7.71 (1H, d, J = 8 Hz, H-5) and 7.80 (1H, s, H-8). The two singlet signals at 8.48 (1H, s, H-4) and 10.44 (1H, s) were evidenced for the presence of proton on the pyridine ring (ring A) fused to benzene ring and aldehyde proton, respectively.

The proton decoupled ^{13}C NMR spectrum (100 MHz, $CDCl_3$, Appendix 10) of compound **132** (Table 5, Appendix 10) revealed the total of twelve peaks at δ_C 14.4 (methyl), 62.7 (methylene), 119.9 (C-3), 122.6 (C-10), 125.9 (C-6), 126.5 (C-8), 130.7 (C-5), 138.6 (C-7), 139.1 (C-4), 149.4 (C-9), 161.6 (C-2) and 189.0. The latter is accounted to the presence of carbonyl functional group in the structure of compound **132**. Analysis of the DEPT-135 NMR spectrum of compound **132** revealed the presence of seven peaks one point down and six point up at δ_C 62.7 (methylene), 14.4 (methyl), 139.1 (C-4), 130.7 (C-5), 125.9 (C-6), 126.5 (C-8) and 188.9 (carbonyl carbon).

Table 5: The ^{1}H, ^{13}C NMR and DEPT-135 spectral data of compound **132** in $CDCl_3$.

Position	^{1}H	^{13}C	DEPT-135
2	-	161.6	-
3	-	119.9	-
4	8.48 (1H, s)	139.1	139.1
5	7.71 (1H, d, *J* = 8 Hz)	130.7	130.7
6	7.33 (1H, d, *J* = 12 Hz)	125.9	125.9
7	-	138.6	-
8	7.80 (1H, s)	126.5	126.5
9	-	149.4	-
10	-	122.6	-
-CHO	10.32 (1H, s)	189.0	188.9
$-OCH_2-$	4.61 (2H, q, *J* = 8.00 Hz)	62.7	62.7
$-CH_3$	1.50 (3H, t, *J* = 6.00 Hz)	14.4	14.4

Based on the above analysis, the structure **132** has been assigned to this compound (Figure 12).

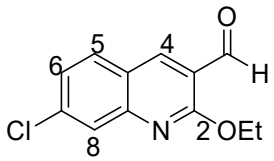

132

Figure 12: Structure of 7-chloro-2-ethoxyquinoline-3-carbaldehyde (**132**)

4.2.6 Characterization of 2-chloroquinoline-3-carbonitrile (133)

Compound **133** was obtained as yellow crystal melting point 132-134 °C with yield 89%. TLC (*n*-hexane: EtOAc, 5:1) gave rise to a spot at Rf = 0.66, visualized under UV lamp at long-wave (365 nm). The UV-Vis spectrum (MeOH) of this compound displayed absorption band at λmax

357 nm presumably due to π→π* transition of bonding electron to empty ant-bonding orbital caused by energy.

The ^{1}H NMR spectrum (400 MHz, $CDCl_3$) of compound **133** (Table 6, Appendix 11) showed peaks due to the presence of benzene ring (ring B) fused to pyridine having the A_2B_2 spin pattern was the evidenced from peaks at δ_H 7.75 (1H, t, J = 6 Hz, H-6), 7.96 (1H, t, J = 8 Hz, H-7), 8.10 (1H, d, J = 8 Hz, H-5) and 8.60 (1H, d, H-8). The singlet signal at 7.32 (1H, s, H-4) was accounted to proton on the pyridine ring (ring A) fused to benzene ring.

The proton decoupled ^{13}C NMR spectrum (100 MHz, $CDCl_3$) of compound 133 (Table 6, Appendix 12) revealed the total of ten peaks at δ_C 107.9 (C-3), 125.1 (C-10), 128.1 (C-8), 128.8 (C-5), 128.9 (C-6), 133.7 (C-7), 144.9 (C-4), 148.2 (C-9), 148.2 (C-2) and 115.1. The latter is accounted to the presence of carbonyl functional group in the structure of compound **133**. Analysis of the DEPT-135 NMR spectrum of compound **133** revealed the presence of five peaks at δ_C 144.9 (C-4), 128.8 (C-5), 129.0 (C-6), 133.7 (C-7) and 128.1 (C-8).

Table 6: The ^{1}H, ^{13}C NMR and DEPT-135 spectral data of compound **133** in $CDCl_3$.

Position	^{1}H	^{13}C	DEPT-135
2	-	148.2	-
3	-	107.9	-
4	7.32 (1H, s)	144.9	144.9
5	8.10 (1H, d, J = 8.00 Hz)	128.8	128.8
6	7.75 (1H, t, J = 6.00 Hz)	128.9	129.0
7	7.96 (1H, t, J = 8.00 Hz	133.7	133.7
8	8.60 (1H, d)	128.1	128.1
9	-	148.2	-
10	-	125.1	-
-C≡N	-	115.1	-

Based on the above analysis, the structure **133** has been assigned to this compound (Figure 13).

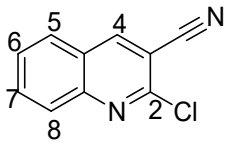

133

Figure 13: Structure of 2-chloroquinoline-3-carbonitrile (**133**)

4.3 Antibacterial activity of compounds 129-133

Quinolines are pharmacologically active compounds used to treat various life threatening diseases. In an attempt to find analogues compounds against bacteria, a series of quinoline derivatives have been synthesized and subsequently evaluated for their antibacterial activities against various strain of bacterial pathogens. The results obtained are depicted in Table 1 and Figure 8. The data in Table 1 shows that all synthesized compounds displayed weak to moderate activities against all tested bacterial strains.

Table 7: The inhibition zone of synthetic compounds (**129-133**) in mm (mean ± SD)

Compounds	Concentrations in µg/mL	Bacteria strains and Zone of Inhibition in mm			
		E. coli	*S. aureus*	*P. aeruginosa*	*S. pyogenes*
129	100	7.00 ± 0.04	9.00 ± 0.03	9.00 ± 0.04	8.00 ± 0.01
	200	9.00 ± 0.01	11.00 ± 0.03	11.00 ± 0.03	10.00 ± 0.04
130	100	9.00 ± 0.00	8.00 ± 0.01	7.00 ± 0.04	7.00 ± 0.01
	200	11.00 ± 0.04	9.00 ± 0.00	8.00 ± 0.01	8.00 ± 0.03
131	100	8.00 ± 0.00	8.00 ± 0.00	8.00 ± 0.03	10.00 ± 0.04
	200	10.00 ± 0.01	9.00 ± 0.01	9.00 ± 0.04	11.00 ± 0.02
132	100	10.00 ± 0.00	8.00 ± 0.01	9.00 ± 0.04	7.00 ± 0.03
	200	12.00 ± 0.00	9.00 ± 0.04	10.00 ± 0.00	10.00 ± 0.03
133	100	8.00 ± 0.02	7.00 ± 0.01	8.00 ± 0.00	8.00 ± 0.02
	200	9.00 ± 0.04	10.00 ± 0.01	8.00 ± 0.00	9.00 ± 0.02
Amoxicillin	100	16.00 ± 0.00	15.00 ± 0.01	16.00 ± 0.04	16.00 ± 0.03
	200	18.00 ± 0.01	17.00 ± 0.01	18.00 ± 0.00	18.00 ± 0.03

Results are mean ± SD of duplicate experiments; Amoxicillin is used as positive control

The mean inhibition zone ranged from lowest (7 mm at 100 µg/mL) to the highest (12 mm 200 µg/mL). Two compounds; **132** and **130** showed good activities against *E. coli* at mean inhibition zones of 12.00 ± 0.00 and 11.00 ± 0.04 mm, and the compound **129** also good activity against *S. aureus* and *P. aeruginosa* with 11.00 ± 0.03 mm at 200 µg/mL when compared with standard amoxicillin. The compound **131** at 200 µg/mL concentration showed good activity against *S. pyrogenes* with mean inhibition of 11.00 ± 0.02 mm. The other two compounds (**129** and **132**) showed medium activities against other strains of bacteria, while compound **133** showed medium mean inhibition zone against three other bacteria (*S. aureus, P. aeruginosa* and *S. pyrogenes*). The compound **131** also showed medium inhibition zone against strains of bacteria except *S.*

pyrogenes. All synthesized compounds were compared with standard drug tablet (Amoxicillin). The synthesized compounds have stronger activities when compared with the compounds reported in literature, which differ in substituents and functional groups. These activities might be due to chlorine substituted at 7-position, and the amide and nitrile functional groups. The antibacterial activity of the synthesized analogs of quinoline was graphically further presented in Figure 8.

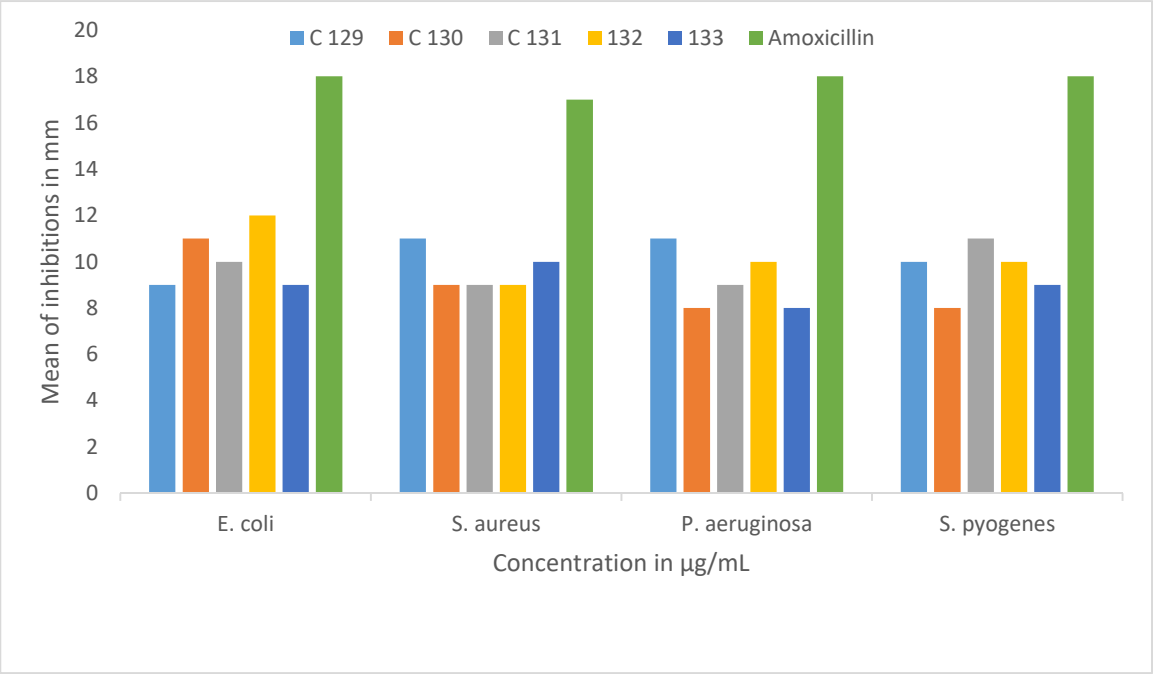

Figure 14: The inhibition zone of the synthetic compounds in mm (mean ± SD) at 200µg/mL

4.4 Radical scavenging activity of synthesized compounds (128-133).

DPPH assay was conducted to evaluate the antioxidant activity of synthesis compounds as scavengers of free radicals. Compounds exhibiting antioxidant activity reduced the absorbance at 517 nm, which is due to DPPH radical in addition to their ability to turn the purple color of DPPH to yellow or colorless. In this work, the radical scavenging activity of the synthesized compounds were evaluated using DPPH, and the findings are depicted in Table 2.

Table 8: Percentage inhibition and IC_{50} of synthesized compounds (**128-132**) and ascorbic acid

Conc.	Compounds					
µg/mL	**128**	**129**	**130**	**131**	**132**	**Ascorbic acid**
10.00	16.92	50.77	68.82	13.08	55.00	91.15
5.00	14.62	10.77	67.70	9.62	21.54	73.08
2.50	14.00	5.38	65.45	5.77	15.00	35.00
1.25	11.92	4.23	65.17	4.62	13.85	11.15
IC_{50} (mol/L)	74.72	2.17	0.31	16.78	4.32	2.41

The DPPH radical scavenging activity of the synthesized compounds was compared with ascorbic acid which is used as standard, and the result is graphically presented in Figure 9.

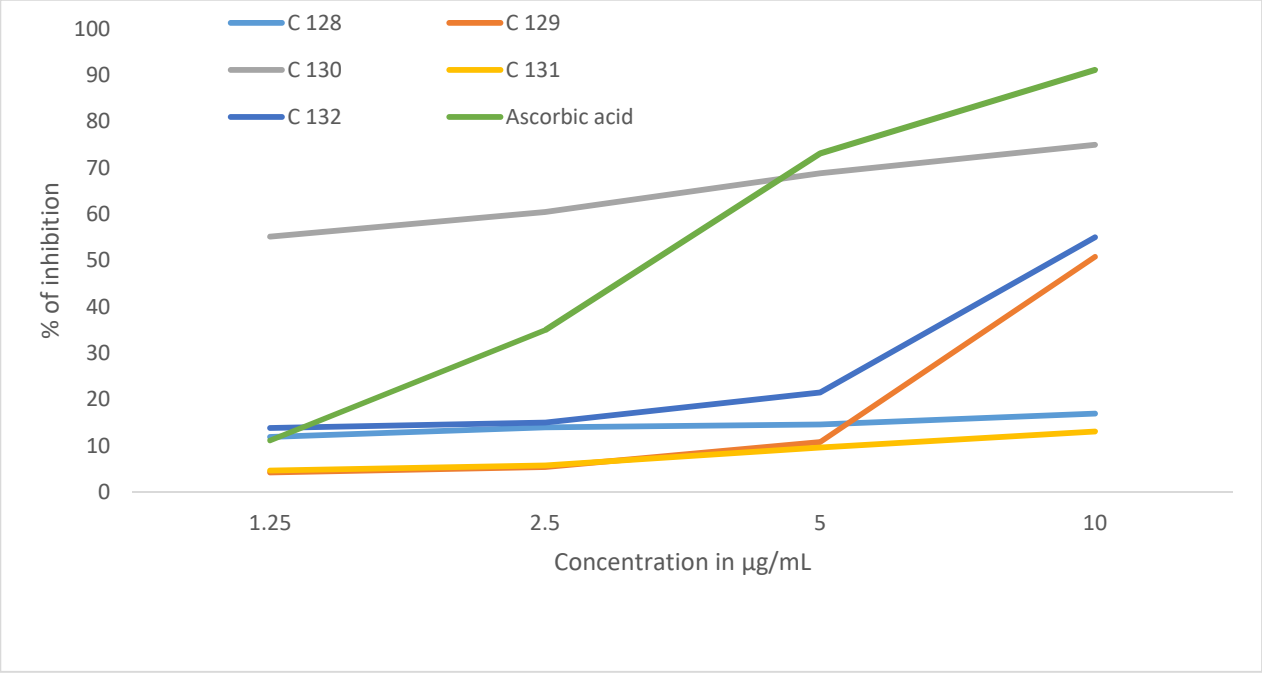

Figure 15: The percentage inhibition of free radical DPPH by the synthesized compounds

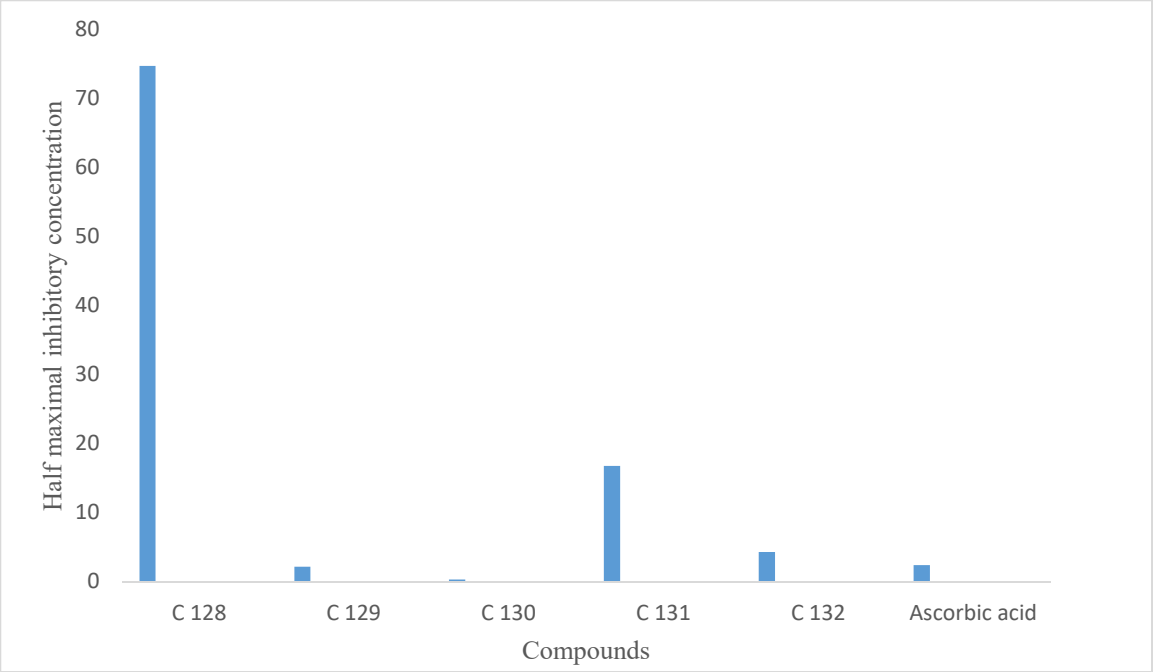

Figure 16: The IC_{50} of free radical DPPH by synthesized compounds

Generally antioxidant of the synthesized compounds in this work was medium to high relative to ascorbic acid at the same concentration. The percentage inhibition of compound **130** at 2.50 and 1.25 µg/mL much greater than that of ascorbic acid, which have 0.31 µg/mL of IC_{50} and medium in other two concentration. The percentage inhibition of compound **132** at 10.00 µg/mL, 5.00 µg/mL and 2.50 µg/mL is medium when compared with that of ascorbic acid and high in 1.25 µg/mL concentration. The percentage inhibition of compound **129** is medium (10.00 µg/mL) to low (in other concentration) relative to ascorbic acid, but low IC_{50} (2.17 µg/mL) relative to ascorbic acid. The percentage inhibition of compound **131** is almost low in all concentration relative to ascorbic acid. DPPH is a stable free radical accepting hydrogen from a corresponding donor, which causes it to lose the characteristic deep purple (λmax 517 nm) color. Compound **133**, doesn't have such easily transferable hydrogen, so that doesn't have percentage inhibition at all concentration. The absorbance of compound **133** is almost equal with the absorbance of control which is DPPH in methanol and DMSO depending on solubility of compounds.

4.5 *In silico* molecular docking analysis of the synthesized compounds (129-133) against *E. coli DNA gyrase B.*

The DNA gyrase, an enzyme belonging to a member of bacterial *topoisomerase*, controls the topology of DNA during transcription, replication, and recombination by introducing transient breaks to both DNA strands. In this regard, bacterial DNA gyrase is essential for bacterial survival and therefore necessary to be exploited as an antibacterial drug target. Therefore, in this study, the molecular docking analysis of the synthesized compounds was conducted to investigate their binding pattern with DNA gyrase and compared them with standard inhibitor (ciprofloxacin). The synthesized compounds (**129-133**) were found to have minimum binding energy ranging from -6.1 to -6.6 kcal/mol (Table 3), with good result achieved with compound **132** (-6.6 kcal/mol). The binding affinity, H-bond, and residual interaction of five compounds and ciprofloxacin were summarized in Table 3.

Table 9: Molecular docking value of synthetic compounds (**129-133**) against *E.coli* DNA gyraseB

Compounds	Affinity (kcal/mol)	H-bond	Residual Amino acid Interactions	
			Hydrophobic/Pi-Cation/Pi-Anion/ Pi-Alkyl interactions	Van-der Walls interactions
129	-6.1	Gly-77	Asp-73, Glu-50, Ile-78, Ile-94	Ala-47, Arg-76, Gly-75, Pro-79, Asn-46, Thr-165
130	-6.4	Asp-73, Asn-46, Gly-77	Glu-50, Pro-79, Ile-78, Arg-76	Ala-47, Gly-75, Thr-165
131	-6.3	Asp-73, Arg-76, Gly-77	Ala-47, Ile-78, Asn-46, Ile-94	Glu-50, Gly-75
132	-6.6	Asp-73, Gly-77, Thr-165	Ala-47, Ile-78, Asn-46, Ile-94	Glu-50, Val-43, Pro-79
133	-6.2	Gly-77	Asp-73, Ile-78, Ile-94	Ala-47, Glu-50, Asn-46, Gly-75, Pro-79
Ciprofloxacin	-7.2	Asp-73, Arg-76, Thr-165	Glu-50, Gly-77, Ile-78, Asn-46	Ala-47

Compared to ciprofloxacin, the synthesized compounds (**129**, **130** and **133**) showed similar residual interaction (Van-der Walls interaction) profile with amino acid residues Ala-47. The compounds (**129-133**) showed similar residual interactions (hydrophobic/Pi-cation/Pi-anion/ Pi-alkyl interactions) with amino acid residues Ile-78. Also the compounds **129** and **130**, and **131** and **132** showed similar residual interactions (hydrophobic/Pi-cation/Pi-anion/ Pi-alkyl interactions) with amino acid residues Glu-50, and Asn-46 respectively. The compounds **130**, **131** and **132** showed additional hydrogen bonding interactions with amino acid residues Asp-73,

and compounds **131** (Arg-76) and **132** (Thr-165) have shown additional hydrogen bonding interactions with amino acid residues. The *in silico* interaction results match the *in vitro* analysis of the synthesized compounds showed good activities against *E. coli*, among which compounds **130** (-6.4 kcal/mol) and **132** (-6.6 kcal/mol) revealed better activity. The energy of synthesized compounds in this study were less than that of reported in the literature [35], which haven't chlorine at 7-position of quinoline. This was indicated the synthesized compounds higher activity against *E. coli* due to synthesized quinoline derivatives have chlorine substituent at 7-position. The compounds **130** and **132** docking results partially matched the ciprofloxacin interactions with amino acid residues. Therefore, compounds **130** and **132** might have the best antibacterial agents among the synthesized compounds in this study. The 3-dimensional binding interaction of synthesized compounds (**129-133**) and ciprofloxacin against *E. coli* gyrase B complex is illustrated below.

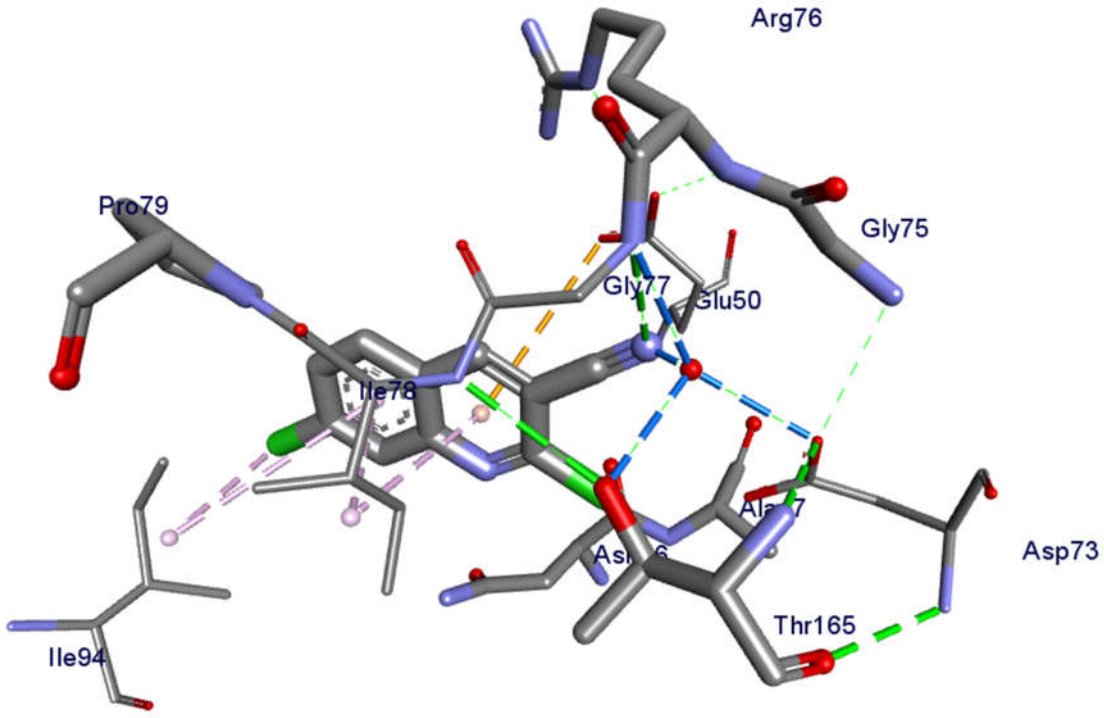

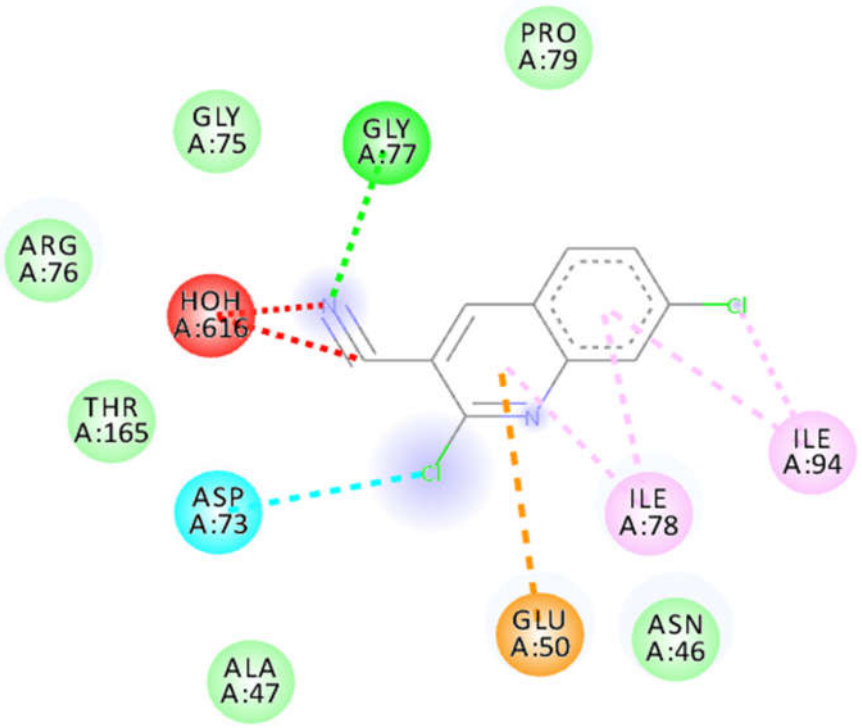

Figure 17: The binding interactions of compound **129** against *E. coli* DNA gyraseB (PDB ID: 6F86).

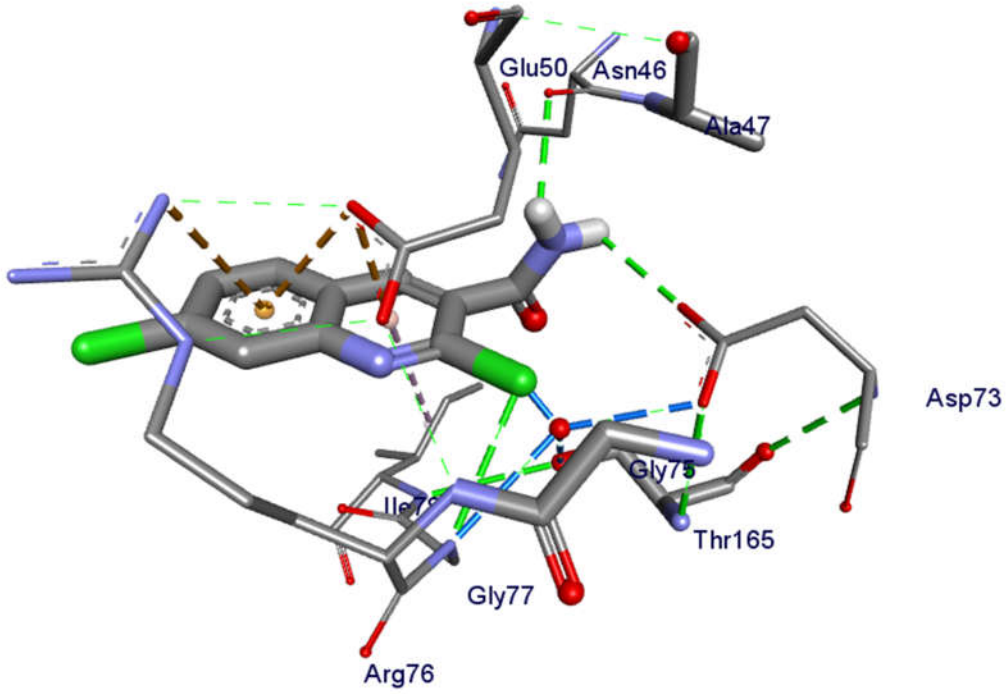

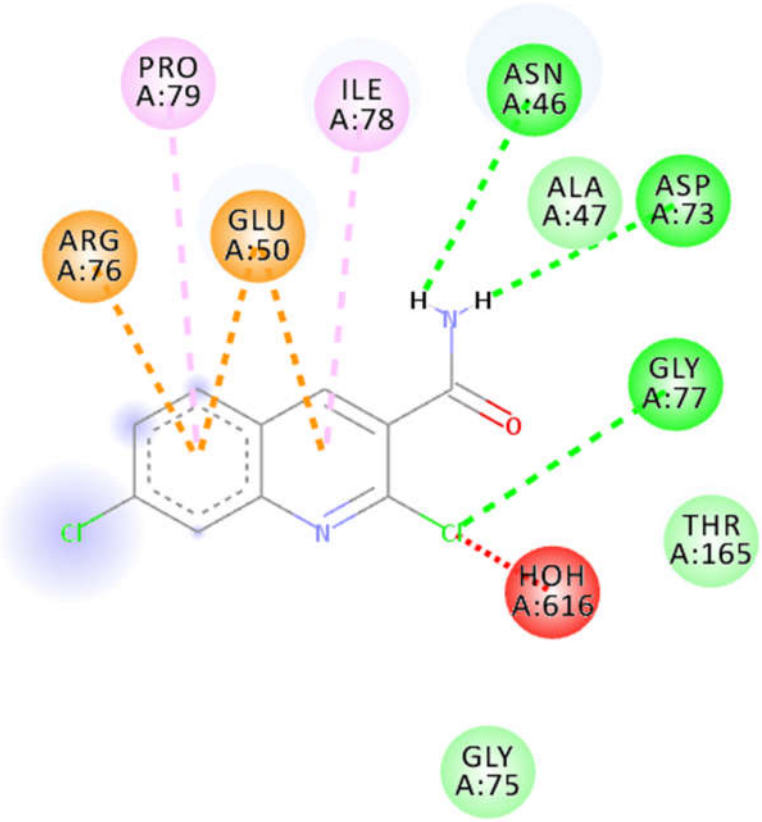

Figure 18: The binding interactions of compound **130** against *E. coli* DNA gyraseB (PDB ID: 6F86).

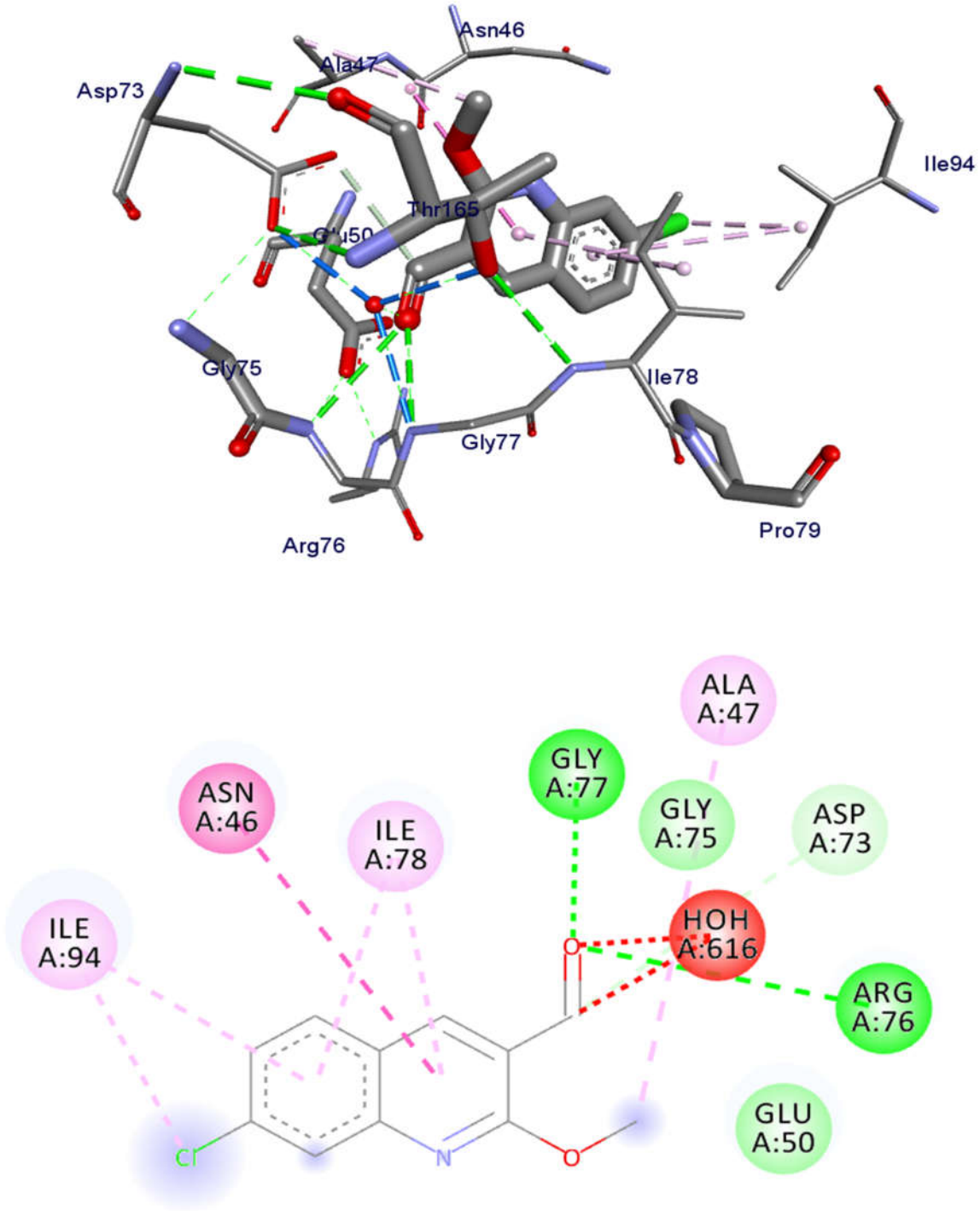

Figure 19: The binding interactions of compound **131** against *E. coli* DNA gyraseB (PDB ID: 6F86).

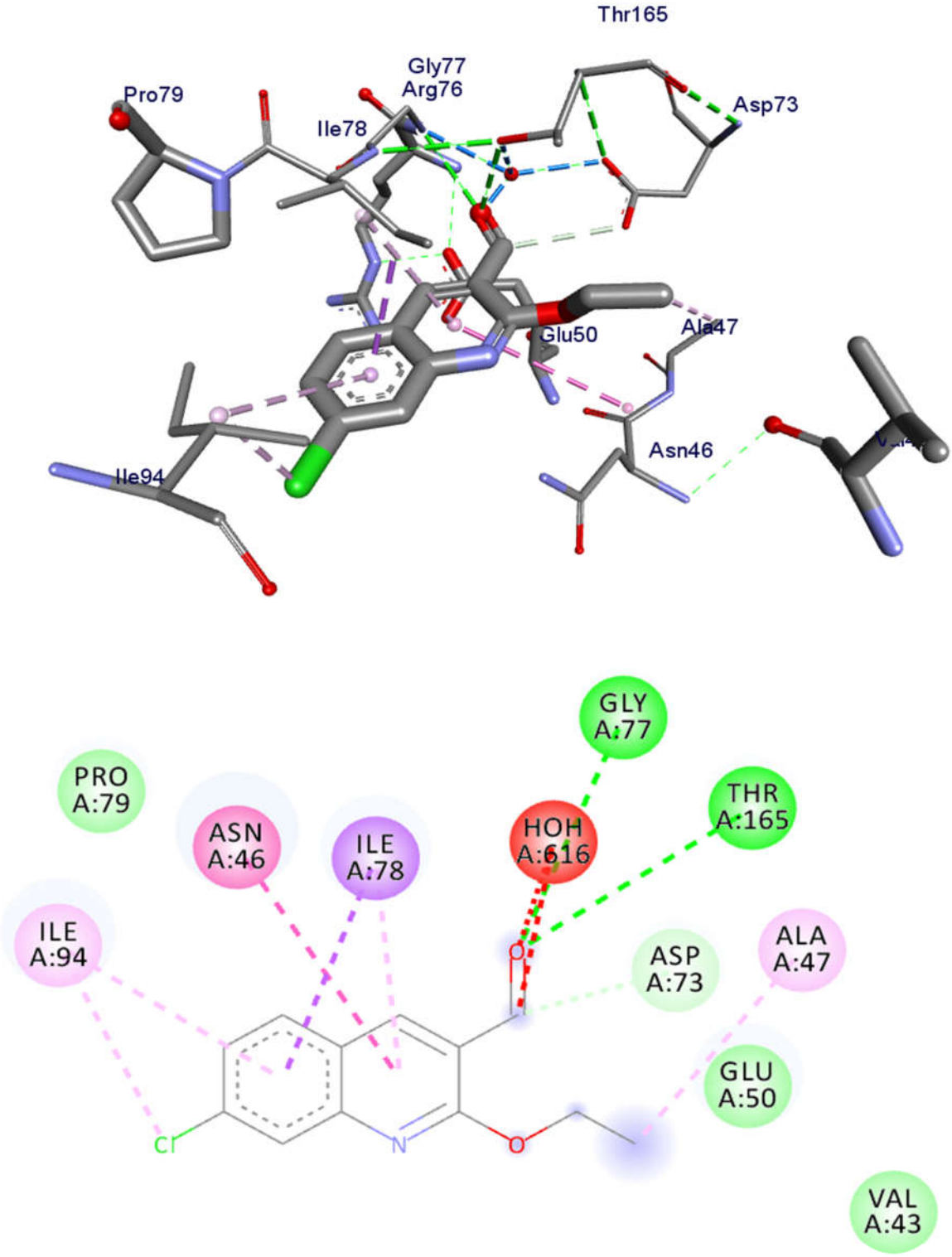

Figure 20: The binding interactions of compound **132** against *E. coli* DNA gyraseB (PDB ID: 6F86).

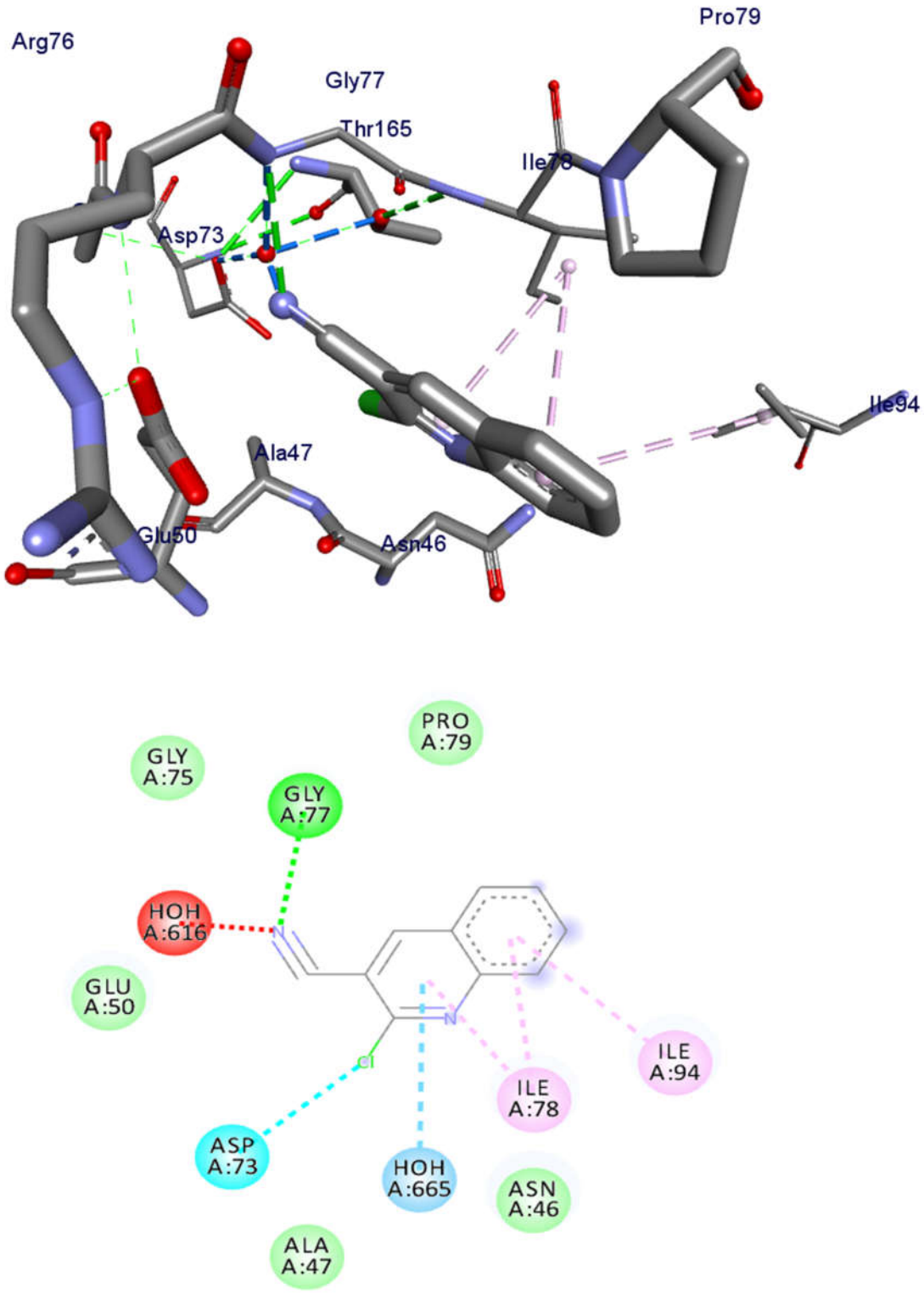

Figure 21: The binding interactions of compound **133** against *E. coli* DNA gyraseB (PDB ID: 6F86).

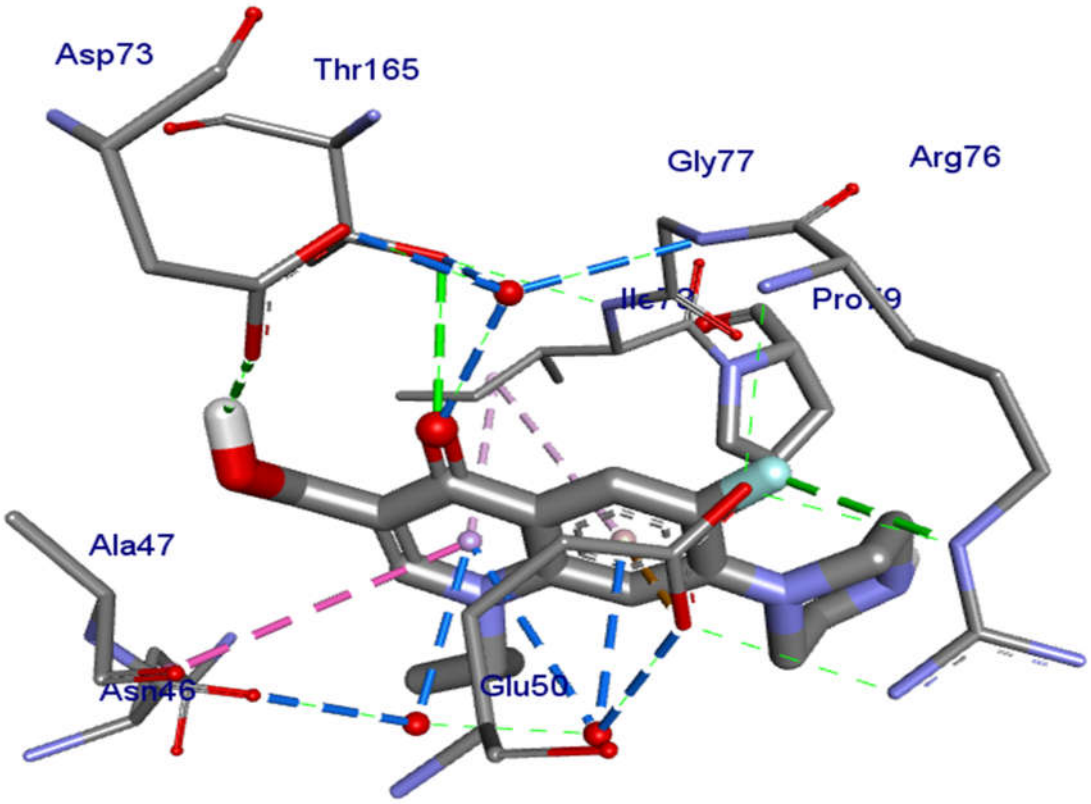
Asp73
Thr165
Gly77
Arg76
Ala47
Asn46
Glu50

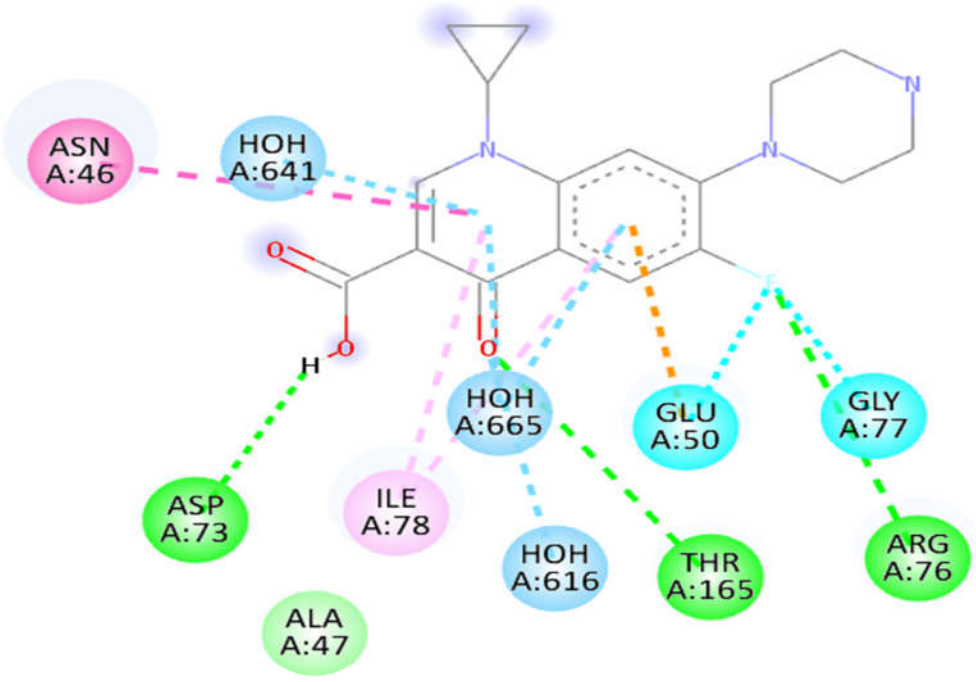

Figure 22: The binding interactions of Ciprofloxacin against *E. coli* DNA gyraseB (PDB ID: 6F86).

4.6 *In silico* molecular docking analysis of the synthesized compounds (129-133) against Human *Topoisomerase IIα.*

The type two *topoisomerase* is an enzyme belonging to a human *topoisomerase* that cut both strands of the DNA helix simultaneously in order to manage DNA tangles and supercoils. They use the hydrolysis of ATP, unlike type I *topoisomerase*. Human DNA *topoisomerase II* is an important target in anticancer therapy. The human *topoisomerase II* enzyme is essential to controls the topology of DNA during transcription, replication, and recombination by introducing transient breaks to both DNA strands. Therefore, in this study, the molecular docking analysis of the synthesized compounds was conducted to investigate their binding pattern with DNA *topoisomerase II-α* and compared them with standard inhibitor (Vosaroxin), which is anticancer drug. The synthesized compounds (**129-133**) were found to have minimum binding energy ranging from -6.9 to -7.3 kcal/mol (Table 4), with best results achieved with compound

132 (-7.3 kcal/mol), **129** (-7.1 kcal/mol) and **130** (-7.1 kcal/mol). The binding affinity, H-bond, and residual interaction of five compounds and vosaroxin were summarized in Table 4.

Table 10: Molecular docking value of synthesized compounds (**129-133**) against Human *Topoisomerase IIα* (PDB ID: 4fm9)

Compounds	Affinity (kcal/mol)	H-bond	**Residual Amino acid Interactions**	
			Hydrophobic/Pi-Cation/Pi-Anion/ Pi-Alkyl interactions	Van-der Walls interactions
129	-7.1	--	Pro-593, Leu-705, Gln-542	Asp-541, Glu-702, Lys-550, Ser-547, Asp-543, Gln-544, Asp-683, Tyr-684
130	-7.1	Leu-685, Gln-542	Leu-705, Pro-593, Lys-701, Tyr-686	Asp-683, Tyr-684, Glu-702, Ser-547, Tyr-590
131	-6.9	Ser-547, Leu-685, Gln-542	Pro-593, Leu-705, Lys-701	Asp-683, Tyr-684, Leu-592, Ser-591, Tyr-590, Ile-577
132	-7.3	Ser-591, Leu-685, Glu-702, Tyr-590, Leu-592, Gln-542	Pro-593, Leu-705, Lys-701	Asp-683, Asp-543, Ile-577
133	-7.0	Leu-685	Ile-577, Tyr-686, Leu-705	Ser-547, Lys-550, Gln-542, Tyr-590, Ser-591, Tyr-684, Lys-701, Glu-702
Vosaroxin	-7.2	Ser-591, Leu-685, Leu-592	Leu-705, Ile-577, Pro-593	Glu-682, Tyr-684, Arg-672, Gln-542

Compared to vosaroxin, the synthesized compounds (**129**, **130, 131** and **133**) showed similar residual interactions (Van-der Walls interaction) with amino acid residues Tyr-684. The

compound **133** also showed similar residual interactions with amino acid residue Gln-542. The compounds (**129-132**) showed similar residual interactions (hydrophobic/Pi-cation/Pi-anion/ Pi-alkyl interactions) with amino acid residues Leu-705 and Pro-593. Also the compound **133** showed similar residual interactions (hydrophobic/Pi-cation/Pi-anion/ Pi-alkyl interactions) with amino acid residues Leu-705 and Ile-577. The compound **132** showed additional hydrogen bonding interactions with amino acid residues Ser-591 and Leu-685. The compounds **130**, **131** and **133** also showed additional hydrogen bonding interactions with amino acid residues Leu-685. The compounds **129**, **130** and **133** docking results partially matched the vosaroxin interactions with amino acid residues. The compound **132** docking results stronger than that vosaroxin interactions with amino acid residues. Therefore, compounds **129, 130** and **132** might have the best anticancer agents among the synthesized compounds in this study. The 3-dimensional binding interaction of synthesized compounds (**129-133**) and vosaroxin against human *topoisomerase II-α* is illustrated below.

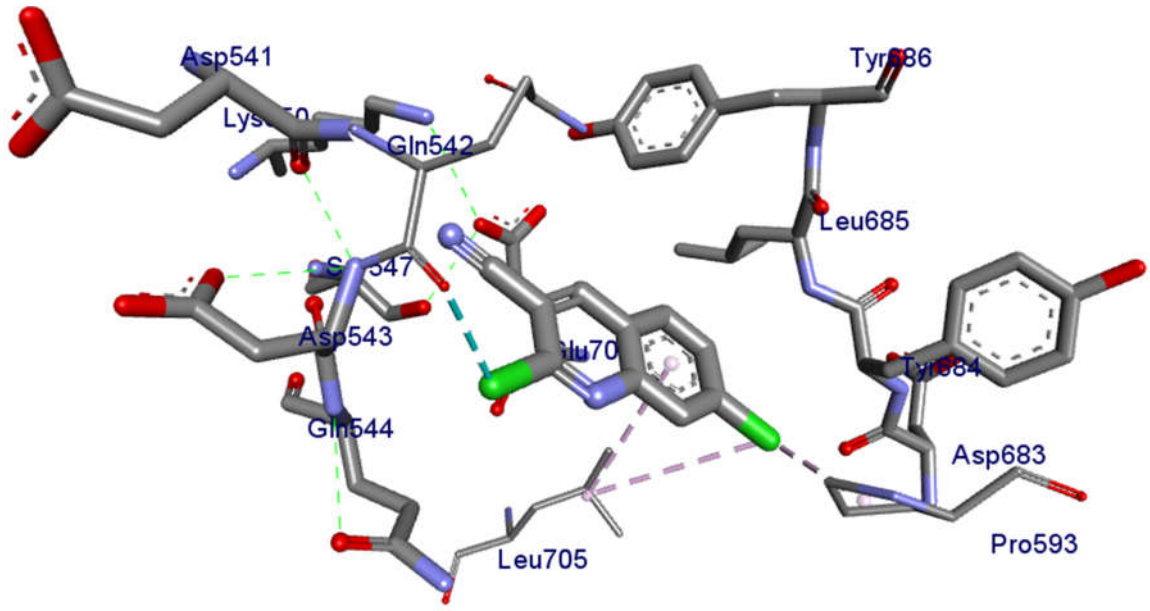

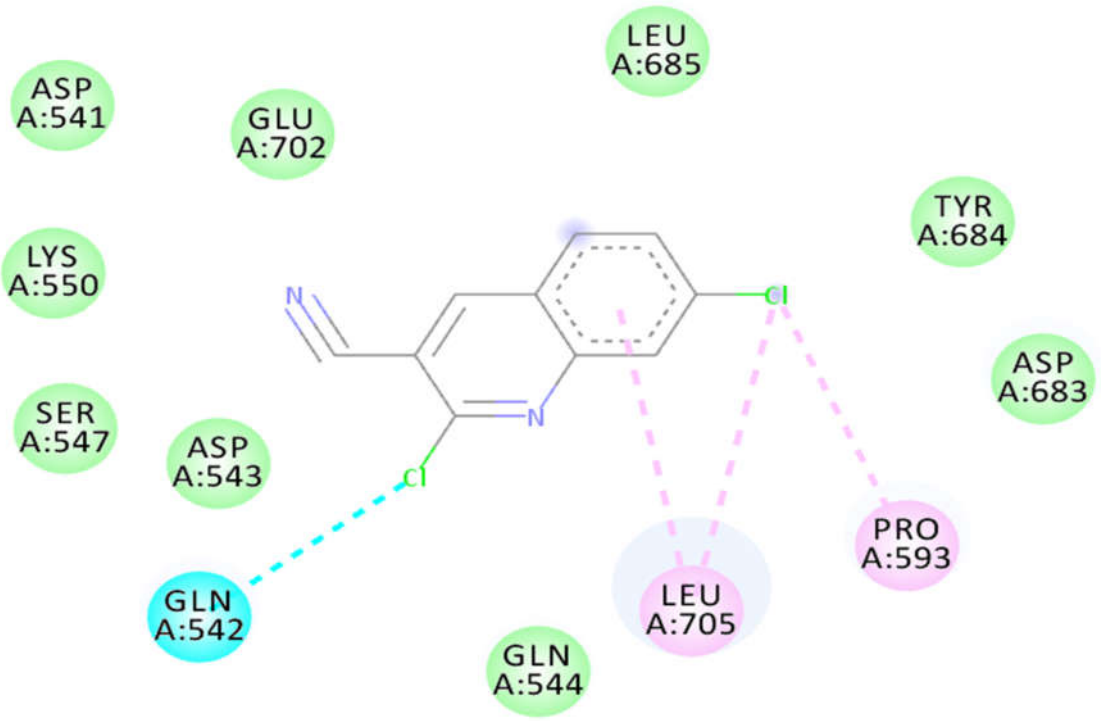

Figure 23: The binding interactions of compound **129** against Human *Topoisomerase IIα* (PDB ID: 4fm9).

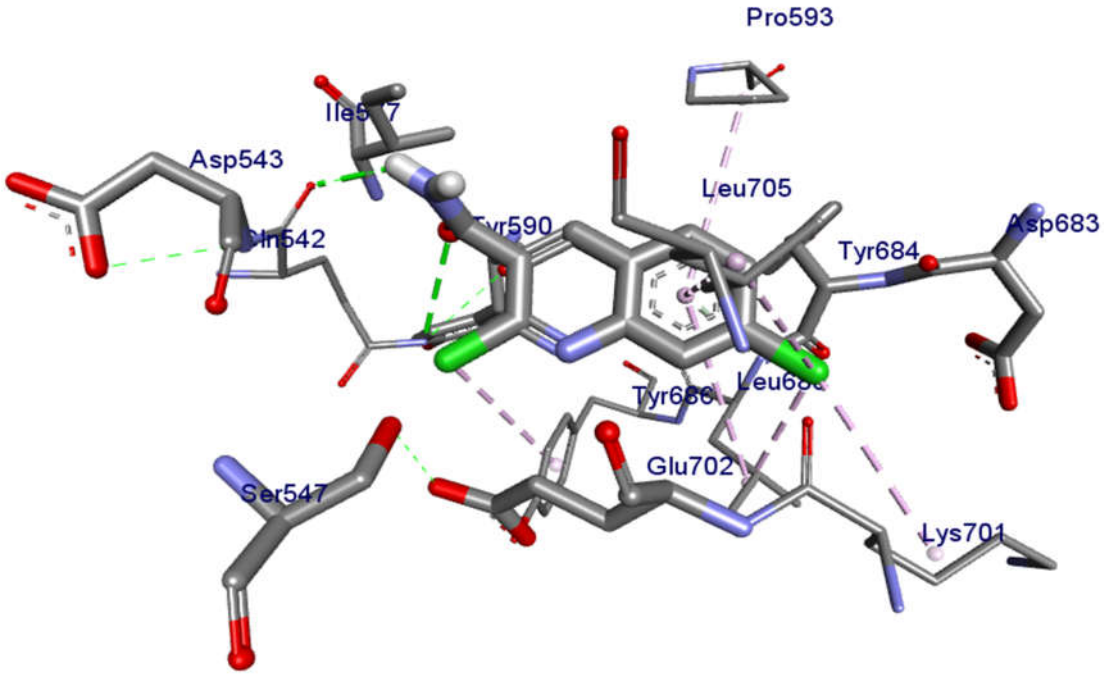

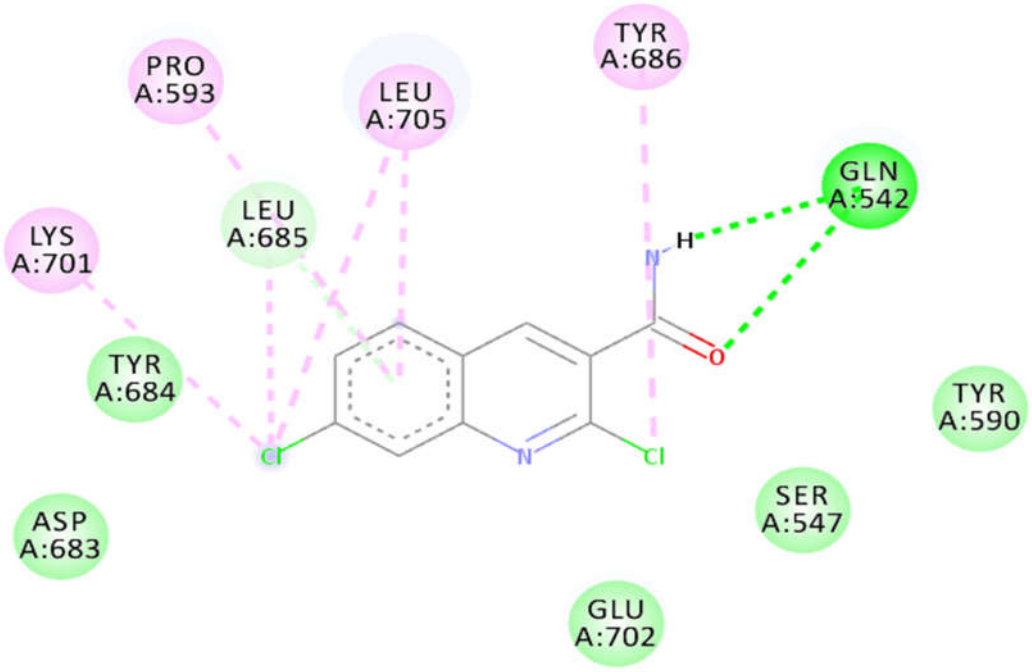

Figure 24: The binding interactions of compound **130** against Human *Topoisomerase IIα* (PDB ID: 4fm9).

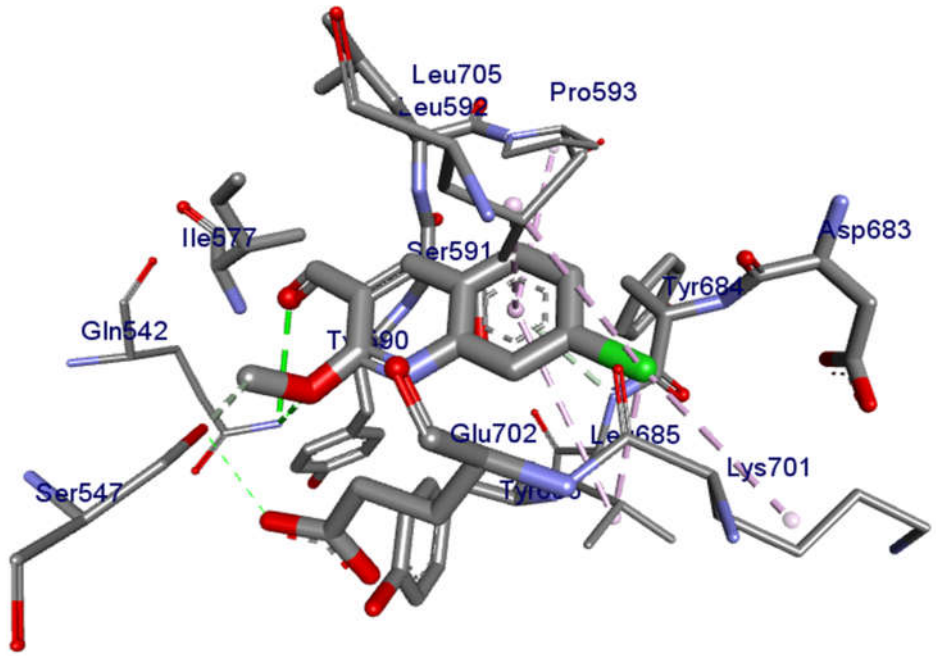

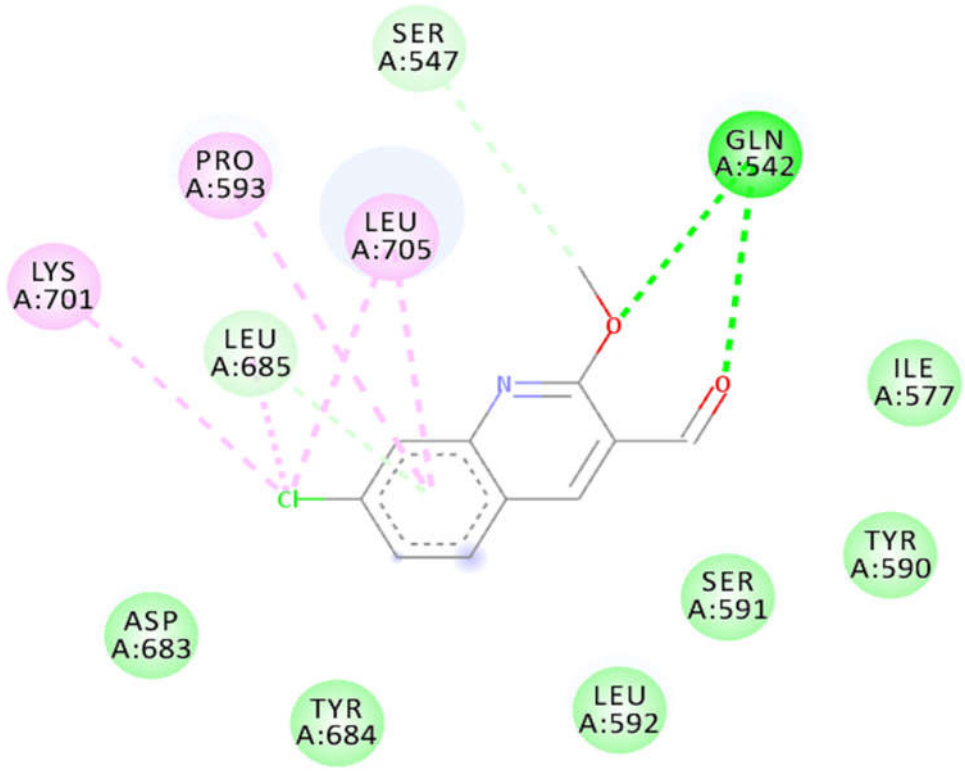

Figure 25: The binding interactions of compound **131** against Human *Topoisomerase IIα* (PDB ID: 4fm9).

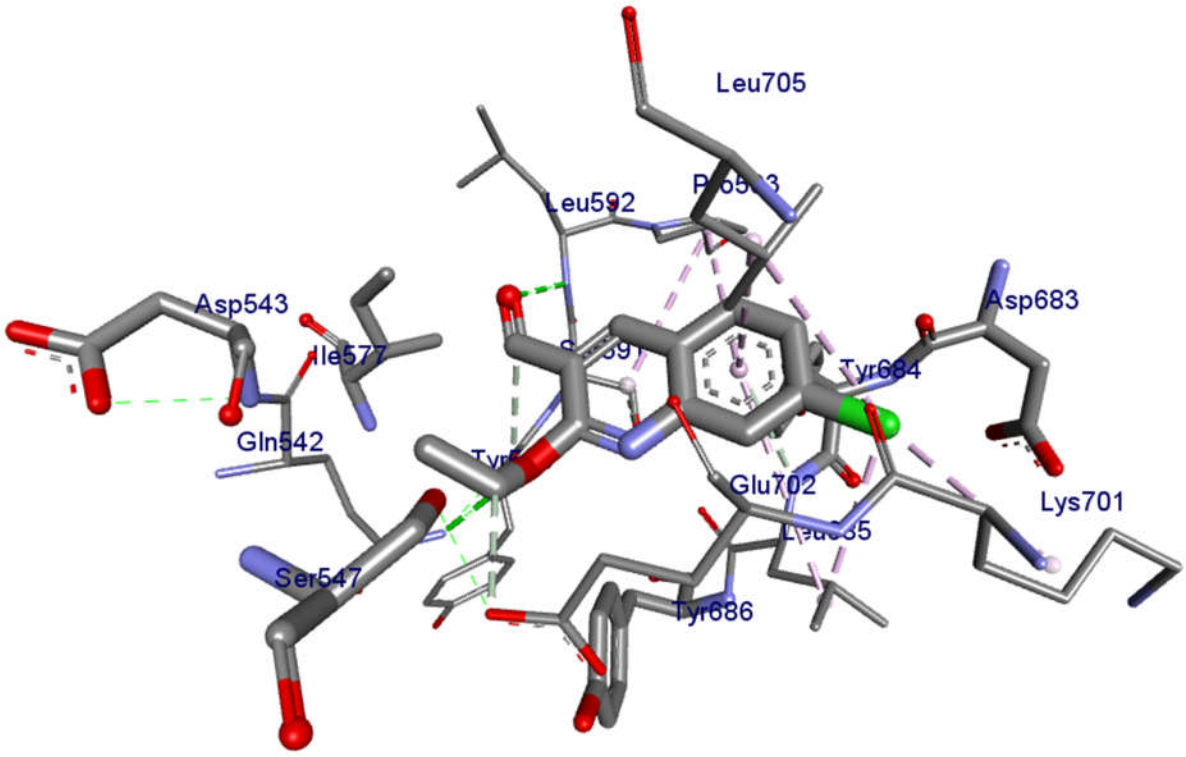

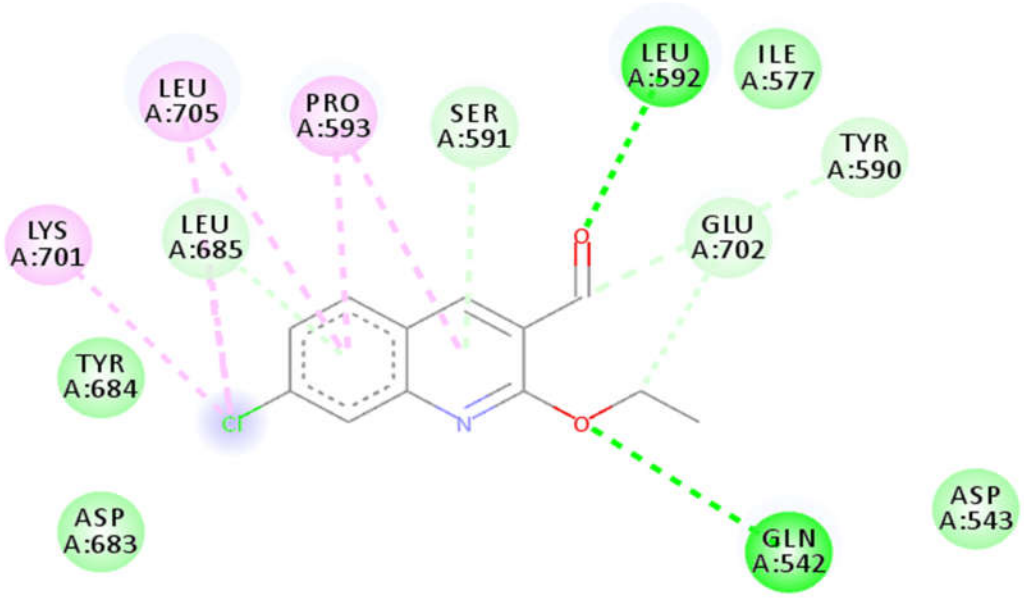

Figure 26: The binding interactions of compound **132** against Human *Topoisomerase IIα* (PDB ID: 4fm9).

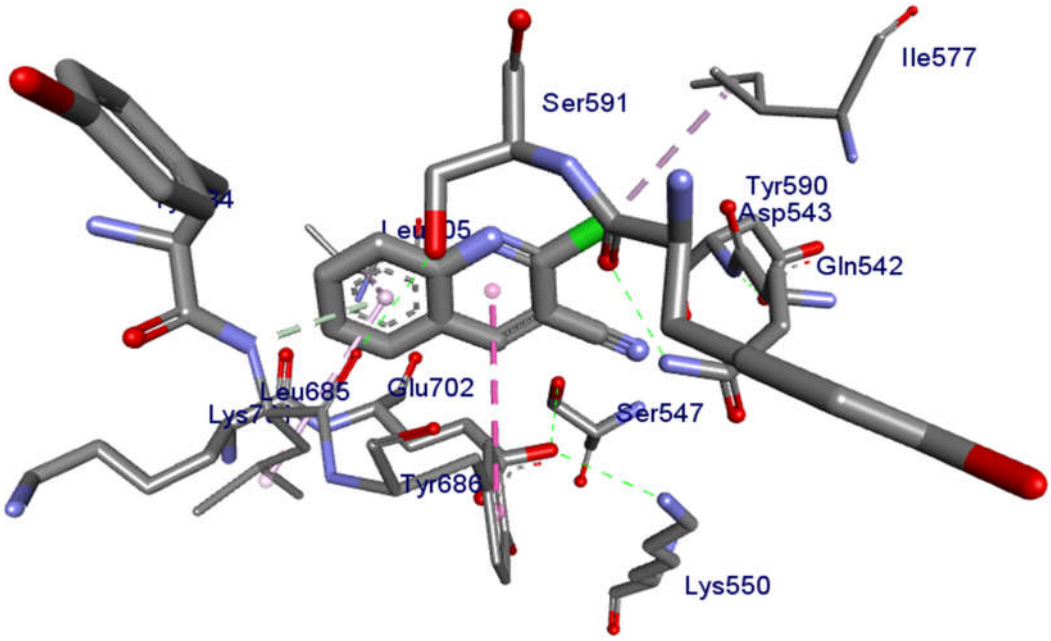

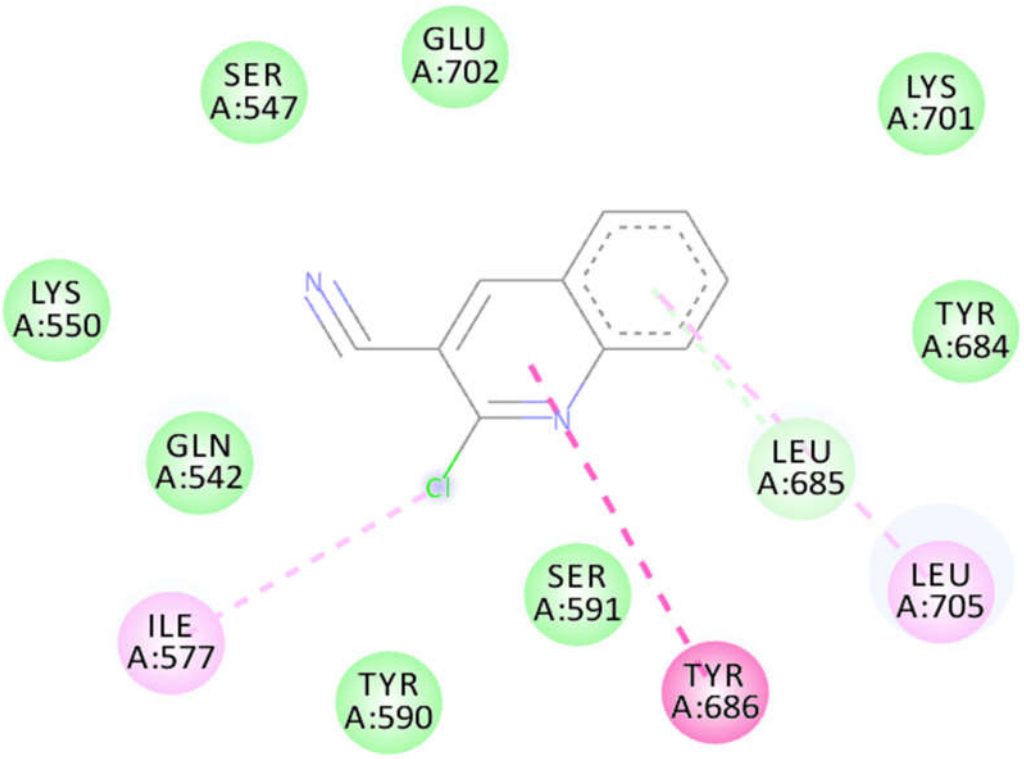

Figure 27: The binding interactions of compound **133** against Human *Topoisomerase IIα* (PDB ID: 4fm9).

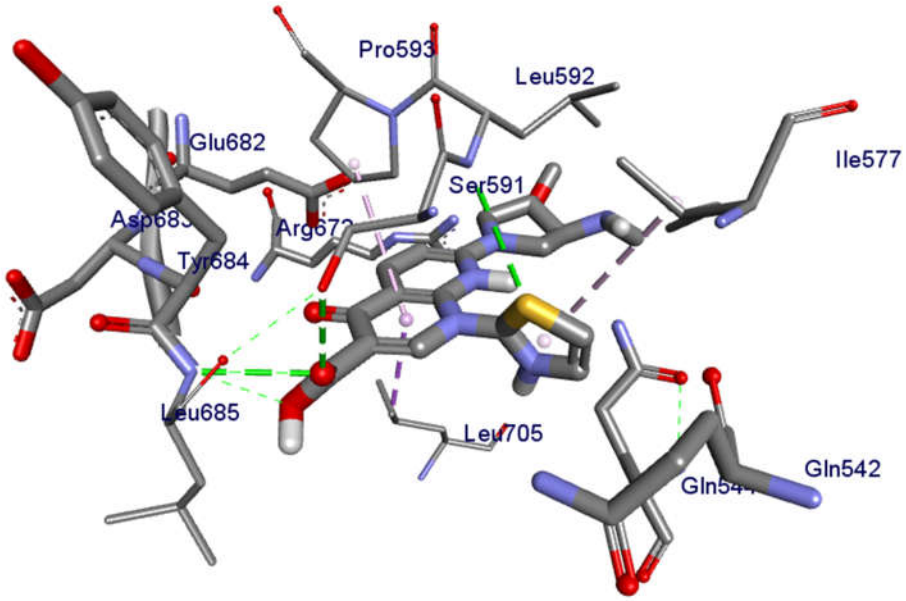

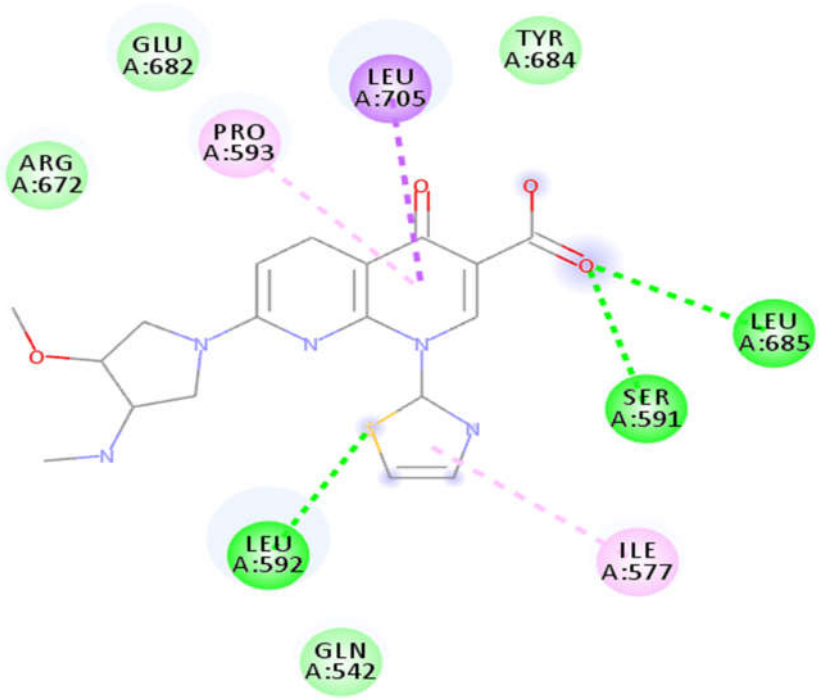

Figure 28: The binding interactions of vosaroxin against Human *Topoisomerase IIα* (PDB ID: 4fm9).

A drug-likeness prediction model introduced by Wagener *et al*. (2000), involved molecular descriptors related to numbers of different atom types and decision trees for discriminating between potential drugs and non-drugs. The drug-likeness of synthesized compounds were depicted in Table 5. ADME describes the disposition and fate of pharmaceutical compounds within an organism, especially in the human body. The primary cause of failure during the drug development phase is poor pharmacokinetics (PK) and toxicity rather than poor efficacy of the candidate compound. The ADME prediction of synthesized compounds were depicted in Table 6. The prediction of compound toxicities is an important part of the drug design development process. ProTox-II incorporates molecular similarity, fragment propensities, most frequent features and machine-learning, based a total of 33 models for the prediction of various toxicity endpoints such as acute toxicity, hepatotoxicity, cytotoxicity, carcinogenicity, mutagenicity, immunotoxicity, adverse outcomes pathways and toxicity targets.

Table 11: Drug-likeness predictions of compounds **129-133** computed by SwissADME.

Compounds	Formula	Mol. Wt. (g/mol)	NRB	NHA	NHD	TPSA ($A^{°2}$)	LogP (cLogP)	Lipinski's rule of Five Violation
129	$C_{10}H_4Cl_2N_2$	223.06	0	2	0	36.68	2.13	0
130	$C_{10}H_6C_{l2}N_2O$	241.07	1	2	1	55.98	1.85	0
131	$C_{11}H_8ClNO_2$	221.64	2	3	0	39.19	2.36	0
132	$C_{12}H_{10}ClNO_2$	235.67	3	3	0	39.19	2.37	0
133	$C_{10}H_5ClN_2$	188.61	0	2	0	36.68	1.91	0
Vosaroxin	$C_{18}H_{19}N_5O_4S$	401.45	5	9	2	136.13	0.963	0

NHD = Number of Hydrogen donor, NHA = Number of Hydrogen acceptor

NRB = Number of rotatable bonds, and TPSA = total polar surface area

The SwissADME predicted results showed that the synthesized compounds **129–133** satisfy Lipinski's rule of five with zero violations for their drug like molecular nature (Table 5). According to the Lipinski's rule of five, the molecular weight of the molecules should be less than 500, the number of hydrogen bond acceptors less than ten, number of hydrogen bond donors less than five and the lipophilicity (cLogP) values should be less than five [55]. The SwissADME predicted LogP values are in the range from 1.85 to 2.37 assuring optimal lipophilicity of the synthesized compounds. In addition, TPSA of the synthesized molecules were used predict percent absorption descriptor. The predicted TPSA value in ($Å^2$) for synthesized compounds were ranged from 36.68 to 55.98 inferring very good absorption. It has been suggested that molecules with a TPSA of 140 $Å^2$ and above would be poorly absorbed (< 10 percent fractional absorption), while compounds with a TPSA less than 60 $Å^2$ would be well absorbed (> 90 percent) [56].

Table 12: ADME predictions of compounds **129-133** computed by SwissADME and PreADMET.

Compounds	Chemical Formula	Skin Permeation Value (log Kp) cm/s	GI Absorption	BBB Permeability	Inhibitor Interaction (SwissADME/PreADMET)					
					P-gp substrate	CYP1A2 inhibitor	CYP2C19 inhibitor	CYP2C9 inhibitor	CYP2D6 inhibitor	CYP3A4 inhibitor
129	$C_{10}H_4Cl_2N_2$	-5.18	High	Yes	No	Yes	Yes	No	No	No
130	$C_{10}H_6C_{l2}N_2O$	-5.88	High	Yes	No	Yes	Yes	No	No	No
131	$C_{11}H_8ClNO_2$	-5.82	High	Yes	No	Yes	Yes	No	No	No
132	$C_{12}H_{10}ClNO_2$	-5.64	High	Yes	No	Yes	Yes	No	No	No
133	$C_{10}H_5ClN_2$	-5.41	High	Yes	No	Yes	No	No	No	No
Vosaroxin	$C_{18}H_{19}N_5O_4S$	-8.98	High	No	Yes	Yes	No	No	No	No

GI = Gastro-Intestinal, BBB = Blood Brain Barrier, P-gp = P-glycoprotein, CYP = Cytochrome-P

Pharmacokinetically, all synthesizes compounds have high GI absorption, Blood Brain Barrier (BBB) permeability, medium skin permeation value and none of the synthesized compounds were predicted to as P-glycoprotein substrate (Table 6). Under normal physiological conditions, the substance enter to the brain requires lipid soluble, less than 400 Daltons, and not substrate of active efflux transporters (AET). In this study, all synthesized compounds were passed through blood brain. Besides, the interaction of therapeutic molecules with cytochromes P450 (CYP) isoforms as substrate of these enzymes has been proposed to screen a therapeutically active molecule. It is reported that the inhibition of CYP isoezymes is certainly one major cause of pharmacokinetics-related drug-drug interactions there by leading to toxic or adverse effects due to the lower clearance and accumulation of the drug or its metabolites [57]. The synthesized compounds were none inhibitors of three enzymes namely; CYP2C9, CYP2D6 and CYP3A4,

and inhibitors of CYP1A2 and CYP2C19 except compound **133** not inhibited CYP2C19. All synthesized compounds were similar with vosaroxin in all enzymes, except CYP2C19 which was not inhibited by compounds **129-132.**

Table 13: Toxicity prediction of compounds **129-133** computed by Pro-Tox II and OSIRIS Property Explorer.

Compounds	Formula	LD_{50} (mg/kg)	Toxicity Class	Organ Toxicity				
				Hepatotoxicity	Carcinogenicity	Immunotoxicity	Mutagenicity	Cytotoxicity
129	$C_{10}H_4Cl_2N_2$	5000	5	Inactive	Inactive	Inactive	Inactive	Inactive
130	$C_{10}H_6C_{l2}N_2O$	705	4	Inactive	Inactive	Inactive	Inactive	Inactive
131	$C_{11}H_8ClNO_2$	2190	5	Inactive	Active	Inactive	Inactive	Inactive
132	$C_{12}H_{10}ClNO_2$	2190	5	Inactive	Active	Inactive	Inactive	Inactive
133	$C_{10}H_5ClN_2$	1100	4	Inactive	Inactive	Inactive	Inactive	Inactive
Vosaroxin	$C_{18}H_{19}N_5O_4S$	500	4	Active	Inactive	Inactive	Inactive	Inactive

The organ toxicity (hepatotoxicity) and toxicological end points (carcinogenicity, immunotoxicity, mutagenicity and cytotoxicity) of the synthesized compounds were predicted. The Pro Tox II predicted organ toxicity results revealed that all the synthesized compounds were inactive in hepatotoxicity, immunotoxicity, mutagenicity and cytotoxicity. The compounds **129**,**130** and **133** were also inactive in carcinogenicity and compounds **131** and **132** have carcinogenic properties. Almost all synthesized compounds have similar with vosaroxin in immunotoxicity, mutagenicity, cytotoxicity and carcinogenicity properties, but none hepatotoxicity whereas vosaroxin was hepatotoxic. LD_{50} is the amount of substance given all at

once, which causes the death of 50% (one half) of a group of tested animals. It's one way to measure the acute toxicity of materials. The order of toxicity of synthesized compounds toward human body **130** (LD_{50} = 705) > **133** (LD_{50} =1100) > **131** and **132** (LD_{50} =2190) > **129** (LD_{50} = 5000). The "Lethal Dose" of compound **129** was higher than other synthesized compounds, whereas the compound **130** was least. In this study, "Lethal Dose" of compound **130** was closer to control (vosaroxin) than other synthesized compounds.

5. CONCLUSION and RECOMMENDATION

The quinoline heterocycle is a useful scaffold to develop bioactive molecules. In the present work, a series of quinoline derivatives were synthesized by Vilsmeier–Haack reaction. Methanol and Ethanol (nucleophiles) were introduced into 2,7-dichloroquinoline-3-carbaldehyde by substitution of chlorine at 2-position using potassium carbonate in DMF solvent. The carbaldehyde functional group of 2,7-dichloroquinoline-3-carbaldehyde and 2-chloroquinoline-3-carbaldehyde was further manipulated to nitriles using phosphorous oxychloride and sodium azide. The nitrile functional group of 2,7-dichloroquinoline-3-carbonitrile was converted to amide using acetic acid and sulfuric acid. All synthesized compounds were characterized by ^{1}H NMR, ^{13}C NMR, and UV-Vis spectroscopy. The antibacterial activities of the synthesized compounds were screened by the disc-diffusion method against two Gram-negative and two Gram-positive bacteria, and most of them were found to have weak to moderate activities against the bacterial strains used for the screening. Among them, two compounds; **132** and **130** showed good activities against *E. coli* at mean inhibition zones of 12 ± 0 and 11 ± 0.04 mm, and the compound **129** also good activity against *S. aureus* and *P. aeruginosa* with 11 ± 0.03 mm at 200µg/mL when compared with standard amoxicillin. The compound **131** at 200µg/mL concentration showed good activity against *S. pyrogenes* with mean inhibition of 11 ± 0.02 mm. The radical scavenging properties of the synthesized compounds were evaluated by DPPH assay among them; compounds **130** and **129** are high antioxidant activity with IC_{50} of 0.31 and 2.17 µg/mL relative to ascorbic acid respectively. The synthesized compounds were docked against human *topoisomerase IIα* in order to investigate their anticancer potency. The compound **132** showed strong binding affinity (-7.3 kcal/mol) for the enzyme than the reference drug or vosaroxin (-7.2 kcal/mol), which might have better anticancer activity.

As quinoline derivatives may have biological activities it is important to evaluate the antiviral, antifungal, anticancer, anti-inflammatory activities and others activities of synthesized compounds.

The synthesized compounds have two or three reactive site; these may have many options to further derivation and evaluation of biological activities.

Research Fund Acknowledgment

This research project is funded by Adama Science and Technology University under the grant number ASTU/SM-R/269/21, Adama, Ethiopia.

6. REFERENCES

1. Ilango, K., Valentina, P., Subhakar, K., and Kathiravan, M. (2015), 'Design, Synthesis and Biological Screening of 2, 4-Disubstituted Quinolines', *Austin J Anal Pharm Chem*., 2(4): 1048-1068.

2. Eisner, T., Morgan, R.C., Attygalle, A. B., Smedley, S. R., Herath, K. B., and Meinwald, J. (1997), 'Defensive Production of quinoline by a phasmid insect (Oreophoetes peruana)', J. *Exp. Biol.*, 200: 2493–2500.

3. Sharma, P., Kaur, K., Chawla, A., Singh, R., and Singh, R. (2016), 'Review on Biological Activities of Quinoline Derivatives', *Journal of Management, Information Technology and Engineering (BEST: JMITE),* Vol. 2, Issue 1: 1-14.

4. Sandhya, B., Suresh, K., Sushma, D., and Rajiv, K. (2010), 'Structural modifications of quinoline-based antimalarial agents: Recent developments', J Pharm Bioallied Sci., 2(2): 64–71.

5. Sujeet, K. G., and Ashutosh, M. (2016), Synthesis, Characterization & Screening for Anti-Inflammatory & Analgesic Activity of Quinoline Derivatives Bearing Azetidinones Scaffolds', *Anti-Inflammatory & Anti-Allergy Agents in Medicinal Chemistry*, 15: 31-43.

6. Jayakumar, S. B., Praveen, Y., Pramod, N., Shivkumar, B., Shivkumar, H., and Nagendra, R. R. (2012), 'Synthesis, characterization and anti-inflammatory activity of 3-formyl 2-hydroxy quinoline thiosemicarbazides', *Journal of Pharmacy Research*, 5(5): 2735-2737.

7. Shweta, J., Vikash, C., Pankaj, K. J., Kamla, P., Devendra, P., and Ankur, V. (2019), 'Comprehensive review on current developments ofquinoline-based anticancer agents', *Arabian journal of chemistry*, 12: 4920-4946.

8. Peng, T., Chunhui, L., Zhong, P., Anne, M. V., Alekhya, N., Ma, S., Yaqiong, L., Xingmin, S., and Jianfeng, C. (2018), 'Facilely accessible quinoline derivatives as potent antibacterial agents', *Bioorganic & Medicinal Chemistry,* 26: 3573–3579.

9. Himank, K., Vinod, D., Ritika, J., Manojkumar, J., Piyush, A., Prasath, R., Bhavana, P., and Sujit, K. G. (2015), 'Antihypertensive activity of a quinoline appendedchalcone derivative and its site specific bindinginteraction with a relevant target carrier protein', *RSC Adv*., 5: 65496.

10. Sumesh, E., Airody, V. A., and N. Suchetha, Sh. (2009), 'Synthesis and antimicrobial activities of novel quinoline derivatives carrying1,2,4-triazole moiety', *European Journal of Medicinal Chemistry,* 44: 4637–4647.

11. Manske, R. H. and Kula, M. (1953), 'The Skraup Synthesis of Quinolines', *Organic Reactions,* vol. 7: pp. 59-98.

12. Denmark, S. E. and Venkatraman, S. (2006), 'On the Mechanism of the Skraup Doebner-Von Miller Quinoline Synthesis', *Journal of Organic Chemistry,* vol. 71: pp. 668-676.

13. Cohn, E. W. (1930), 'A modification of the Skraup synthesis of quinolone', *Journal of the American Chemical Society,* vol. 52: pp. 3685-3688.

14. Yale, H. L. (1947), 'The Skraup Reaction with Acrolein and its Derivatives. I. The Preparation of 6-Methoxy-8-nitroquinoline', *Journal of the American Chemical Society,* vol. 69: p. 1230.

15. Yale, H. L., and Bernstein, J. (1947), 'The Skraup Reaction with Acrolein and its Derivatives', *Journal of the American Chemical Society,* vol. 70: p. 254.

16. Saggadi, H., Luart, D., Thiebault, N., Polaert, I., Estel, L. and Len, C. (2014), 'Quinoline and phenanthroline preparation starting from glycerol via improved microwave-assisted modified Skraup reaction', *RSC Advances,* vol. 4: pp. 21456-21464.

17. Gaina, L., Cristea, C., Moldovan, C., Porumb, D., Surducan, E., Deleanu, C., Mahamoud, A., Barbe, J., and Silberg, I. A. (2007), 'Microwave-assisted synthesis of phenothiazine and quinolone derivatives', *International Journal of Molecular Sciences,* vol. 8: pp. 70-80.

18. Badger, G., Crocker, H., Ennis, B., Gayler, J., Matthews, W., Raper, W., Samuel, E. L., and Spotswood, T. (1963), 'Studies on the Doebner-Miller, Skraup, and related reactions', *Australian Journal of Chemistry,* vol. 16: pp. 814-827.

19. Marco-Contelles, J., Perez-Mayoral, E., Samadi, A., Carmo, C., and Soriano, E. (2009), 'Recent advances in the Friedlander Reaction', *Chemical Reviews,* vol. 109: pp. 2652-2671.

20. Zhou, P., Hu, B., Zhao, S., Zhang, Q., Wang, Y., Li, X., and Yu, F. (2018), 'An improved Pfitzinger reaction for the direct synthesis of quinoline-4-carboxylic esters/acids mediated by TMSCl', *Tetrahedron letters*, 59: 3116-3119.

21. Al-juboorya, S., and Kubba, M. (2016), 'Synthesis, characterization and antifungal evaluation of some novel quinolone derivatives derived from ethyl p-aminobenzoate', *Der Pharma Chemica*, 8 (4): 63-66.

22. Aghera, V., Patel, J., and Parsania, P. (2008), 'Synthesis, spectral and microbial studies of some novel quinoline derivatives via Vilsmeier–Haack reagent', *ARKIVOC*, (xii): 195-204.

23. Ginelle, A. R., and Bryan, J. C. (2016), 'Recent Advances in Metal-Free Quinoline Synthesis', *Molecules***,** 21: 986.

24. Brouet, J.C., Gu, S., Peet, N. P., and Williams, J. D. (2009), **'**A survey of solvents for the Conrad-Limpach synthesis of 4-hydroxyquinolones', *Synth. Commun.*, *39*: 5193–5196.

25. Bergstrom, F. W. (1944), 'Heterocyclic Nitrogen Compounds', Part IIA. 'Hexacyclic Compounds: Pyridine, Quinoline, and Isoquinoline', *Chem. Rev.,* 35 (2): 156.

26. Thomas, K.D., Airody, V. A., and Suchetha, Sh. (2010), 'Design, synthesis and antimicrobial activities of some new quinoline derivativescarrying 1,2,3-triazole moiety', *European Journal of Medicinal Chemistry,* 45: 3803-3810.

27. Shaharyar, M., Siddiqui, A.A., Ali, M.A., Sriram, D., and Yogeeswari, P. (2006), 'Synthesis and in vitro antimycobacterial activityofN1-nicotinoyl-3-(40-hydroxy-30-methylphenyl)-5-[(sub)phenyl]-2-pyrazolines', *Bioorg. Med. Chem. Lett*., 13: 2213–2220.

28. Meth-Cohn, O., Narine, B., Tarnowski, B. (1981), 'A versatile newsynthesis of quinolines and related fused pyridines, Part 5. Thesynthesis of 2-chloroquinoline-3- carbaldehydes', *J. Chem. Soc.Perkin Trans.,* 1: 1520–1530.

29. Miniyar, P. B., Barmade, M. A., and Mahajan, A. A. (2015), 'Synthesis and biological evaluation of 1-(5-(2-chloroquinolin-3-yl)-3-phenyl-1H-pyrazol-1-yl) ethanone derivatives as potential antimicrobial agents', *Journal of Saudi Chemical Society,* 19: 655–660.

30. Dominguez, J.N., Leon, C., Rodrigues, J., Dominguez, N.G., Gut, J., and Rosenthal, P.J. (2009), 'Synthesis of chlorovinyl sulfones asstructural analogs of chalcones and their antiplasmodialactivities', *Eur. J. Med. Chem*., 44: 1457–1462.

31.Insuasty, B., Tigreros, A., Orozco, F., Quiroga, J., Aboní́a, R., Nogueras, M., Sanchez, A., and Cobo, J. (2010), 'Synthesis of novel pyrazolicanalogues of chalcones and their 3-aryl-4-(3-aryl-4,5-dihydro-1H-pyrazol-5-yl)-1-phenyl-1H-pyrazole derivatives as potentialantitumor agents', Bioorg. *Med. Chem.,* 18: 4965–4974.

32. Bakr, F. Abdel-Wahab, and Rizk, E. K. (2013), '2-Chloroquinoline-3-carbaldehyde II: Synthesis, Reactions, and Applications', *Journal of Chemistry,* Volume 2013, p. 13, Article ID 851297.

33. Konstantinovskii, L. E., Olekhnovitch, R. Y., Korobov, M. S., Nivorozhkin, L. E., and Minkin, V. I. (1991), 'Stereodynamical interconversion of bis(N-aryl-α-isopropyl-β aminovinylthionato) zinc(II) and -cadmium(II)', *Polyhedron*, vol. 10, no. 8: pp. 771–778.

34. Pawar, R. A., Bajare, P. B., and Mundade, S. B. (1990), 'Studies on Vilsmeier-Haack reaction: A new route to 2-chloroquinoline-3-carboxyaldehydes and a furoquinoline derivative', *Journal of the Indian Chemical Society*, vol. 67, no. 8: pp. 685–686.

35. Digafie, Z., Rajalakshmanan, E., Zerihun, B., and Yadessa, M. (2020), 'Synthesis and Antibacterial, Antioxidant, and Molecular Docking Analysis of Some Novel Quinoline Derivatives', *Journal of Chemistry*, Volume 2020, p. 16, Article ID 1324096.

36. Zeleke, D., Yadessa, M., Zerihun, B., and Rajalakshmanan, E. (2021), 'Synthesis, Molecular Docking Analysis, and Evaluation of Antibacterial and Antioxidant Properties of Stilbenes and Pinacol of Quinolines', *Advances in Pharmacological and Pharmaceutical Sciences*, Vol. 2021: 17 pages.

37. Ambika, S., Mrityunjay, K. S., and Singh, R. M. (2006), 'Pyrazolo-fused quinoline analogues: Synthesis of 1H-pyrazolo [3,4-b] quinolines and 3-amino-1H-pyrazolo [3,4-b] quinolines from 3-formyl and 3-cyano-2-chloroquinolines', *Ind. J. Chem*., 45B: 292-96.

38. Jia, W., Liu, Y., Li, W., Liu, Y., Zhang, D., Zhang, P., and Gong, P. (2009), 'Synthesis and in vitro anti-hepatitis B virus activity of 6*H*-[1]benzothiopyrano[4,3-*b*]quinolin-9-ols', *Bioorg. Med. Chem.*, *17*: 4569–4574.

39. Murat, B., Owen, T., Christopher, R. G., Selina, K. S., Greg, M. A., Glenn, M. M., Belamy, B. Ch., Naresh, K., and David, S. C. B. (2009), 'Synthesis, Characterization and Anti-Cancer Activity of Hydrazide Derivatives Incorporating a Quinoline Moiety', *Molecules x***,** 21: 916.

40. Rao, K. R., Bhanumathi, N., and Sattur, P. B. (1991), 'Synthesis of novel quino[2,3-*b*][1,5]benzodiazepin-12-ones', *J. Heterocycl. Chem.*, 28: 1339–1340.

41. Ibrahim, Ali, M., Tarek, M. Y., Emad, M. E., and Rizk, E. K. (2016), 'New Potential Antimalarial Agents: Design, Synthesis and Biological Evaluation of Some Novel Quinoline Derivatives as Antimalarial Agents', *Molecules*, 21: 909.

42. Sevene, E., Gonz*á*lez, R., and Men*é*ndez, C. (2010), 'Current knowledge and challenges of antimalarial drugs for treatment and prevention in pregnancy', *Expert Opin. Pharmacother*., 11: 1277–1293.

43. Xhamla, N., Naki, T. and Blessing, A. A. (2017), 'Quinoline-Based Hybrid Compounds with Antimalarial Activity', *Molecules*, 22: 2268.

44. Baba, A., Kawamura, N., Makino, H., Ohta, Y., Taketomi, S., and Sohda, T. (1996), 'Studies on disease-modifying antirheumatic drugs: synthesis of novel quinoline and quinazoline derivatives and their anti-inflammatory effect', *Journal of Medicinal Chemistry,* vol. 39: pp. 5176-5182.

45. Shraddha, M. P., Kinjal, D. P., Rajesh, H. V., Shyamali, N. P., and Hitesh, D. P. (2014), 'Recent advances in the synthesis of quinolones', *RSCAdv*., 4: 24463–24476.

46. Chen, Y. L., Huang, C. J., Huang, Z.Y., Tseng, C. H., Chang, F. S., Yang, S. H., Lin, S. R., and Tzeng, C. C. (2006), 'Synthesis and antiproliferative evaluation of certain 4-anilino-8-methoxy-2-phenylquinoline and 4-anilino-8-hydroxy-2-phenylquinoline derivatives', *Bioorg. Med. Chem.*, *14*: 3098–3105.

47. Adsule, S., Barve, V., Chen, D., Ahmed, F., Dou, Q. P., Padhye, S., and Sarkar, F. H. (2006), 'Novel Schiff base copper complexes of quinoline-2 carboxaldehyde as proteasome inhibitors in human prostate cancer cells', *J. Med. Chem.,* 49: 7242–7246.

48. Shi, A., Nguyen, T. A., Battina, S. K., Rana, S., Takemoto, D. J., Chiang, P.K., Hua, D.H. (2008), 'Synthesis and anti-breast cancer activities of substituted quinolones', *Bioorg. Med. Chem. Lett.*, 18: 3364–3368.

49. Cortes, J. E., Kantarjian, H. M., Brummendorf, T. H., Kim, D.W., Turkina, A. G., Shen, Z. X., Pasquini, R., Khoury, H. J., Arkin, S., Volkert, A., et al. (2011), 'Safety and efficacy of bosutinib (SKI 606) in chronic phase Philadelphia chromosome-positive chronic myeloid leukemia patients with resistance or intolerance to imatinib', *Blood,* 118: 4567–4576.

50. Cortes, J. E., Kim, D.-W., Kantarjian, H. M., Brümmendorf, T. H., Dyagil, I., Griskevicius, L., Malhotra, H., Powell, C., Gogat, K., Countouriotis, A. M., et al. (2012), 'Bosutinib versus Imatinib in Newly Diagnosed Chronic-Phase Chronic Myeloid Leukemia: Results from the BELA Trial', *J. Clin. Oncol.,* 30: 3486–3492.

51. Prabodh, Ch. S., Ankit, J., and Sandeep, J. (2009), 'Fluoroquinolone antibacterials: a review on chemistry, microbiology and therapeutic prospects', *Acta Poloniae Pharmaceutica ñ Drug Research,* Vol. 66 No. 6: pp. 587-604.

52. Nur, B., Azierah, A., Muhammad, M. M., and Khamsah, S. M. (2018), 'Chemical Composition and Antioxidant Activity of Stingless Bee Propolis from Different Extraction Methods', *International Journal of Engineering and Technology,* 7 (4.43): 90-95.

53. Raksha, M., Bharat, B., and Dhani, R. (2018), 'Variation in Antioxidant Activity of a Rattan Species, *Plectocomia himalayana* Griff by DPPH assay based on two different methods of Methanol Extraction', *Pharmacognosy and Phytochemistry*, 10 (2).

54. Antonio, G., Laurence, G., Perrine, S., Amelie, L., Severine, R., Amaury, F., and Patrick, D. (2011), 'Impact of aryloxy-linked quinazolines: A novel series of selective VEGFR-2 receptor tyrosine kinase inhibitors', *Bioorganic and Medicinal Chemistry Letters*, 21: 2106-2112.

55. Lipinski, C. A., *et al.* (1997), 'Experimental and computational approaches to estimate solubility and permeability in drug discovery and development settings', *Advanced drug delivery reviews*, 23(1-3): p. 3-25.

56. Clark, D. E. (1999), 'Rapid calculation of polar molecular surface area and its application to the prediction of transport phenomena. 1. Prediction of intestinal absorption', *Journal of pharmaceutical sciences,* 88(8): p. 807-814.

57. Hollenberg, P. F. (2002), 'Characteristics and common properties of inhibitors, inducers, and activators of CYP enzymes', *Drug metabolism reviews*, 34(1-2): p. 17-35.

APPENDIXS

Appendix 1: ^{1}H-NMR spectrum (400 MHz, $CDCl_3$ and MeOD-*d4*) of compound **128**

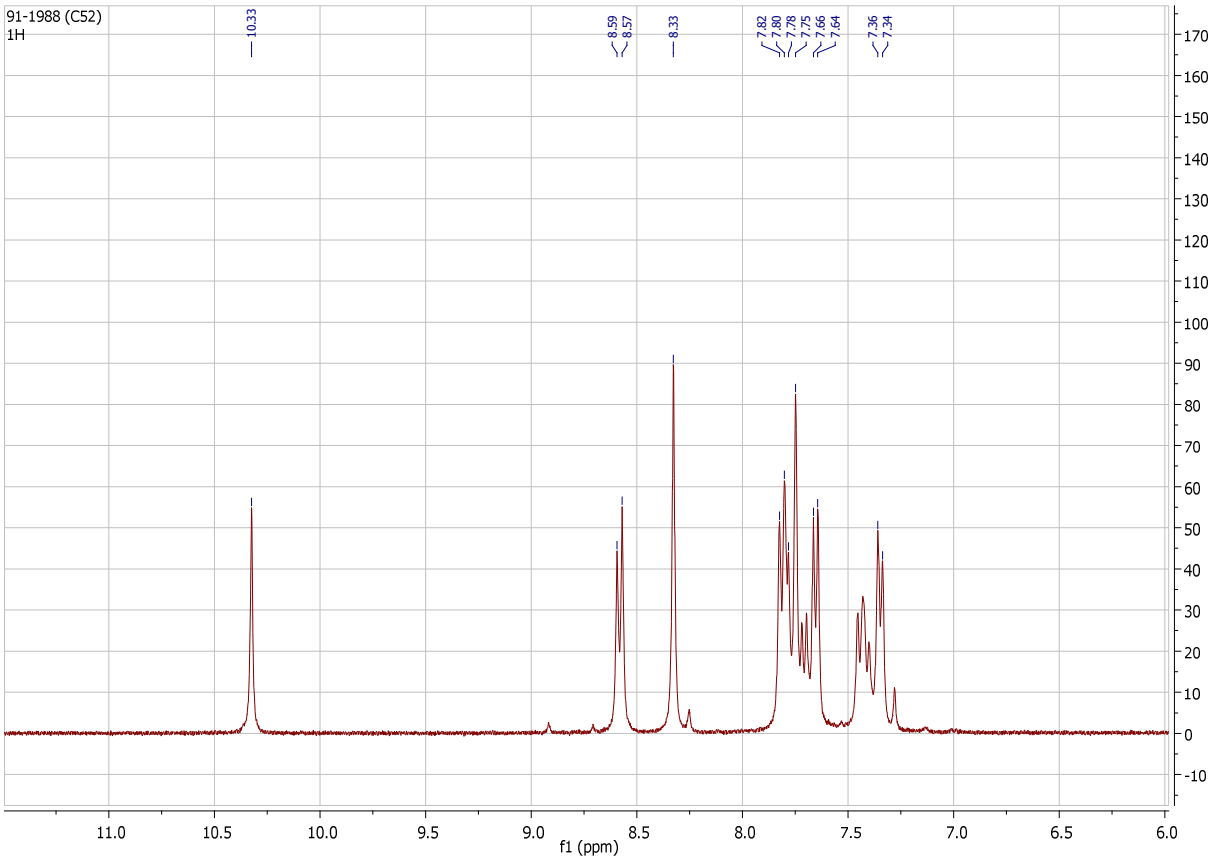

Appendix 2: ^{13}C-NMR spectrum (100 MHz, $CDCl_3$ and MeOD-*d4*) of compound **128**

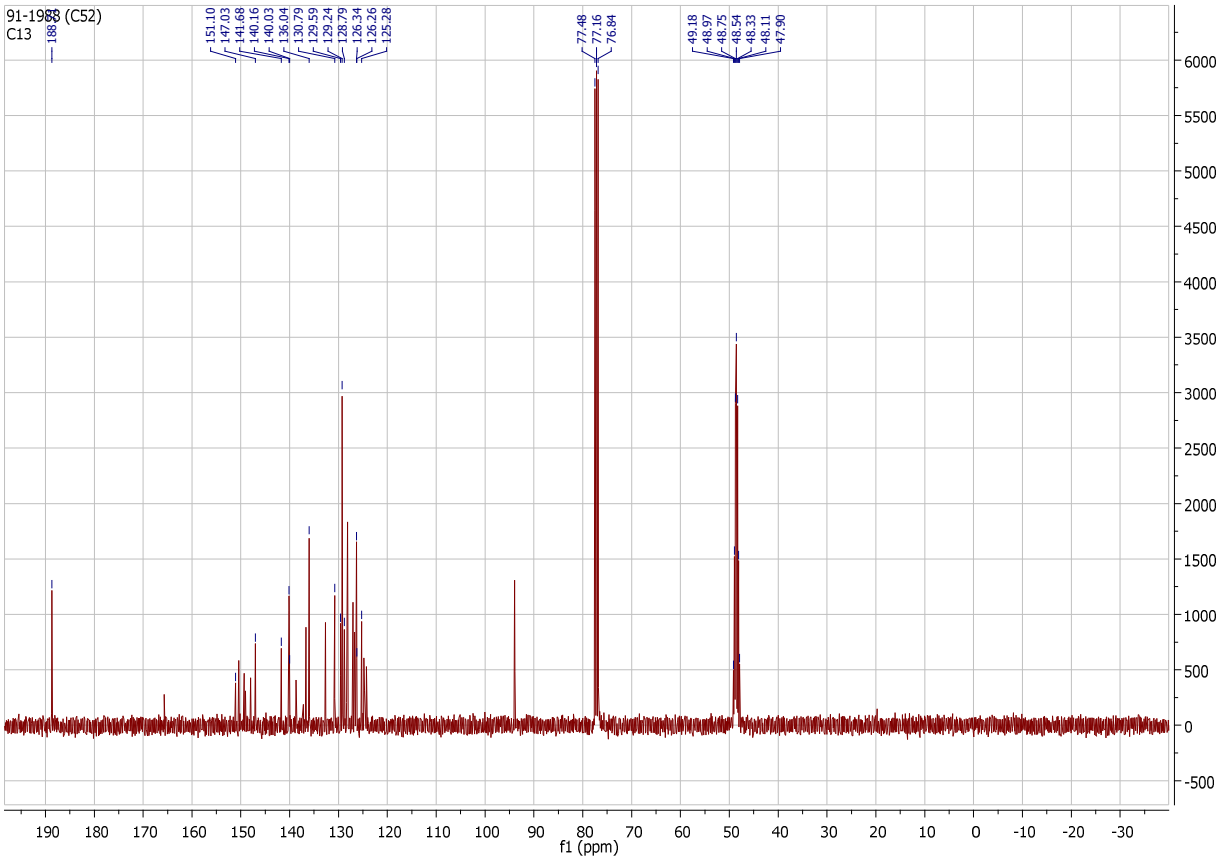

Appendix 3: ^{1}H-NMR spectrum (400 MHz, $CDCl_3$ and MeOD-*d4*) of compound **129**

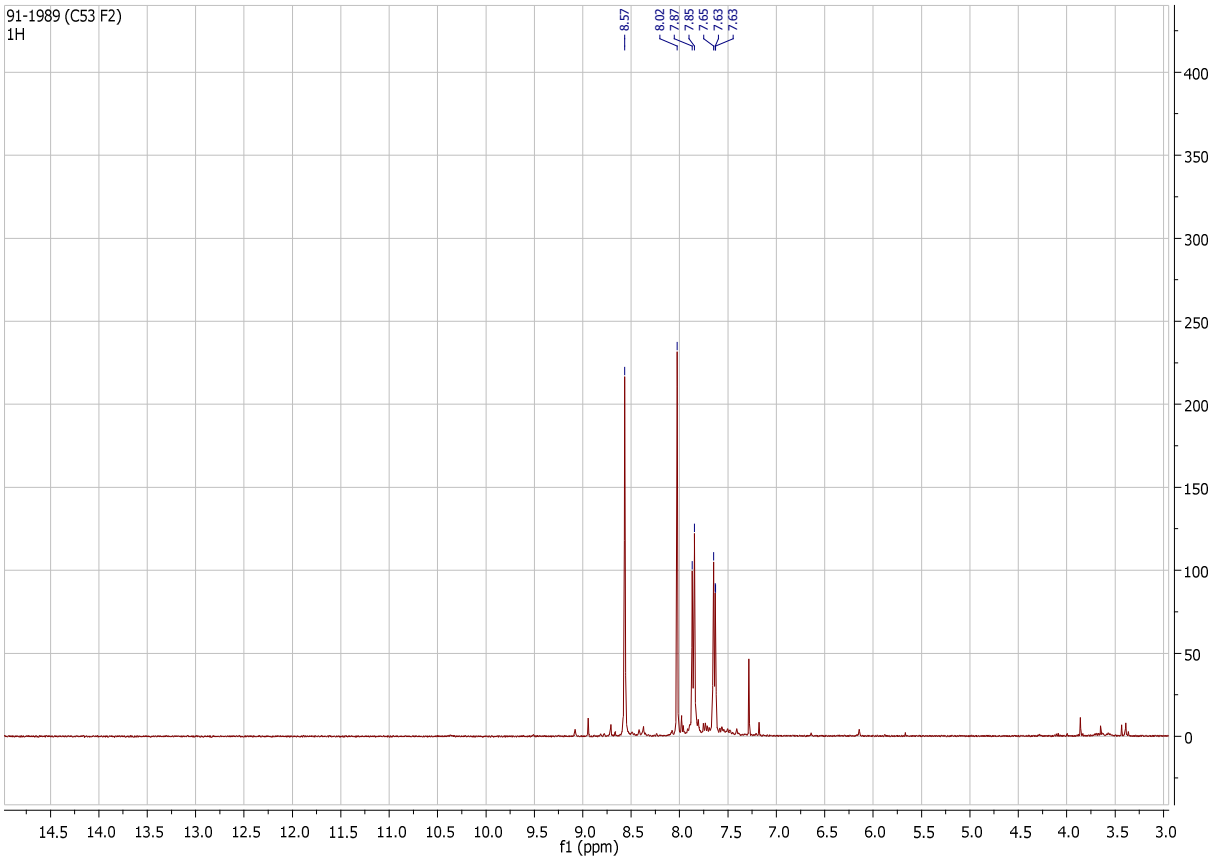

Appendix 4: ^{13}C-NMR spectrum (100 MHz, $CDCl_3$ and MeOD-*d4*) of compound **129**

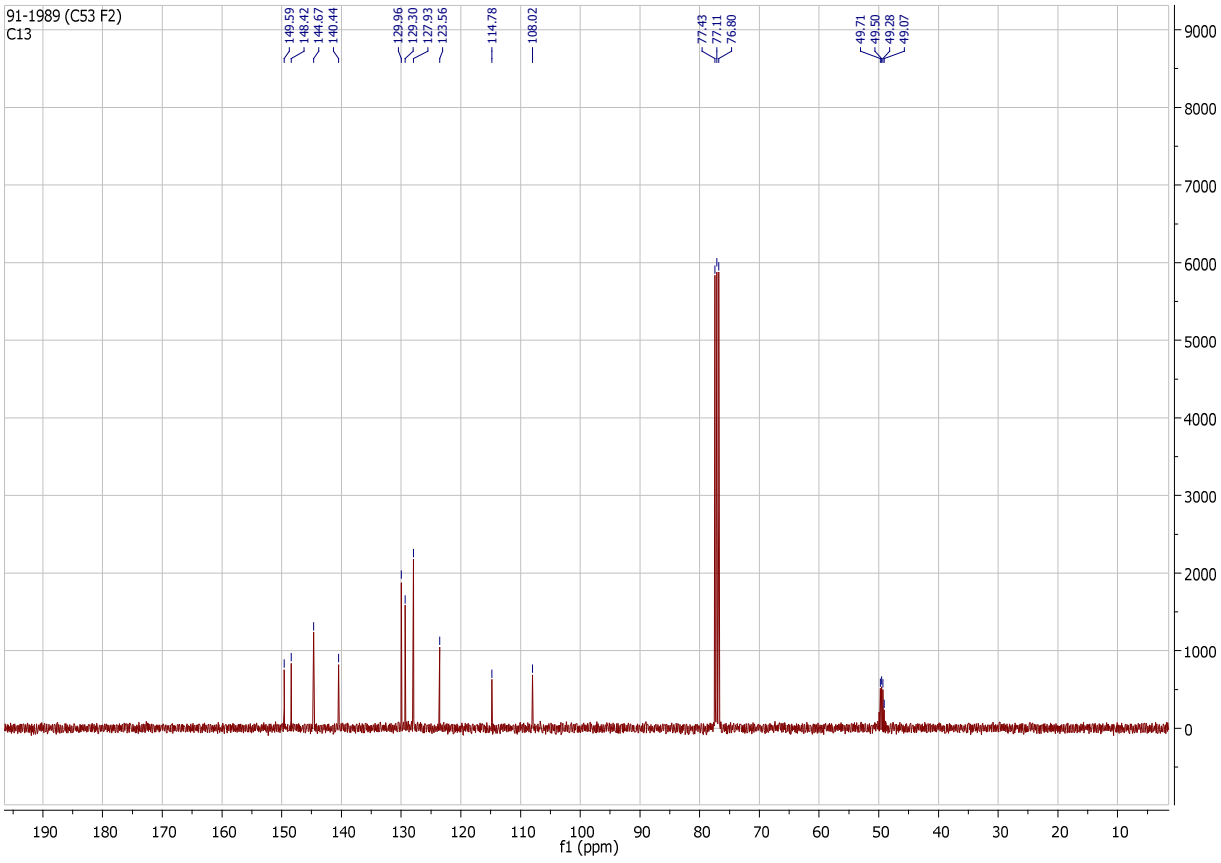

Appendix 5: ^{1}H-NMR spectrum (400 MHz, DMSO-*d6*) of compound **130**

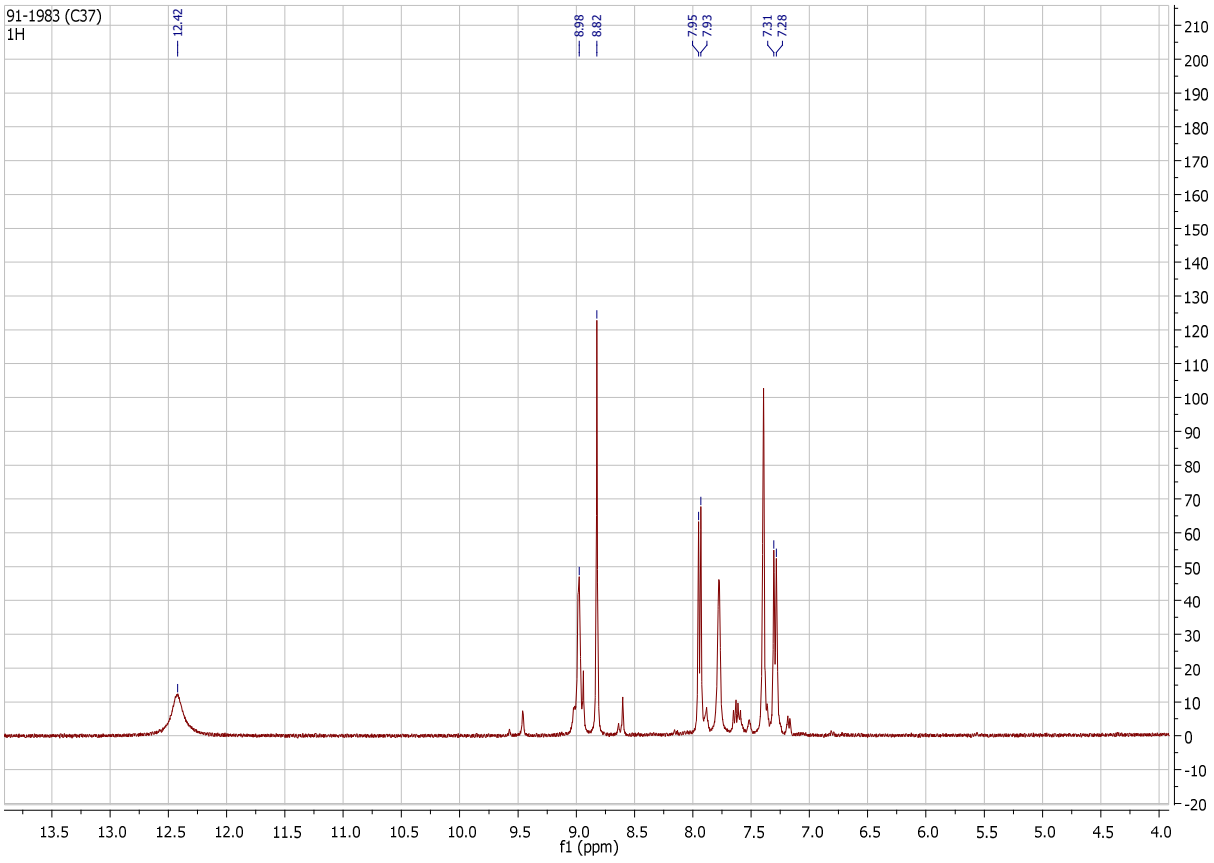

Appendix 6: ^{13}C-NMR spectrum (100 MHz, DMSO-*d6*) of compound **130**

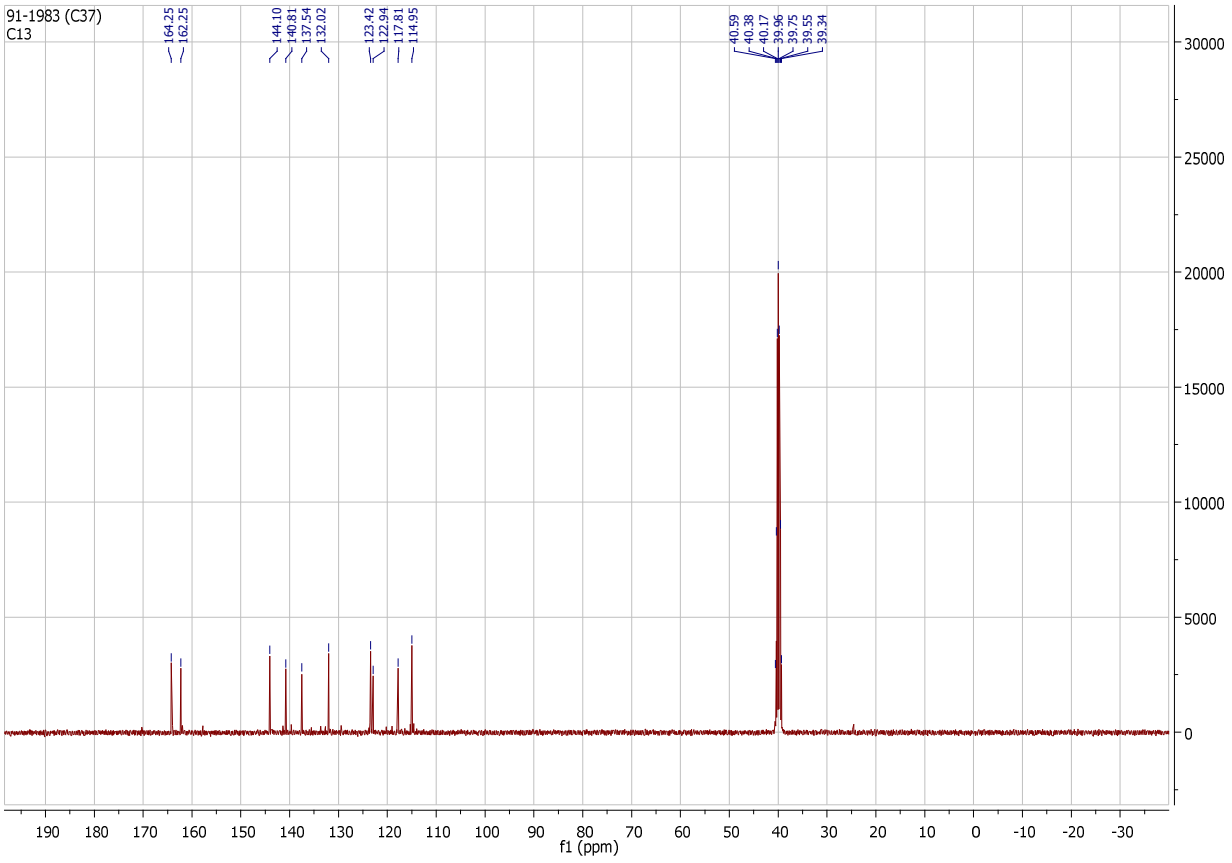

Appendix 7: ^{1}H-NMR spectrum (400 MHz, $CDCl_3$ and MeOD-*d4*) of compound **131**

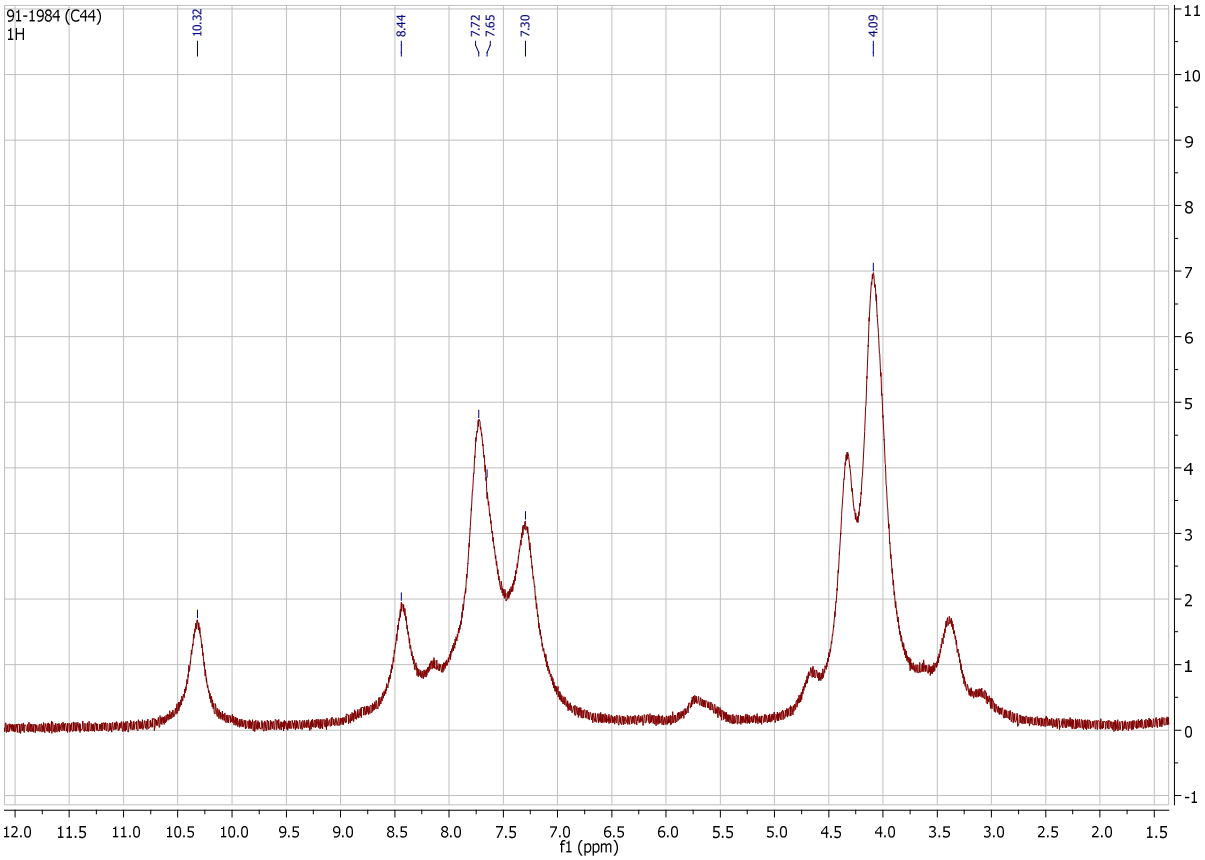

Appendix 8: ^{13}C-NMR spectrum (100 MHz, $CDCl_3$ and MeOD-*d4*) of compound **131**

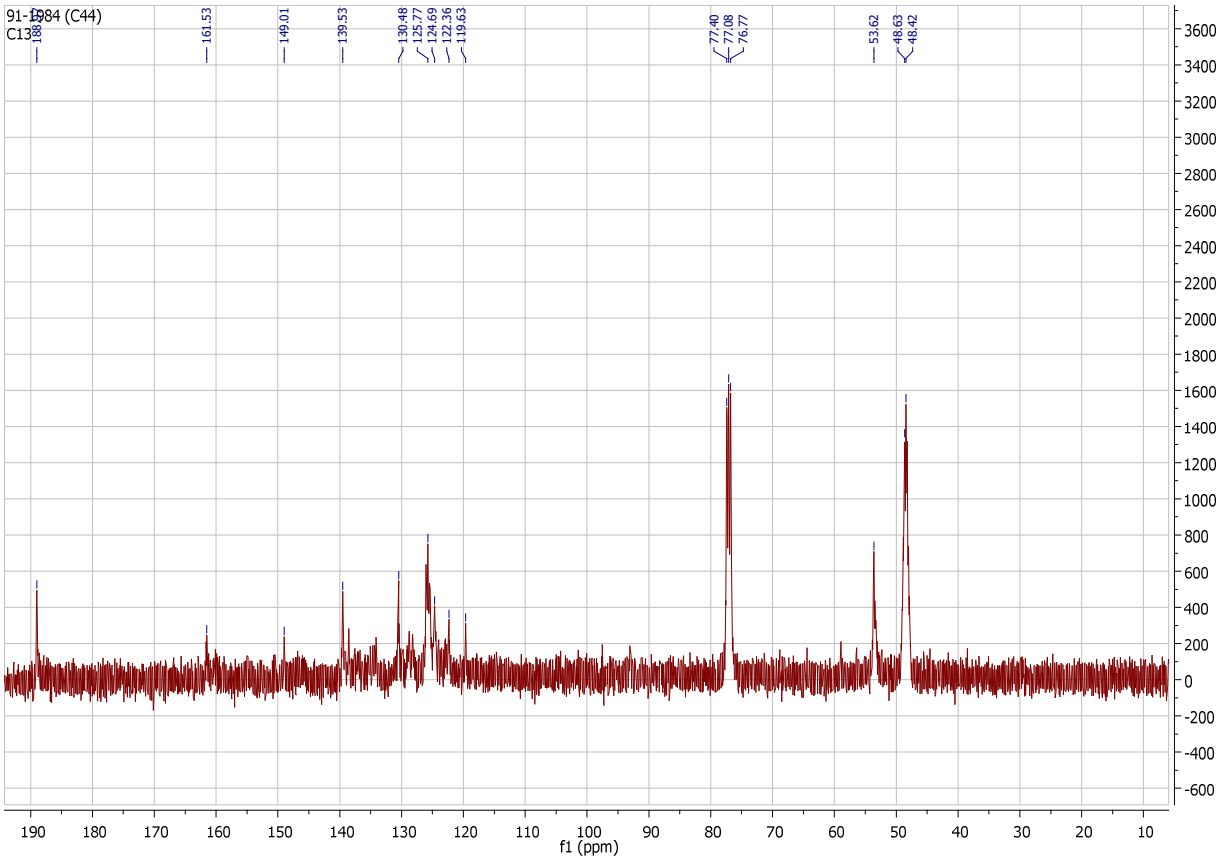

Appendix 9: ^{1}H-NMR spectrum (400 MHz, $CDCl_3$) of compound **132**

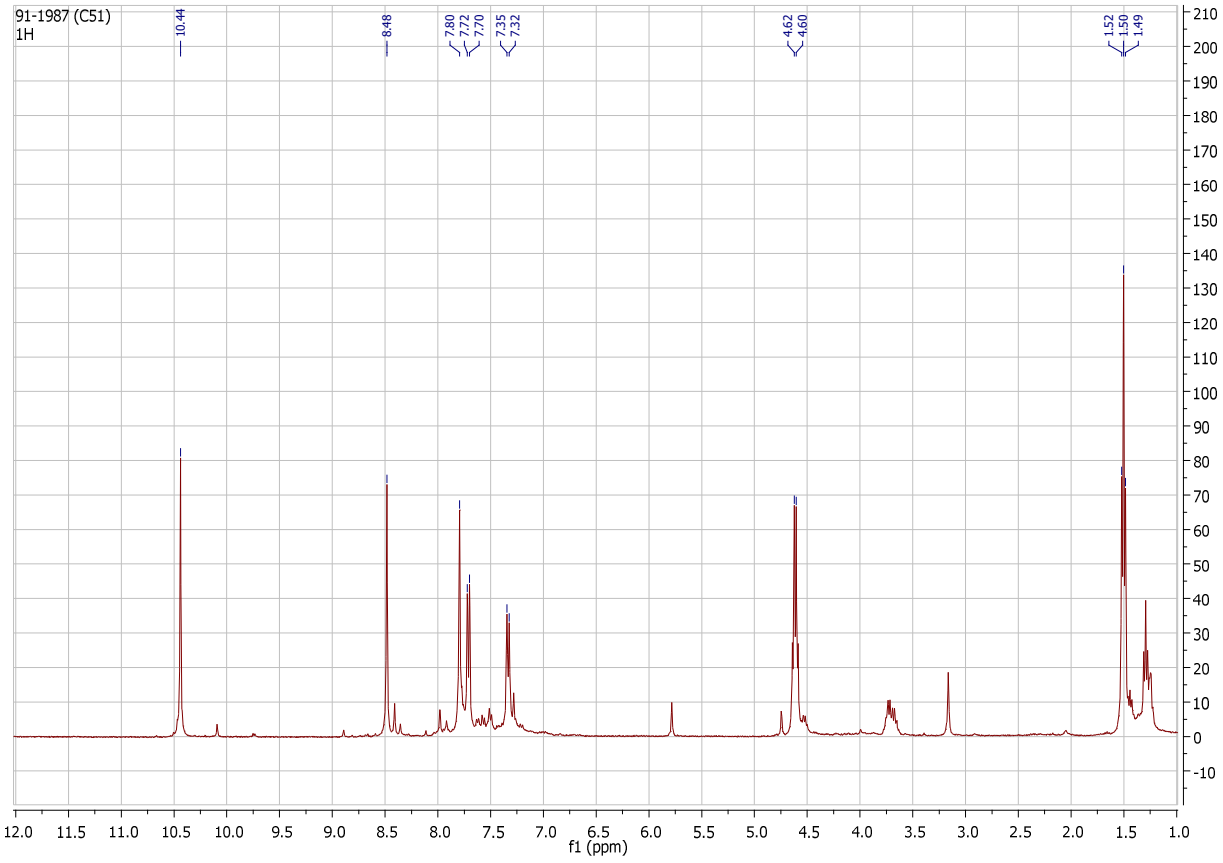

Appendix 10: ^{13}C-NMR spectrum (100 MHz, $CDCl_3$) of compound **132**

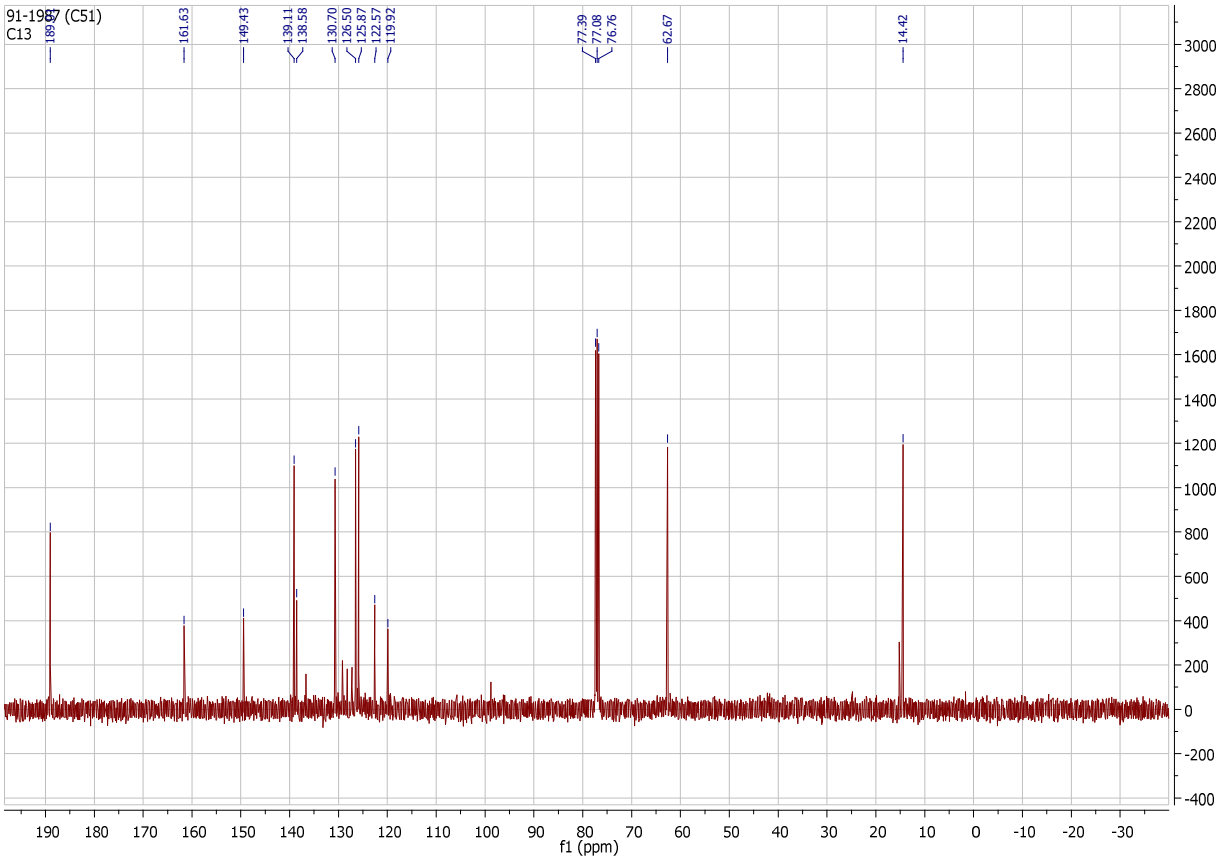

Appendix 11: ^{1}H-NMR spectrum (400 MHz, $CDCl_3$) of compound **133**

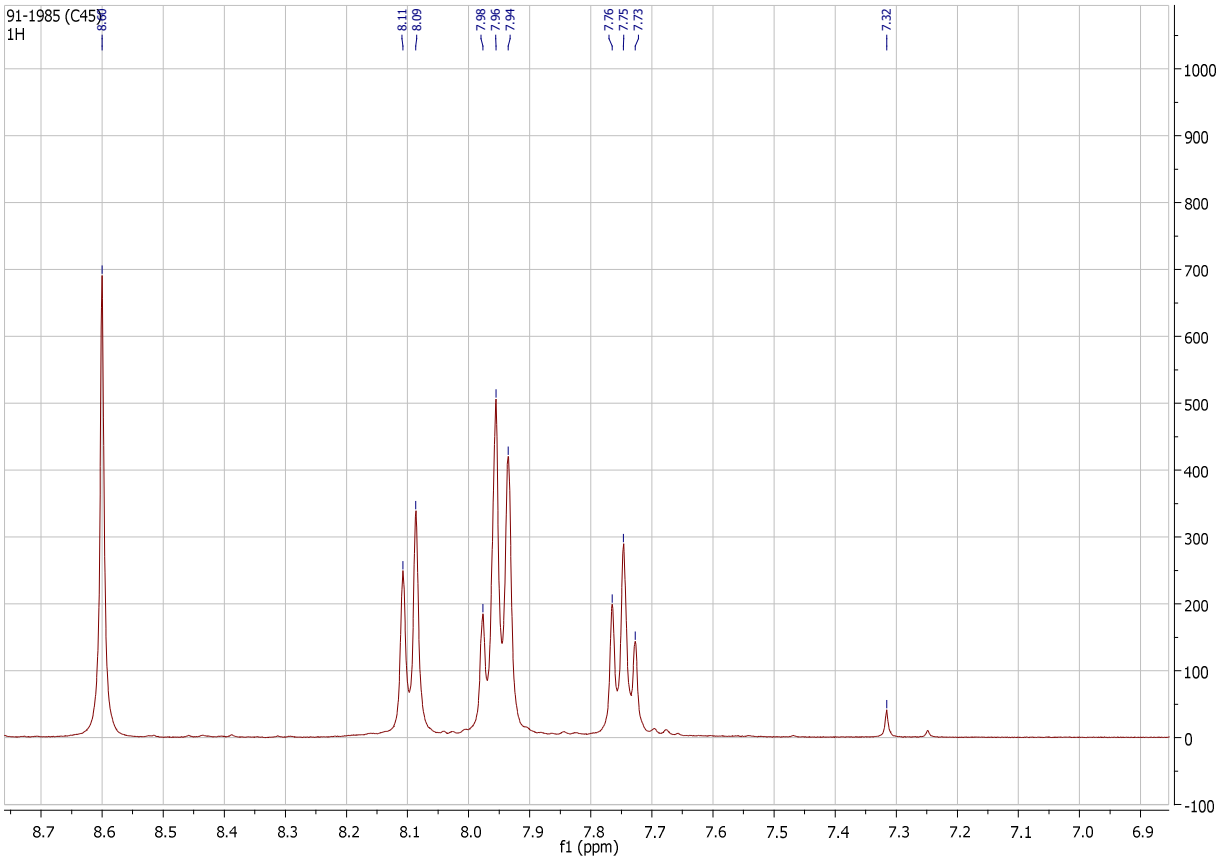

Appendix 12: ^{13}C-NMR spectrum (100 MHz, $CDCl_3$) of compound **133**